Proceedings of the 7th U.S. / Japan Natural Resources (UJNR) Panel on Earthquake Research

Compiled by Shane T. Detweiler and William L. Ellsworth

Open-File Report 2008-1335

U.S. Department of the Interior
U.S. Geological Survey

U.S. Department of the Interior
DIRK KEMPTHORNE, Secretary

U.S. Geological Survey
Mark D. Myers, Director

U.S. Geological Survey, Reston, Virginia 2008

For product and ordering information:
World Wide Web: http://www.usgs.gov/pubprod
Telephone: 1-888-ASK-USGS

For more information on the USGS—the Federal source for science about the Earth,
its natural and living resources, natural hazards, and the environment:
World Wide Web: http://www.usgs.gov
Telephone: 1-888-ASK-USGS

Suggested citation:
Detweiler, Shane T., and Ellsworth, William L., 2008, Compilers, Proceedings of the 7th U.S. / Japan Natural Resources (UJNR) Panel on Earthquake Research: U.S. Geological Survey Open-File Report 2008-1335, 99 p. [http://pubs.usgs.gov/of/2008/1335/].

The abstracts in this volume are published as they were submitted. Abstracts authored entirely by non-USGS authors do not represent the views or position of the U.S. Geological Survey or the U.S. government and are published solely as part of the Proceedings volume.

Any use of trade, product, or firm names is for descriptive purposes only and does not imply endorsement by the U.S. Government.

Although this report is in the public domain, permission must be secured from the individual copyright owners to reproduce any copyrighted material contained within this report.

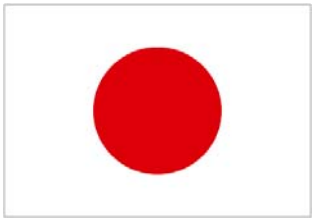

Proceedings of the 7th U.S. / Japan Natural Resources (UJNR) Panel on Earthquake Research

Seattle, Wash. USA 27-30 Oct. 2008

Compiled by Shane T. Detweiler and William L. Ellsworth

This page intentionally left blank

UJNR Participants

Dr. Ryosuke Ando
Geological Survey of Japan, AIST
ryo-ando@aist.go.jp

Dr. David Applegate (U.S.-side Chairman)
Earthquake Hazards Program Coordinator
U.S. Geological Survey
applegate@usgs.gov

Dr. Rick Benson
Incorporated Research Institutions for Seismology (IRIS)
rick@iris.washington.edu

Dr. Greg Beroza
Stanford University
beroza@stanford.edu

Dr. Rich Briggs
U.S. Geological Survey
rbirggs@usgs.gov

Dr. Jody Bourgeois
University of Washington
bourgeois@ess.washington.edu

Dr. Tom Brocher
U.S. Geological Survey
brocher@usgs.gov

Dr. Ikuo Cho
Geological Survey of Japan, AIST
ikuo-cho@aist.go.jp

Dr. Ken Creager
University of Washington
kcc@ess.washington.edu

Mr. Shane Detweiler (U.S.-side Secretary)
U.S. Geological Survey
shane@usgs.gov

Dr. James Dieterich
University of California, Riverside
James.dieterich@ucr.edu

Dr. William Ellsworth
U.S. Geological Survey
ellsworth@usgs.gov

Dr. Geoff Ely
University of Southern California
gely@usc.edu

Dr. Joan Gomberg
U.S. Geological Survey
gomberg@usgs.gov

Dr. Gavin Hayes
U.S. Geological Survey
ghayes@usgs.gov

Dr. Steve Hickman
U.S. Geological Survey
hickman@usgs.gov

Dr. David Hill
U.S. Geological Survey
hill@usgs.gov

Dr. Naoshi Hirata
Earthquake Research Institute
hirata@eri.u-tokyo.ac.jp

Dr. Hitoshi Hirose
National Research Institute for Earth Science and Disaster Prevention
hirose@bosai.go.jp

Dr. Shigeki Horiuchi
National Research Institute for Earth Science and Disaster Prevention
horiuchi@bosai.go.jp

Dr. Heidi Houston
University of Washington
Heidi.houston@gmail.com

Dr. Tetsuro Imakiire
Geographical Survey Institute
imq@gsi.go.jp

Dr. Miaki Ishii
Harvard University
ishii@eps.hardvard.edu

Dr. Kaj Johnson
Indiana University
kajjohns@indiana.edu

Dr. Hisanori Kimura
National Research Institute for Earth Science and Disaster Prevention
kimura@bosai.go.jp

Dr. Kenji Kinoshita (Japan-side Chairman Representative)
Deputy Director-General
Geographical Survey Institute
kinoshita@gsi.go.jp

Dr. Bill Leith
U.S. Geological Survey
wleith@usgs.gov

Dr. Rowena Lohman
Cornell University
rolohman@gmail.com

Ms. Elizabeth Martin
University of Washington
memartin@u.washington.edu

Dr. Hiroshi Masaharu
Geographical Survey Institute
masaharu@gsi.go.jp

Dr. Norio Matsumoto
Geological Survey of Japan, AIST
n.matsumoto@aist.go.jp

Dr. Jeff McGuire
Woods Hole Oceanographic Institution
jmcguire@whoi.edu

Dr. Meghan Miller
President, UNAVCO Inc.
meghan@unavco.org

Dr. Takuya Nishimura
Geographical Survey Institute
t_nishimura@gsi.go.jp

Dr. Shin-ichi Noguchi
National Research Institute for Earth Science and Disaster Prevention
shin@bosai.go.jp

Dr. Kazushige Obara
National Research Institute for Earth Science and Disaster Prevention
obara@bosai.go.jp

Dr. Susan Owen
Jet Propulsion Laboratory
Susan.Owen@jpl.nasa.gov

Dr. Garry Rogers
Natural Resources Canada
grogers@nrcan-rncan.qc.ca

Dr. Justin Rubinstein
U.S. Geological Survey
jrubinstein@usgs.gov

Dr. Makoto Saito
Japan Meteorological Agency
msaito@met.kishuo.go.jp

Dr. Hiroshi P. Sato
Geographical Survey Institute
hsato@gsi.go.jp

Dr. David Schmidt
University of Oregon
das@uoregon.edu

Dr. David Shelly
U.S. Geological Survey
dshelly@usgs.gov

Dr. Brian Sherrod
U.S. Geological Survey
bsherrod@usgs.gov

Dr. Bunichiro Shibazaki
Building Research Institute

bshiba@kenken.go.jp

Dr. Bridget Smith-Konter
University of Texas, El Paso
brkonter@utep.edu

Dr. Bill Steele
University of Washington
bill@ess.washington.edu

Dr. Tetsuya Takeda
National Research Institute for Earth Science and Disaster Prevention
ttakeda@bosai.go.jp

Dr. Wayne Thatcher
U.S. Geological Survey
thatcher@usgs.gov

Dr. Mikio Tobita
Geographical Survey Institute
tobita@gsi.go.jp

Dr. Shinji Toda
Geological Survey of Japan, AIST
s-toda@aist.go.jp

Dr. John Vidale
University of Washington
John_vidale@mac.com

Dr. Charles Wicks
U.S. Geological Survey
cwicks@usgs.gov

Dr. Eva Zanzerkia
National Science Foundation
ezanzerk@nsf.gov

This page intentionally left blank

AGENDA

7th UJNR Earthquake Research Panel Meeting

October 27-30, 2008

University of Washington Urban Horticultural Center & Greater Seattle Field Trip

Monday 27 October 2008

0800 Registration

0845 Meet at bus for field trip "Evidence of an active Seattle Fault from Alki Pt. to Lk. Sammamish"

1230 Stop for lunch

1730 Return to hotel

1800 Dinner on own

Tuesday 28 October 2008

0715 Breakfast on own

0815 Welcoming Remarks by Panel Co-Chairs **David Applegate** and **Kazuo Komaki**
Session I- Session Chairs **Hiroshi Masaharu** and **Meghan Miller**

0830 **Hiroshi Masaharu** "New Activities and Role of the Coordinating Committee for Earthquake Prediction"

0850 **Eva Zanzerkia** "Earth Sciences at the National Science Foundation: Understanding Earthquake Processes and Hazards Though Science, Facilities and Computation"

0910 **Naoshi Hirata** "Japanese new earthquake research programs : new comprehensive and basic policy for the promotion of seismic research, and new research program for prediction of earthquake and volcanic eruption"

0930 **Meghan Miller** "Plate Boundary Observatory – Integrated geodetic networks for observing fault deformation mechanisms across the temporal spectrum"

0950 **Shinji Toda** "Recent destructive inland earthquakes off major active faults: Implications for future updates of the seismic hazard map in Japan"

1010 Break

1030 Session II- Session Chairs **Craig Weaver** and **Ikuo Cho**

Tom Brocher "Recent Science on the Hayward Fault"

1050 **Ikuo Cho** "Physically-based approach to long-term forecasts of earthquakes on active faults: Evaluation of stress triggering effects"

1110 **Jim Dieterich** "Characteristics of Earthquake Occurrence and Rupture Propagation in Fault Systems"

1130 **Craig Weaver** "Seattle Urban Seismic Hazard Maps: Detailed ground shaking estimates in the urban environment. Who Cares?" (talk given by Joan Gomberg)

1150 Lunch

1310 Session III– Session Chairs **Shigeki Horiuchi and Jeff McGuire**

Geoff Ely "Large-scale dynamic earthquake rupture simulations for southern California"

1330 **Shigeki Horiuchi** "Earthquake Early Warning in Japan"

1350 **Kenji Kinoshita** "GSI's urgent countermeasure activities against earthquake disaster"

1410 **Jeff McGuire** "The potential for seafloor based earthquake early warning in subduction zones"

1430 **Makoto Saito** "Earthquake Information for Disaster Mitigation in Japan"

1450 **Break**

1510 Session IV- Session Chairs **Hisanori Kimura** and **Bill Ellsworth**

Steve Hickman "Structure, composition and mechanical behavior of the San Andreas Fault in central California: Recent results from SAFOD downhole measurements and core analyses"

1530 **Hisanori Kimura** "Detailed distribution and activity of small repeating earthquakes at the Kanto region, central Japan"

1550 **Kaj Johnson** "What can we learn about frictional properties of faults from postseismic earthquake studies?"

1610 **Bill Ellsworth** "Micro-, nano- and picoearthquakes: implications for fault friction and fault mechanics"

1630 **Miaki Ishii** "Monitoring Rupture Process of Giant Earthquakes Using the Japanese Hi-net Array"

1650 **Greg Beroza** "Strong Ground Motion Prediction Using the Ambient Seismic Field"

1710 Introduction to Posters, short presentations by:

Chuck Wicks, "Modeling the slip distribution and fault geometry of the February 21, 2008 Mw 6.0 Wells Nevada Earthquake using InSAR"

Rick Benson "The IRIS DMC: Global Real-Time Collection and Distribution of Seismological Data and Products"
Headquarters for Earthquake Research Promotion "National seismic hazard maps for Japan (2008)"
Sato et al. "Crustal movements detected by seafloor geodetic observation"
Fuyuki Hirose "Anomalous depth distribution of deep low-frequency earthquakes at the northeast Tokai district"

1900 Opening Banquet & No-Host Bar at University of Washington Waterfront Activity Center

Wednesday 29 October 2008

0730 Breakfast on own

0830 Session V-Session Chairs **Wayne Thatcher** and **Mikio Tobita**

Wayne Thatcher "How the Continents Deform: the Evidence from Tectonic Geodesy"

0850 **Norio Matsumoto** "Observation well network of groundwater and borehole strain monitoring for a prediction research of the Tonankai and Nankai earthquakes"

0910 **Bridget Smith-Konter** "Stress evolution of the San Andreas Fault System: Hindcast stress accumulation models and stress rate uncertainties"

0930 **Mikio Tobita** "SAR-derived deformation fields and a fault model of the 2008 Wenchuan Earthquake"

0950 **Rowena Lohman** "Atmospheric, topographic, crustal and parameterization errors: At what point do they significantly affect our models of moderate to large earthquakes?"

1010 **Ryosuke Ando** "Physical source modeling for the 2008 Iwate-Miyagi Nairiku, Japan, Earthquake"

1030 Break and Poster Viewing

1050 Session VI- Session Chairs **T. Nishimura** and **Brian Sherrod**

Brian Sherrod "Finding concealed active faults: examples of active faults concealed beneath thick vegetation and glacial deposits in the Puget Lowland, Washington"

1110 **Takuya Nishimura** "Fault model of the 2007 M6.8 Chuetsu-oki earthquake, central Japan and triggered episodic deformation in the adjacent active folding area"

1130 **Susan Owen** "Earthquake Research Programs at NASA: Advancing Earthquake Prediction and Characterization through Observations and Modeling"

1150 **Hiroshi P. Sato** "Comparison of satellite image interpretations between ALOS/PRISM and IKONOS, in the case of landslides triggered by Wenchuan (Sichuan) EQ"

1210 Lunch

1330 Session VII- Session Chairs **Elizabeth Martin** and **Shin-ichi Noguchi**

Rich Briggs "Inferring megathrust rupture areas from forearc structure: Promise and perils"

1350 **Gavin Hayes** "Resolving the geometry of global subduction zone interfaces - working towards improved earthquake source modeling"

1410 **Shin-ichi Noguchi** "The 2004 Great Sumatra Earthquake as a critical phenomenon and an accelerating seismicity along the Indian-Eurasian plate boundary zone"

1430 **Elizabeth Martin** "Previous tsunamis in Thailand"

1450 **Jody Bourgeois** "Studies of Seismicity and Paleoseismicity in the Kuril Biocomplexity Project [KBP]"

1510 Break and Poster Viewing

1530 Session VIII- Chairs **Kazushige Obara** and **Ken Creager**

Kazushige Obara "Phenomenology of episodic tremor and slip in southwest Japan--Spatio-temporal characteristics and segmentation"

1550 **Garry Rogers** "ETS in Canada: 25 Years of Observations"

1610 **Bunichiro Shibazaki** "Modeling short-term slow slip events in the deeper parts of the Nankai trough subduction zone"

1630 **Ken Creager** "Cascadia Episodic Tremor and Slip"

1650 **David Schmidt** "Assessment of slow slip events on the Cascadia subduction zone, 1998-2008"

1710 **Tetsuro Imakiire** "Detection of short term slow slip event by GEONET routine analysis"

1730 **John Vidale** "What does tremor really look like? - Results from a 1km, 80-element array on hard rock"

1750 Poster Viewing

1830 Free Time and dinner on own

Thursday 30 October 2008

0730 Breakfast on own

0830 Session IX- Session Chairs **Joan Gomberg** and **Hitoshi Hirose**

Hitoshi Hirose "Recurrence behavior of short-term slow slip and correlated non-volcanic tremor episodes in western Shikoku, southwest Japan"

0850 **Justin Rubinstein** "Bursts and Waves: The Response of Non-Volcanic Tremor to External Stressing"

0910 **Joan Gomberg** "Observations and implications of triggered tremor"

0930 **David Hill** "Surface Wave Triggering Potential"

0950 Break

1010 **Heidi Houston** "Scaling and the relation between tremor and slow slip"

1030 **Tetsuya Takeda** "Seismic exploration of deep low-frequency tremor area in western Shikoku, Japan"

1050 **David Shelly** "Precise relative location of San Andreas Fault tremors near Cholame, CA"

1110 Closing remarks by Panel Co-Chairs **David Applegate** and **Kazuo Komaki**

1130 Group photo

1145 Distribute box lunches

1200 Board Bus – depart for Earthquake Engineering field trip to Safeco Field

1800 Return to hotel

Friday 31 October 2008

0730 Breakfast on own

0900 Board Bus for Seattle International Airport (depart)

This page intentionally left blank

TABLE OF CONTENTS

This page intentionally left blank

SESSION I

ABSTRACTS

New Activities and Role of the Coordinating Committee for Earthquake Prediction

Hiroshi MASAHARU, Tetsuro IMAKIIRE, Mikio TOBITA and Riichi KAWAMOTO
Geographical Survey Institute (GSI)

The Coordinating Committee for Earthquake Prediction (CCEP) was established in 1969 based on the "Proposition on the Second Earthquake Prediction Plan" by the Geodesy Council. The purpose of CCEP was to constantly exchange information on observation and research and make overall judgment about the information. The latter purpose has been changed to making scientific discussion on earthquake prediction. Evaluation of seismic activities in Japan is now done by the Earthquake Research Committee under the Headquarters for Earthquake Research Promotion. CCEP holds regular meetings four times a year and holds unscheduled meetings when a large earthquake takes place. The committee is made up of about thirty members from organizations that carry out regular observation on seismicity and/or crustal deformation, i.e. universities, Japan Meteorological Agency, National Research Institute for Earth Science and Disaster Prevention, Geological Survey of Japan, Hydrographic and Oceanographic Department, Japan Agency for Marine-Earth Science and Technology and GSI. GSI serves as the secretariat of CCEP since its establishment. CCEP publishes its report biannually. The contents are made open at CCEP's website (http://cais.gsi.go.jp/KAIHOU/index.html). This CCEP report makes valuable archives of observation data about earthquakes.

CCEP has reviewed its role and style of activities, especially agenda of meetings according to the circumstances of earthquake research and the review of the Propositions. Since 2000, the meeting spends nearly half of its time to the presentations and discussions on a selected topic. The Working Group for Advancement of Future Activities of CCEP now discuss making the main part of meetings be the presentations and discussions on important themes for promoting earthquake prediction research. In 2008, CCEP decided to abolish its designation of Areas for Specified Observation. According to CCEP's designation, earthquake observation had been prompted. But now whole Japan is covered by dense observing system that was expected to set up in the Areas for Specified Observation. Therefore the area designation finished its role and the task shifted to research themes targeting whole Japan. The newest "Proposition on the Promotion of Observation and Research Plan for Earthquake and Volcanic Eruption Prediction" submitted in July 2008 states that 'Esteeming its activities so far positively, CCEP should make its role clearly as the information exchange mainly of the monitoring results of seismic activities and crustal deformation and discussion on advancement of monitoring techniques.' Based on this, CCEP starts to the next phase where main agenda will be the discussion of themes. CCEP has played an important role in earthquake prediction in Japan under the leadership of chairmen of the committee and contribution of committee members. CCEP is expected to continue playing important role in renewed activities.

Framework of earthquake research of Japan

Minister for Internal Affairs and Communications
Minister of Education, Culture, Sports, Science and Technology
Minister of Economy, Trade and Industry
Minister of Land, Infrastructure, Transport and Tourism

Report ←

Council for Science and Technology

Establish the propulsion program of earthquake prediction research (by the Subdivision on Geodesy)	Ministry of Education,Culture, Sports, Science and Technology (MEXT)

Headquarters for Earthquake Research Promotion (established in Jul. 1995)	MEXT

1. Planning of comprehensive and basic policies
2. Coordination of budgets and other administrative works
3. Establishment of comprehensive survey and observation plans
4. Collection, arrangement, analysis and comprehensive evaluation of survey results
5. Public announcements based on the comprehensive evaluations

Survey and research information ←

general coordination →

Coordinating Committee for Earthquake Prediction (CCEP.) (established in Apr.1969)

Exchanging information and making academic investigation on the observation and the research about the earthquake prediction	GSI

information ←

Earthquake Assessment Committee for the Areas under the Intensified Measures against Earthquake Disasters (established in Aug.1983)	
Short-term earthquake prediction for the areas under the intensified measures	JMA

Central Disaster Management Council (established in 1961)	Cabinet Office

Observation data for the areas under the intensified measures ←

- **Geographical Survey Institute (GSI)**
- National Research Institute for Earth Science and Disaster Prevention (NIED)
- National universities
- Geological Survey of Japan ,National Institute of Advanced Industrial Science and Technology (AIST)
- Hydrographic and Oceanographic Department, Japan Coast Guard
- Japan Meteorological Agency (JMA)
- Japan Agency for Marine-Earth Science and Technology (JAMSTEC)

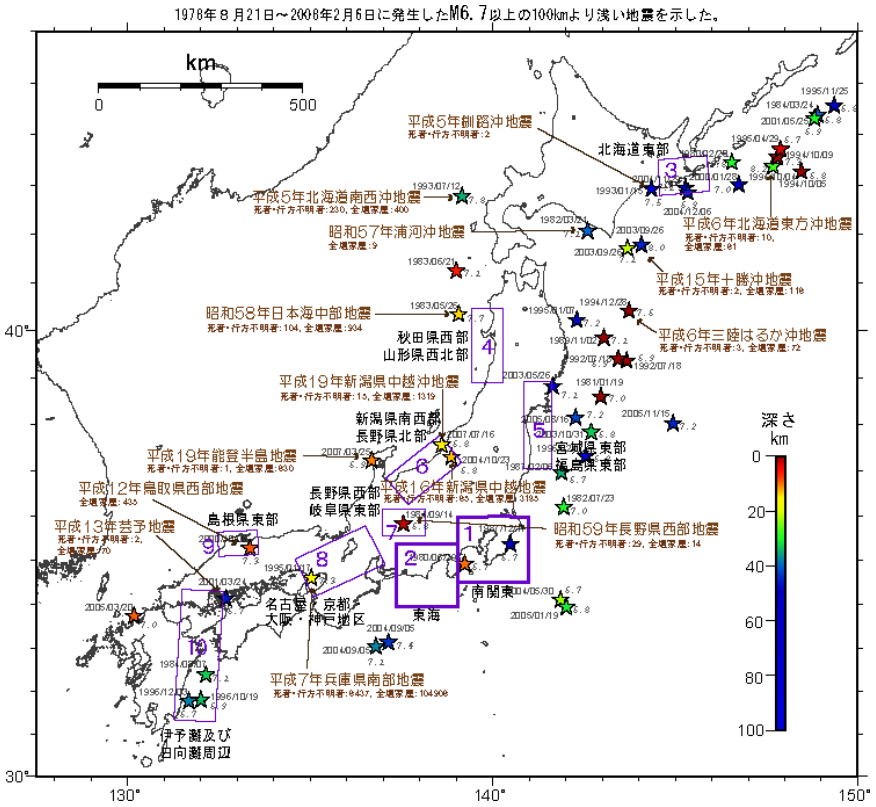

The left figure shows the relationship between designated areas and earthquakes with M6.7 or larger that happened after designation. These large earthquakes happened in or near the designated areas (except Tokai area).

Various kinds of observation data are collected and they contributed to promoting earthquake prediction research.

Earth Sciences at the National Science Foundation: Understanding Earthquake Processes and Hazards Though Science, Facilities and Computation

By Eva Zanzerkia
National Science Foundation

With the completion of the EarthScope Facility construction, the availability of new and densely sampled datasets and the NSF's emphasis on computationally innovative and collaborative science, the Earth science community is poised to make unprecedented advances in the study of earthquake processes and crustal structure. The Deep Earth Processes (DEP) Section, in the Earth Sciences Division, Geosciences Directorate, serves as a hub for the community's interaction with the Foundation, providing support for fundamental research on earthquakes and other natural hazards, tectonics, geodynamics, as well as research facilitated by the EarthScope program. EarthScope is a multidisciplinary program to study the structure and evolution of the North American continent and the physical processes responsible for earthquakes and volcanic eruptions.

The DEP programs support science that encompasses observational, experimental and theoretical studies of natural hazards and the structure and deformation of the earth. These programs support a variety of technique developments, such as microatoll studies, and other paleoseismic methods to date subduction zone earthquakes, new videography and infrasound techniques to observe volcanic eruption, and the development of tomography methods using ambient seismic noise. Recent fault mechanics projects range from observations of episodic slip and tremor in Japan, Hawaii, and Cascadia to laboratory studies of rupture processes using photogrammetric materials and frictional models of fault slip and earthquake occurrence in complex fault systems.

The section also supports facilities and computational resources. These include funding for Geoinformatics, cyberinfrastructure specifically for the Earth Sciences, the Computational Infrastructure for Geodynamics, data collection and archiving resources such as IRIS and UNAVCO, GeoEarthScope and the ALOS/PALSAR consortium, and earth materials databases like EarthChem. All data funded by the National Science Foundation, including EarthScope data, is openly available to the national and international scientific community.

Opportunities, particularly in support of advances in cyberinfrastructure, are available outside of the Geosciences Directorate. As funding for computational advances increase, through federal initiates such as the America Competes Act, the Earth Science, and natural hazards community must take advantage of new programs across the foundation, such as DataNet, PetaApps II and CluE. In addition, multidisciplinary projects combining innovation in computational thinking and Earth Science are invited to Cyber-enabled Discovery and Innovation (CDI). International collaborations are welcomed under this solicitation, as well as the Partnerships for International Research and Education (PIRE) program.

Japanese new Earthquake Research Programs:
New Comprehensive and Basic Policy for the Promotion of Seismic Research, and new Research Program for Prediction of Earthquakes and Volcanoes

Naoshi Hirata
Earthquake Research Institute, the University of Tokyo

It is 10 years since *the Headquarters for Earthquake Research Promotion in Japan* published a document entitled *the Promotion of Earthquake Research—comprehensive and basic policy for the promotion of earthquake observations, surveys, measurements, and researches* (referred to as *the comprehensive and basic policy*; Headquarters for Earthquake Research Promotion, 1997). A structure and contents of the new *comprehensive and basic policy* have been discussed and the new policy will be released next spring. In the policy the new research program for prediction of earthquake and volcanic eruption, which has been recommended by *the Council for Science and Technology of Japan*, is defined as the basic research program, results of which will be one of fundamental inputs for mission-oriented earthquake researches that are conducted by government agencies.

The new *comprehensive and basic policy* (2009-2018) defines three basic objectives to be promoted in ten years:

1) Understanding of near-Trench earthquakes, including a mega-thrust earthquake and an intra-slab earthquake, which is particularly important for the coming mega-thrust earthquakes in the Nankai trough region with high probability of occurrence of event.
2) Systematic collection of information about inland earthquakes for improved evaluation of seismic hazard, with emphasis on off-shore active faults and buried inland source faults.
3) Promotion of communication between researches of seismic hazard science and those of engineering and social sciences for reducing earthquake risk.

The next prediction research program named “The observation and research program for prediction of earthquake and volcanic eruption (2009-2013)” consists of the following four objectives:

1) Development of forecasting system of processes of earthquake and volcanic eruption
2) Comprehensive understanding of earthquake and volcanic eruption
3) Development of new technology
4) Organizing structures of administration, research, education, and outreach

Plate Boundary Observatory – Setting the Standard for Community Science through Integrated Geodetic Networks –Monument Design, Open Data, and Observations across the Temporal Spectrum

M. Meghan Miller, Mike Jackson, Charles Meertens, and Susan Eriksson
UNAVCO, 6380 Nautilus Drive, Boulder, CO 80301 USA

The Plate Boundary Observatory (PBO), one of the three components of NSF's EarthScope project, is the proving ground for UNAVCO's capability to construct an integrated geodetic network at plate boundary scale. PBO's dense array of geodetic instrumentation includes networks of 1100 GPS instruments on deeply anchored or bedrock anchored drilled braced monuments, 75 borehole strain meters with co-located seismometers and tilt meters, five long-baseline strain meters, a pool of 100 portable GPS instruments that are available for individual science investigations. In addition, a suite of imagery products (LiDAR, InSAR) and geochronology services that support assessment of longer-term deformation provide constraints on decadal to millennium scale deformation. Integration of these data sets provides mapping of the kinematics of the Earth at temporal scales that span seconds to millennia, with the goal of investigating: the forces, spatial distribution, and evolution of plate-boundary deformation; earthquake nucleation processes; and magmatic processes.

This project showcases UNAVCO's capability for rapid development of facility construction, scalable deployments, and the UNAVCO science community's commitment to establishing unified data formats, data base access, and open data exchange. GPS analyses provided under the project substantially increase the breadth of the investigator community and provide time series and velocity fields for wide use; high-end data analysis labs within the science community continue to provide independent analyses that innovate in support of specific science goals, and higher order products such as strain rate field derivations. Results affirm the benefit of a large investment in stable monuments, coupled to the Earth through drilled braced construction of several types.

All of the data from EarthScope are freely and openly available to the scientific community, the educational community, and the public. Wide access to the data and research results of the networks will lead to faster progress in scientific research and hazard reduction. EarthScope also provides an excellent opportunity for integrating scientific research and education while advancing the Earth Sciences with diverse audiences.

Recent Destructive Inland Earthquakes off Major Active Faults: Implications for Future Updates of the Seismic Hazard map in Japan

Shinji Toda

Active Fault Research Center, Geological Survey of Japan, National Institute of Advanced Industrial Science and Technology (AIST)

Several recent large inland earthquakes in Japan since the 1995 Kobe earthquake have struck the lower probability areas mapped by the Earthquake Research Committee (ERC) of the Headquarters for Earthquake Research Promotion in 2005. Here we seek the reason why M6-7 class inland earthquakes occurred more frequently than ERC forecasted revisiting the emergence rate of tectonic surface ruptures in the past ~85 years.

The most of the M≥6.5 shallow inland earthquakes have been believed to be accompanied with tectonic sufrace ruptures. Together with the characteristic earthquake concept, the empirical equation between Mjma and L have been widely used to estimate M when evaluating the seismic potential of an active fault. However, some of the reported surface breaks were extremely short relative to their source faults and amount of slip was faint, which do not allow us to retrospectively estimate sizes of the earthquakes and cannot be saved as a distinctive geologic record. From such a backdrop, here we re-examined the surface rupturing earthquakes since 1923 when JMA official catalog starts. We first selected all the earthquakes with Mjma ≥ 6.5 and shallower than 30 km in inland area since 1923 (Fig. 1). We then picked up the surface rupturing earthquakes documented by published papers, and categorized them into three, Rank 1, Rank 2, and Rank 3, depending on how much the rupture represented dimension of the source fault at the Earth's surface. We counted the number of Rank 1 ruptures which lengths are longer than 60% of the source fault and found five out of 30 M≥ 6.5 earthquakes, and four out of 10 M≥7.0 earthquakes produced the Rank 1 ruptures (Table 1). In other words, only 17% of M≥6.5 and 40% of M≥7.0 shallow earthquakes left the surface breaks which correspond to their source fault dimension. Since most of active faults in Japan are not maturely developed, we would simply regard the accumulated landform produced by the frequent surface ruptures as a distinctive active fault. We thus speculate that the number of potential destructive earthquakes of M6-7 estimated from the major active faults would be

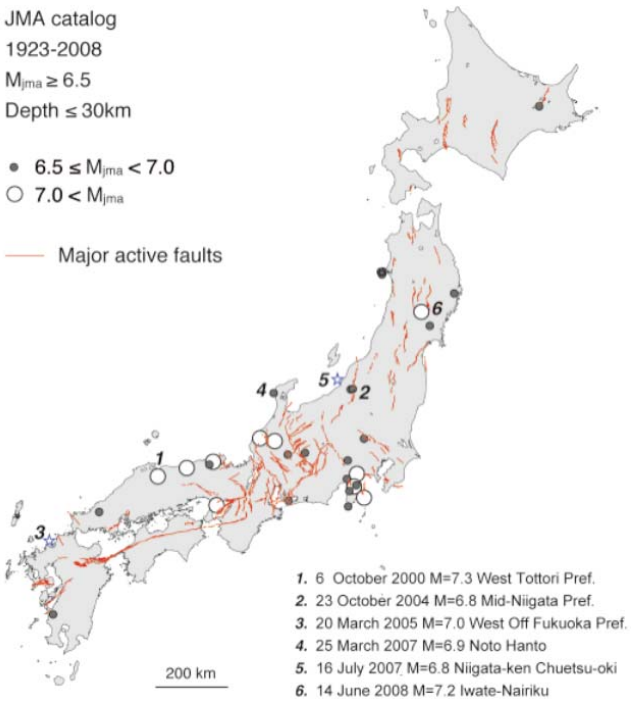

Fig. 1. Inland destructive earthquakes since 1923.

clearly underestimated. For the future updates of the probabilistic map, we may need to add these deficit of the M6-7 size shocks considering all late Quaternary deformation off the major active faults.

≥ Mjma	Number of Earthquakes	Earthquake Rate (No. per Year)	Number of Rank 1 Surface Rupturing Shocks	Emerging Rate of Rank 1 Surface Rupture (%)
6.0	78	0.92	-	0
6.5	30	0.36	5	17
7.0	10	0.11	4	40

Table 1. Seismicity rate of M≥6.0 inland earthquakes and rate of surface rupturing earthquakes

SESSION II

ABSTRACTS

The 1868 Hayward Earthquake Alliance: A Case Study - Using an Earthquake Anniversary to Promote Earthquake Preparedness

Thomas M. Brocher[1], Susan Garcia[1], Brad T. Aagaard[1], John J. Boatwright[1], Tim Dawson[2], Margaret Hellweg[3], Keith L. Knudsen[4], Jeanne Perkins[5], David P. Schwartz[1], Phillip W. Stoffer[1], Mary Lou Zoback[6]

[1] U.S. Geological Survey, Menlo Park, Calif. U.S.A.
[2] California Geological Survey, Menlo Park, Calif. U.S.A.
[3] Berkeley Seismological Laboratory, University of California, Berkeley, Calif. U.S.A.
[4] California Geological Survey, Sacramento Calif., U.S.A.
[5] Association of Bay Area Governments, Oakland, Calif. U.S.A.
[6] Risk Management Solutions, Newark, Calif. U.S.A.

October 21st, 2008, marked the 140th anniversary of the M6.8 1868 Hayward Earthquake, the last damaging earthquake on the southern Hayward Fault. This anniversary was used to help publicize the seismic hazards associated with the fault because: (1) the past five such earthquakes on the Hayward Fault occurred about 140 years apart on average, and (2) the Hayward-Rodgers Creek Fault system is the most likely (with a probability of 31%) fault in the Bay Area to produce a M6.7 or greater earthquake in the next 30 years. To promote earthquake awareness and preparedness, over 140 public and private agencies and companies and many individuals joined the public/private nonprofit 1868 Hayward Earthquake Alliance (1868alliance.org). The Alliance sponsored many activities including a public commemoration at Mission San Jose in Fremont, which survived the 1868 earthquake. This event was followed by an earthquake drill at Bay Area schools involving more than 70,000 students. The anniversary prompted the Silver Sentinel, an earthquake response exercise based on the scenario of an earthquake on the Hayward Fault conducted by Bay Area County Offices of Emergency Services. Sixty other public and private agencies also participated in this exercise. The California Seismic Safety Commission and KPIX (CBS affiliate) produced professional videos designed for school classrooms promoting "Drop, Cover, and Hold On." Starting in October 2007, the Alliance and the U.S. Geological Survey held a sequence of press conferences to announce the release of new research on the Hayward Fault as well as new loss estimates for a Hayward Fault earthquake. These included: (1) a ShakeMap for the 1868 Hayward earthquake, (2) a report by the U. S. Bureau of Labor Statistics forecasting the number of employees, employers, and wages predicted to be within areas most strongly shaken by a Hayward Fault earthquake, (3) new estimates of the losses associated with a Hayward Fault earthquake, (4) new ground motion simulations of a Hayward Fault earthquake, (5) a new USGS Fact Sheet about the earthquake and the Hayward Fault, (6) a virtual tour of the 1868 earthquake, and (7) a new online field trip guide to the Hayward Fault using locations accessible by car and public transit. Finally, the California Geological Survey and many other Alliance members sponsored the Third Conference on Earthquake Hazards in the East Bay at CSU East Bay in Hayward for the three days following the 140th anniversary. The 1868 Alliance hopes to commemorate the anniversary of the 1868 Hayward Earthquake every year to maintain and increase public awareness of this fault, the hazards it and other East Bay Faults pose, and the ongoing need for earthquake preparedness and mitigation.

Physically-based Approach to Long-Term Forecasts of Earthquakes on Active Faults: Evaluation of Stress Triggering Effects

Cho, I., T. Tada and Y. Kuwahara
Geological Survey of Japan, AIST

We have started a research program to improve the accuracy of long-term forecasts for earthquakes on active faults by taking a physically-based approach. Most importantly, we are interested in intraplate earthquakes, not in plate boundary earthquakes that have been modeled by many researchers. In the modeling of plate boundary earthquakes, a rate- and state-dependent friction law is often used to reproduce the patterns of aseismic and seismic slip. The calculation techniques have advanced so much that it is now possible to deal with the interaction of multiple faults. On the other hand, modeling techniques for intraplate earthquakes have not been fully explored, and we have to begin by asking whether we can safely adapt the models of plate boundary earthquakes for intraplate earthquakes as well.

From the practical viewpoint, we do consider that adapting the physical model of plate boundary earthquakes for intraplate earthquakes is a reasonable choice. We should be mindful, however, that there is considerable ambiguity in the model parameters of intraplate earthquakes, including the fault geometry and the mode of loading. History of earthquake occurrences, which we need both for constructing and validating the model, is also ambiguous due to the long recurrence intervals (~1000 yr). This makes it difficult to deal with multiple faults: We generally rely on Monte Carlo simulation in earthquake forecasting, but this is quick to become unfeasible when the dimension of the parameter space becomes too large.

We introduce for computational convenience the idea of stress triggering, by which we mean that stress perturbations (static stress steps) from nearby faults are represented simply as external forces acting on the fault of interest. We pay special attention to a single fault and analyze how the external stress steps affect the degree of imminence of the next earthquake on that fault.

To be more specific, we have chosen to take the following steps. 1) Make a physical model of the fault of interest and simulate a regular earthquake cycle with no stress steps intervening. 2) List up the history of nearby earthquakes based on historical documents or geology-based catalogues. Evaluate the history of external stress steps acting on that fault and recalculate earthquake cycles with those stress steps taken into account. 3) Conduct Monte Carlo simulation by repeating Steps 1 and 2, under different sets of parameters, to obtain the probability distribution for the time to the next earthquake.

We illustrate the above framework with some preliminary results. We call for fruitful discussions so that we can better orient ourselves in our future work.

Characteristics of Earthquake Occurrence and Rupture Propagation in Fault Systems

James Dieterich
Keith Richards-Dinger

University of California, Riverside

We are applying a computationally efficient fault system earthquake simulator to explore possible applications for regional evaluations of earthquake probabilities. The simulations incorporate rate- and state-dependent constitutive properties with high-resolution representations of fault systems, and quasi-dynamic rupture propagation. Fault sections that make up the fault system are represented as continuous smooth surfaces, surfaces with a random fractal roughness, and discontinuous fractally segmented faults. Simulated earthquake catalogs have up to one million earthquakes that span a magnitude range from roughly M4.5 to M8. Comparisons with fully dynamic finite element calculations demonstrate that the model is quite accurate. The simulated seismicity has strong temporal and spatial clustering in the form of foreshocks and aftershocks and occasional large-earthquake pairs. We find that fault system geometry plays the primary role in establishing the characteristics of stress evolution that control earthquake recurrence statistics. Empirical density distributions of earthquake recurrence times at a specific point on a fault depend strongly on magnitude and take a variety complex forms that change with position within the fault system. Because fault system geometry is an observable that has a great impact on recurrence statistics, we propose using fault system earthquake simulators to define empirical probability density distributions for use in regional assessments of earthquake probabilities. A variety of specialize density distributions specially tailored to probabilistic evaluations can be constructed.

We have also begun study of effects of stress state on rupture propagation. Comparisons with fully dynamic finite element models show that RSQsim replicates the rupture propagation process quite well. Of necessity current deterministic rupture simulations for ground motion studies must use initial “composed” stress states. Those stress assumptions may not be dynamically consistent with stresses that evolve in fault systems as a consequence of previous earthquake ruptures. We find that the average stress level, relative to sliding strength, for “composed” stress models are significantly higher than evolved stresses in multi-event simulations, which lead to much more coherent rupture propagation than ruptures dynamically evolved stresses initial. These effects may have a significant impact on ground motions predicted from rupture simulations.

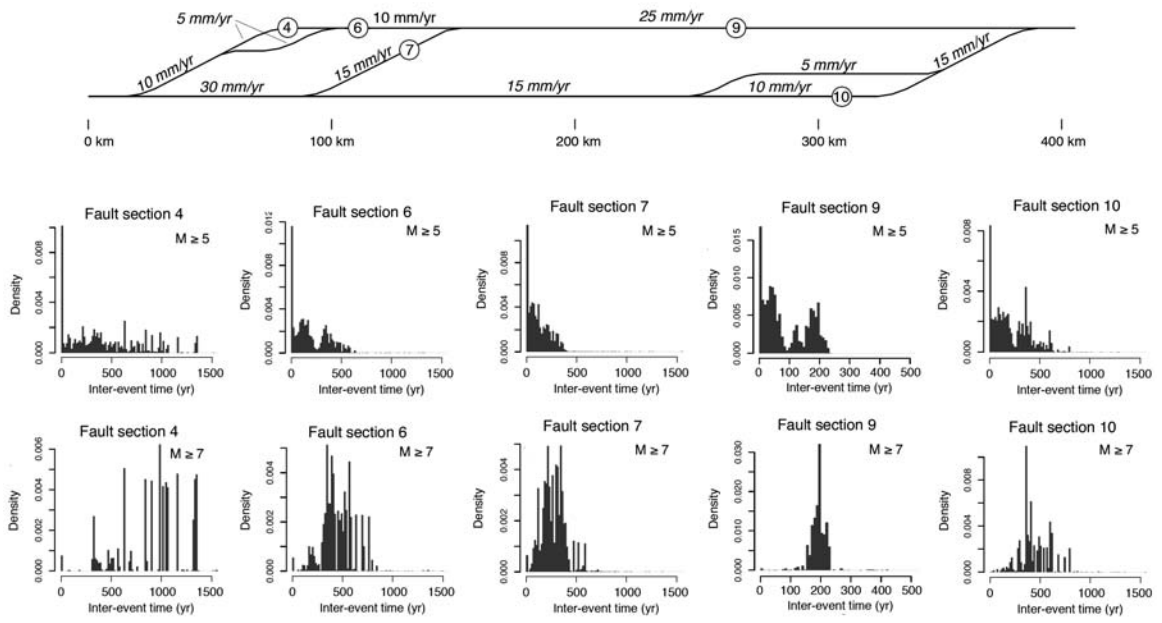

Figure 1. Empirical density distributions for earthquake recurrence in a simple fault system (top).

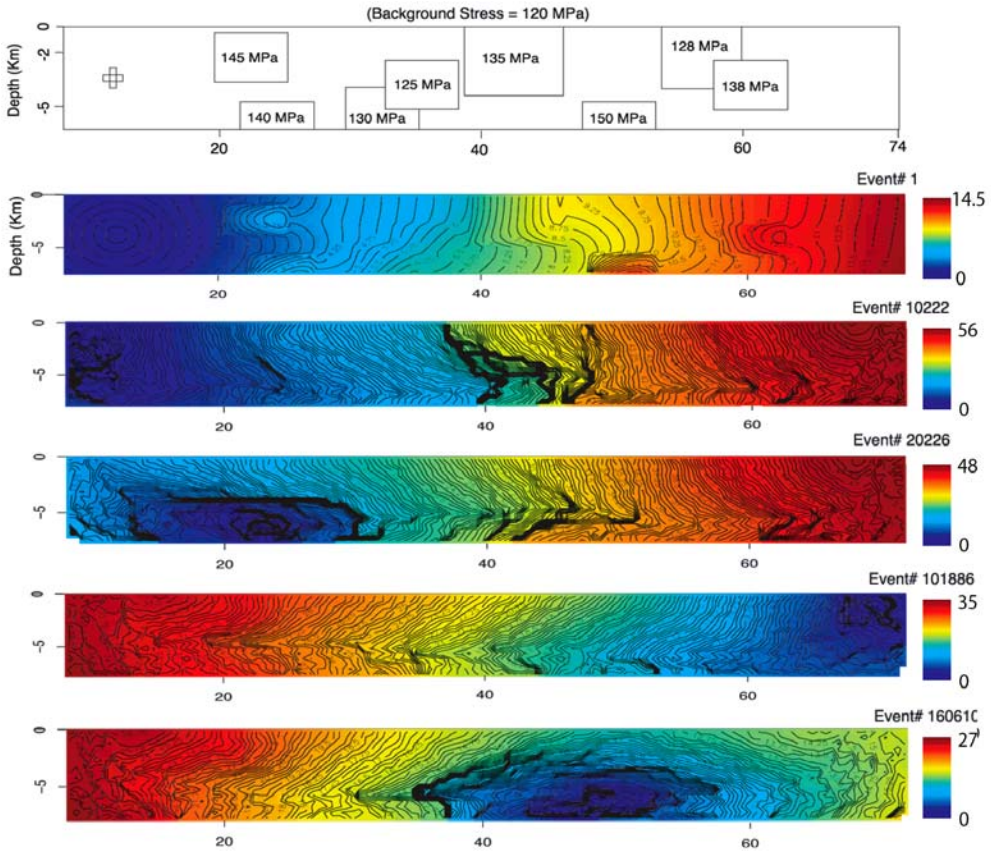

Figure 2. Rupture propagation with "composed" initial stress state (Event 1) and evolved stresses that spontaneous developed following Event 1 in multi-event simulation of 200,000 earthquakes. Contours give rupture position of rupture front at 0.25 s intervals. Note lower and much more variable rupture speeds in the evolved stress simulations.

Seattle Urban Seismic Hazard Maps: New Tools for Resiliency

Craig Weaver and Art Frankel
U.S. Geological Survey

The USGS has produced a new series of earthquake hazard maps for the City of Seattle. These 'urban seismic hazard' maps provide a much higher-resolution view of the potential for strong earthquake shaking than the only other maps of this type covering Seattle, the National Seismic Hazard maps. This new view is particularly important for Seattle, which sits atop a sedimentary basin that strongly affects the patterns of earthquake ground shaking and therefore, of potential damage. The subsurface geologic structure of the Seattle basin amplifies and lengthens the duration of strong shaking in some places and in others dampens motions. The seismic waves that shake the ground may be focused and defocused, and thus enhanced and diminished, because of the complex structures the waves travel through and the way in which faults break during an earthquake. A large earthquake fault break grows like a propagating crack, radiating seismic waves along the way. This can lead to a pile-up of wave energy in front of the fault and spread it out behind. The new urban hazard maps include all these effects, while the national maps do not.

The Seattle urban seismic hazard maps are 'probabilistic' – that is, they portray the severity of shaking the city is likely to experience accounting for all the potential earthquakes that would affect Seattle: on the Seattle and other shallow faults, great Cascadia subduction zone plate interface earthquakes, and deep ones like the 2001 Nisqually earthquake. The hazard is mapped in terms of the shaking level Seattle is likely to experience in a 50-year time window. For example, in the map in Figure 1a shows a 2% chance of the ground motions in Seattle being at least as strong as those shown some time during a 50-year period. These motions have an oscillation period of 1 second.

The highest hazard within the Seattle basin is found in areas of artificial fill and young alluvium (soils and sands), including Harbor Island, Pioneer Square, and in the Interbay, Fremont and Montlake-University of Washington neighborhoods. Other areas within the basin on more consolidated soils (north of Safeco Field), such as downtown Seattle, show elevated hazard compared to rock sites outside of the basin. Outside the Seattle basin, very high hazard also is predicted in the alluvial Duwamish valley.

The public use of the newly released maps is impressive. The maps are the starting point for the design of the replacement 520 Evergreen Point bridge. The City of Seattle is using the maps to help underpin a proposed ordinance requiring retrofitting certain kinds of unreinforced masonry buildings. A recent inventory of these buildings found that Seattle has about 1000, many in high hazard areas identified on the new Seattle Urban Seismic Hazard maps (Figure 1b). Unreinforced masonry buildings have suffered significant damage during three earthquakes since 1949 and have been declared by the Mayor of Seattle as a public safety issue. The USGS has discussed the new maps with insurance groups and public health officials to help with their long-range planning.

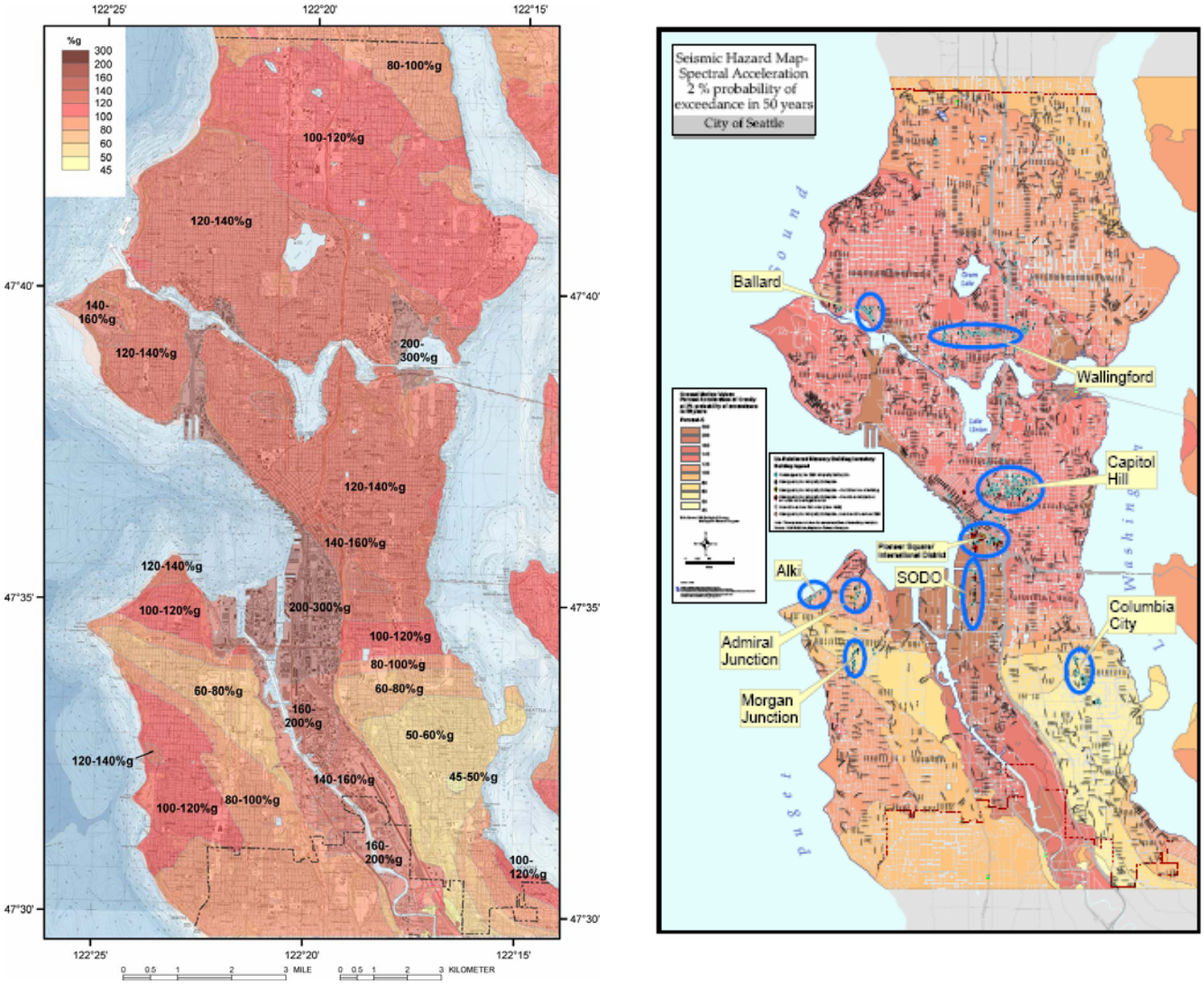

Figure 1: a. Urban Seismic Hazard map for Seattle with a 2% chance of being exceeded during a 50-year period (motions shown have an oscillation period of 1 second). b. Location of unreinforced masonry buildings superimposed on 2% in 50 1 second Seattle Urban Seismic Hazard map.

SESSION III

ABSTRACTS

Large-scale Dynamic Earthquake Rupture Simulations for southern California

Geoffrey Ely
University of Southern California

Ground motions in southern California can be significantly influenced by three-dimensional basin wave-propagation effects. As first observed by the TeraShake simulations, a large event on the southern San Andreas fault could excite larger than expected motions at Whittier Narrows due to basin-guided waves. We reexamine the TeraShake scenario with finite-element dynamic rupture simulations to assess sensitivities in ground motion due to: (1) changes in the 3D velocity model (SCEC Community Velocity Model version 3.0 vs. version 4.0), and (2) inclusion of true Earth topography at the free surface. We find that SCEC-CVM 4.0 diminishes basin guided waves at Whittier Narrows, with ground motions closer to those predicted by empirical attenuation relations. We are performing additional simulations over a suite of potential source scenarios for southern California, with the goal of identifying other cases of 3D basin wave-propagation effects. Selection of scenarios is guided by the Uniform California Earthquake Rupture Forecast, as well as results from the CyberShake project. CyberShake computes synthetic seismograms at selected sites (using a 3D model and an exhaustive set of possible sources), the results of which can be interrogated to identify source/site combinations with high basin-wave excitation.

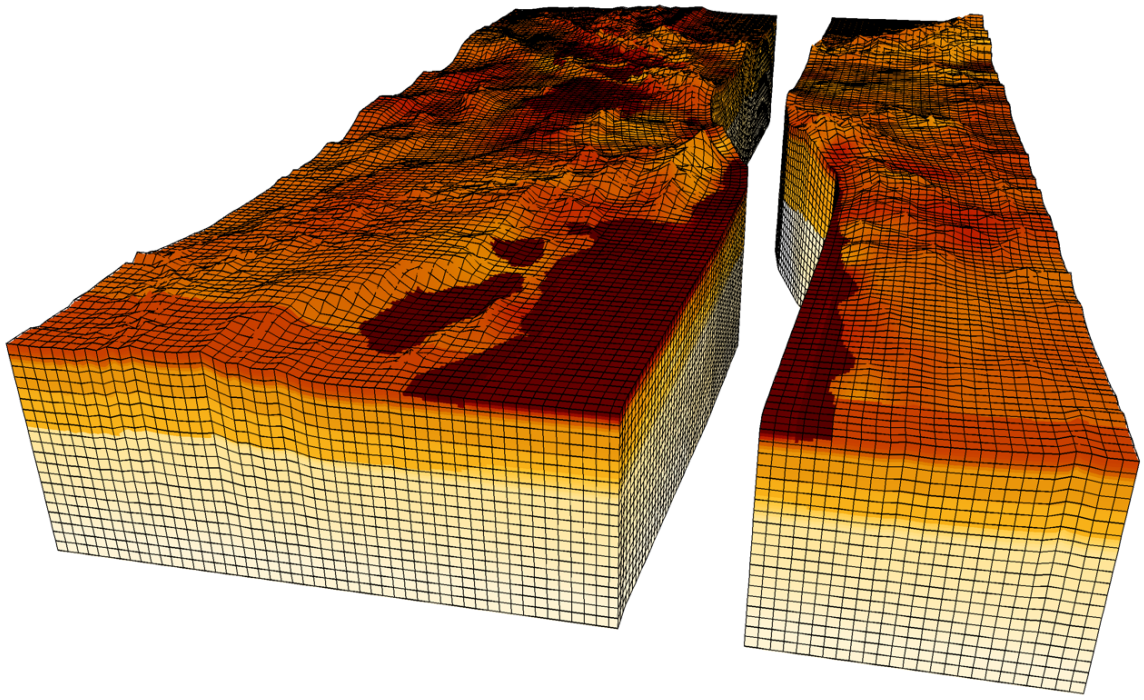

Earthquake Early Warning System in Japan

Shigeki Horiuchi and Hiromitsu Nakamura (NIED, Japan)

We have developed an automatic system for earthquake early warning (EEW) by using Hi-net composed of 800 seismic stations. It determines hypocenter location and magnitude within a few seconds. Our system was installed in JMA who started the practical service of EEW by TV and radio on October, 2007. The followings are the methods and results.

(1) Our automatic system locates hypocenter when more than two stations detect P wave arrival by the use of T^{now}. It has a function to discriminate erroneous arrival times in a case when there are no solutions satisfying T^{now}. This function is very effective for the reliable hypocenter location. It determined hypocenter parameters for about 2,500 events with magnitude larger than 3.0 in a period from May 2005 to May 2008. It is found that 99% of them are nearly correct.

We introduced shaking intensity magnitude in addition to the moment magnitude so as to estimate more reliable shaking intensity. The comparison of estimation errors of shaking intensity by both magnitudes shows that the shaking intensity magnitude decreases estimation errors by 22 %. It is also shown that shaking intensity magnitude can estimate shaking intensity more quickly than the ordinary moment magnitude for events larger than 7. These indicate that the shaking intensity magnitude is effective for the reliable shaking intensity estimation.

We developed a method to estimate hypocentral distance by the use of P wave waveform of single station. Considering that frequencies are higher than 30 Hz, where there is a large amplitude decay by Q for events less than a several ten km, we put an empirical equation determining hypocentral distance using amplitude ratios of high frequency (30Hz) and that of low frequency. As shown in Fig.1, use of high frequency amplitude is effective for the distance estimation.

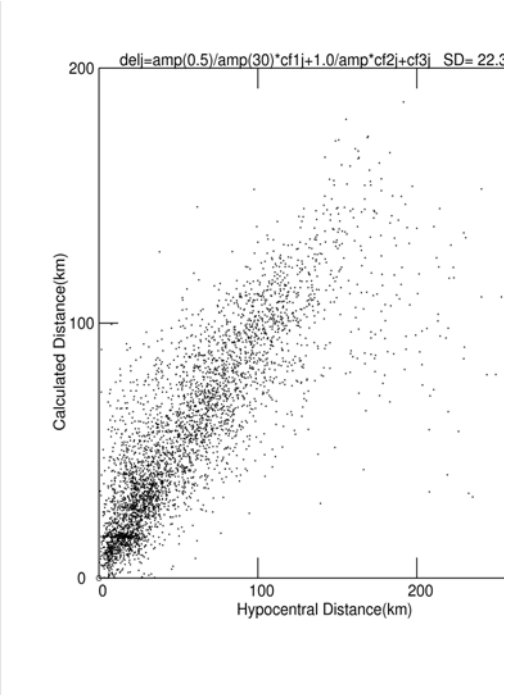

Fig.1 Comparison between observed hypocentral distances and those by the empirical equation.

GSI's Urgent Countermeasure Activities Against Earthquake Disaster

Kenji KINOSHITA, Takashi HARANO, Hiroshi MASAHARU and Tetsuro IMAKIIRE
Geographical Survey Institute (GSI)

Disaster mitigation and disaster management including urgent countermeasures are one of the most important roles of a government. Geographical Survey Institute (GSI) is a governmental agency responsible for surveying and mapping of Japan and is also nominated as one of the “Designated Administrative Organizations” in national level based on “Disaster Countermeasures Basic Act.” This is because basic geospatial data GSI possesses are indispensable for disaster countermeasures and crustal deformation data obtained by repeated surveys and continuous GPS observing stations GEONET are fundamental for monitoring and analyzing earthquake and volcano related phenomena.

In this presentation, we show several types of urgent disaster countermeasure activities of GSI particularly against earthquakes. These activities may be classified into four categories: (1) provision of maps and geospatial information to related public organizations, (2) information gathering and arrangement, (3) grasping crustal deformation caused by the earthquake for clarifying its characteristics, and (4) participating in meetings of government organizations at several levels.

As for item (1), GSI sends image files of compiled topographic maps covering disaster areas on-line to the Prime Minister’s residence and other agencies within one hour after the earthquake. It also sends stock printed topographic maps covering the areas to related organizations of both central and local governments within a day and provides newly arranged printed maps on a scale of 1:30,000 within one or two days. As for item (2), GSI provides a general disaster map by collecting damage information from various sources, mainly mass media and sets up a website to put disaster or damage information from related organizations on a unified web map. GSI also surveys the disaster situation by aerial photographing and field survey. After taking aerial photos, many staff members execute photo interpretation to find and plot disasters and damages on a map. Item (3) grasping crustal deformation is one of the most important and expected GSI’s roles. Within about three hours, the coseismic movement vector diagram observed by GEONET is provided. Earthquake fault models are calculated based on the displacement vectors observed by GEONET. In order to carry out SAR interferometry analysis, data requests are sent to space agencies. GSI provides these data and information to disaster countermeasure meetings of governments (item (4)).

GSI contributes to urgent countermeasure activities of the central and local governments through provision of information. We continue to try improving effectiveness of our activities.

Provision of Topographic Maps to related organizations

(1/30,000)

(1/200,000)

These maps are utilized at the field office of the government

Aerial Photographing

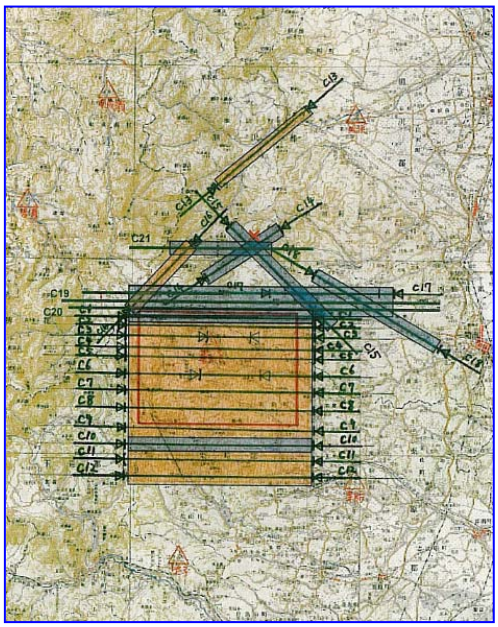

Area of Aerial Photograph

June 15～17

June 18

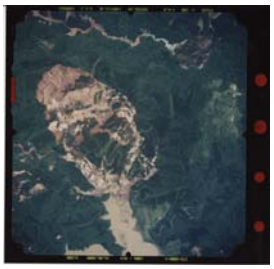

Aerial photo

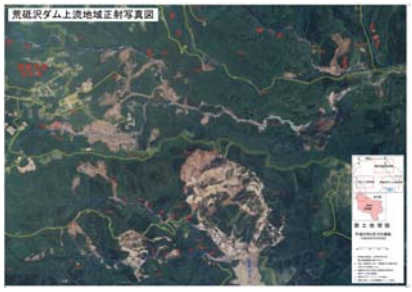

Orthophoto map

Landslide（Upper stream of Aratozawa Dam）

The Potential for Seafloor Based Earthquake Early Warning in Subduction Zones

Jeff McGuire (WHOI), John Collins (WHOI), and Frederick Simons (Princeton University)

Earthquake Early Warning (EEW) algorithms estimate the magnitude of an underway rupture from the first few seconds of the *P*-wave to allow hazard assessment and mitigation before the *S*-wave arrival. Many large subduction-zone earthquakes initiate 50–150 km offshore, potentially allowing seafloor instruments sufficient time to identify large ruptures before the *S*-waves reach land. We tested an EEW algorithm using accelerograms recorded offshore Hokkaido by JAMSTEC in the region of the 2003 M_w 8.1 Tokachi-Oki earthquake and its aftershocks. A wavelet transform of the first ~4 s of the *P*-wave concentrates information about earthquake magnitude from both waveform amplitude and frequency content. We find that wavelets with support of a few seconds provide discriminants for EEW that are both accurate enough to be useful and superior to peak acceleration or peak velocity. Additionally, we observe a scaling of wavelet coefficient magnitude above M_w 6.0 indicating that, at least for the mainshock (M_w 8.1), and largest aftershock (M_w 7.1), the final size of a rupture could have been estimated from the initial portion of the seismogram. Moreover, at least for the Tokachi-Oki event, this size estimate was available from the seafloor data before strong shaking began on land.

The WHOI Ocean Bottom Seismometer (OBS) group recently deployed two seafloor based seismic observatory systems that are successful prototypes for a potential warning system in the offshore region of the Cascadia subduction zone. In 2004/2005, a WHOI OBS was the primary data source for a WHOI-designed, moored-buoy observatory that operated successfully for 1 year at a site west of Vancouver Island [Frye et al., 2006]. An acoustic modem provided communication between the OBS and the buoy, and the link from buoy to shore was over an Iridium satellite link. Low-sample rate seismic data were telemetered on a schedule, and high-rate data (up to 40 Hz) was telemetered on the basis of user-initiated requests. The throughput from OBS to shore amounted to about 0.75 Mbytes/day.

In 2006/2007, WHOI designed and built a cable-based seafloor seismic station for Lighthouse R&D Enterprises, and helped deploy the system 90 km offshore in the Gulf of Oman at a water depth of 1,300 m. This station is equipped with a buried broadband seismometer, strong-motion accelerometer, and Paroscientific depth sensor. All of the data are telemetered ashore in real-time over a dedicated fiber-optic cable to a shore station in Oman. This system has now been running successfully for over a year.

An acoustically-linked observatory suffers from low data throughput (< ~5 kbits/s through water) and by the need for the seafloor instrumentation to have autonomous power and timing. A cable-based observatory is attractive in that it provides power, timing, and ideal telemetry, but seafloor cables are very expensive to permit and lay. Recently, the WHOI buoy group developed an electro-optical-mechanical (EOM) mooring. A prototype system was successfully operated for 13 months offshore Monterey, CA in water depth of 3000 m. The EOM buoy provides power and timing to seafloor instrumentation, and high-speed telemetry between the seafloor and buoy. Telemetry between the buoy and shore is via satellite. Broadcast of a warning derived from running EEW algorithms on the realtime data delivered to the buoy is likely to be achievable with minimal latency. Moreover, recently deployed

satellite telemetry systems allow continuous telemetry at hundreds of kbits/s at moderate tariffs and power requirements. Thus, EOM buoys offer the possibility of near realtime telemetry from the seafloor to shore.

Earthquake Information for Disaster Mitigation in Japan

Makoto Saito,
Earthquake Prediction Information Division, Seismological and Volcanological Department,
Japan Meteorological Agency, msaito@met.kishou.go.jp

Constant and steady efforts have been made in Japan to mitigate earthquake and tsunami disaster, as one of the most important national programs. Japan Meteorological Agency (JMA) is the governmental organization that is responsible for various information issuance on earthquakes and tsunamis, such as Earthquake Early Warning (EEW), tsunami warning and earthquake prediction information of Tokai Earthquake.

When an earthquake takes place, JMA issues series of earthquake information and, if necessary, tsunami warning whose magnitude exceeds the information dissemination criteria. First, JMA issues EEW to the limited users, in several seconds after seismic wave detected at the nearest seismograph from the hypocenter, when the estimated magnitude is grater than 3.5 or predicted seismic intensity is 3 or grater in JMA scale. If predicted seismic intensity is 5 lower or grater, JMA issues EEW to general public via TV and radio according to the Meteorological Service Law. Then JMA issues seismic intensity information in 2 minutes after earthquake occurrence, when observed seismic intensity is 3 or grater in JMA scale. This information is used as a trigger of emergency action taken by disaster prevention organizations. If a tsunamigenic earthquake occurs, JMA issues tsunami warning or tsunami advisory in 2 or 3 minutes after earthquake occurrence based on the database storing tsunami heights and arrival times calculated by numerical simulation. Regarding the Tokai Earthquake with magnitude 8, which is expected to occur in near future at the boundary between Philippine Sea plate and the continental plate, JMA monitors crustal activity by deploying dense network of strainmeters around this region and issues the earthquake prediction information if a slow fault movement thought to be a precursory change of the Tokai Earthquake is detected. JMA has been developing and improving information to be used effectively by related organizations.

In particular, JMA has developed the EEW technology to enable countermeasures against strong motion in cooperation with “Railway Technical Research Institute” and “National Research Institute for Earth Science and Disaster Prevention. The technique consists of quick estimation of hypocenter and magnitude only by the initial portion of seismic wave observed at the stations close to the epicenter. Hence JMA can issue warning before the strong shaking arrival. The dissemination of this innovative information (warning) to the public has started in October 2007. On the Iwate-Miyagi Nairiku Earthquake in 2008 (June 14th 2008), JMA issued an EEW via TV, Radio and other means. In areas near the epicenter, the warning was not in time for evacuation, but in other areas beyond 30km of epicenter many people and organizations could take actions using this warning.

SESSION IV

ABSTRACTS

Structure, Composition and Mechanical Behavior of the San Andreas Fault in central California: Recent Results from SAFOD Downhole Measurements and Core Analyses

Stephen Hickman[1], Mark Zoback[2], William Ellsworth[1], Judith Chester[3], Fred Chester[3], Jim Evans[4], Diane Moore[1], David Kirschner[5], Naomi Boness[6], Thomas Wiersberg[7], Jörg Erzinger[7], Anja Schleicher[8], Ben van der Pluijm[8], John Solum[9]

[1]U.S. Geological Survey (hickman@usgs.gov), [2]Stanford Univ., [3]Texas A&M Univ., [4]Utah State Univ., [5]Saint Louis Univ., [6]Chevron Energy Tech. Co., [7]GeoForschungsZentrum-Germany, [8]Univ. Michigan, [9]Shell Exploration & Production Co.

The San Andreas Fault Observatory at Depth (SAFOD) was drilled to study the physical and chemical processes controlling faulting and earthquake generation along an active, plate-bounding fault at depth. SAFOD is located near Parkfield, California, and penetrates a section of the fault that is moving through a combination of microearthquakes and creep (Figure 1a). In 2004 and 2005, SAFOD was drilled vertically to a depth of 1.5 km and then deviated across the San Andreas Fault Zone to a vertical depth of 3.1 km. In 2007, cores were acquired from holes branching off the main hole to sample directly the country rock and active fault traces.

Geophysical logs define the San Andreas Fault Zone to be about 200 m wide, containing several zones only 2-3 m wide with very low P- and S-wave velocities and low resistivity. Two of these zones have progressively deformed the cemented well casing at measured depths of 3194 m and 3301 m (corresponding to vertical depths of 2.6 - 2.7 km), indicating that they are actively creeping shear zones. Talc and serpentine discovered in drill cuttings associated with the deepest casing deformation zone may be responsible for the anomalously low shear strength and predominantly creeping behavior of the San Andreas Fault at this location. Hydrous clay minerals found as thin-film coatings on polished slip surfaces in cuttings may also be important in controlling fault strength and stability of sliding. There are no indications of anomalous pore pressure within the fault; instead, the fault separates distinct hydrologic regimes, with elevated pore pressure and different geochemical signatures on the northeast side of the fault.

Core was obtained in 2007 across the active deformation zones at 3194 and 3301 m and from just outside the geologically defined San Andreas Fault Zone. Cores crossing the two deformation zones are composed of shales, siltstones and mudstones and contain 1-2 m of a highly foliated, relatively incohesive fault gouge (Figure 1 b). In both cases, this fault gouge exactly correlates in depth with casing deformation and, thus, represents the actively creeping traces of the San Andreas Fault at depth. This fault gouge has an anomalous mineralogy with respect to the adjacent country rock in that it contains veined serpentinite bodies, serpentinite porphyroclasts and an ordered chlorite/smectite phase. Pervasive shearing within the gouge is indicated by anastomozing, slickensided surfaces (Figure 1c), with authigenic clay mineralogy and host-grain/clay microstructures suggestive of extensive fluid-rock interaction and dissolution-precipitation creep. Brecciation and cataclasis in some shales and siltstones associated with these deformation zones as well as in sandstones from the southwest side of the currently active fault may be indicative of past seismogenic faulting and/or cataclastic creep. These cores are now being tested in laboratories at a number of institutions around the

world to study their composition, deformation mechanisms, physical properties and rheological behavior.

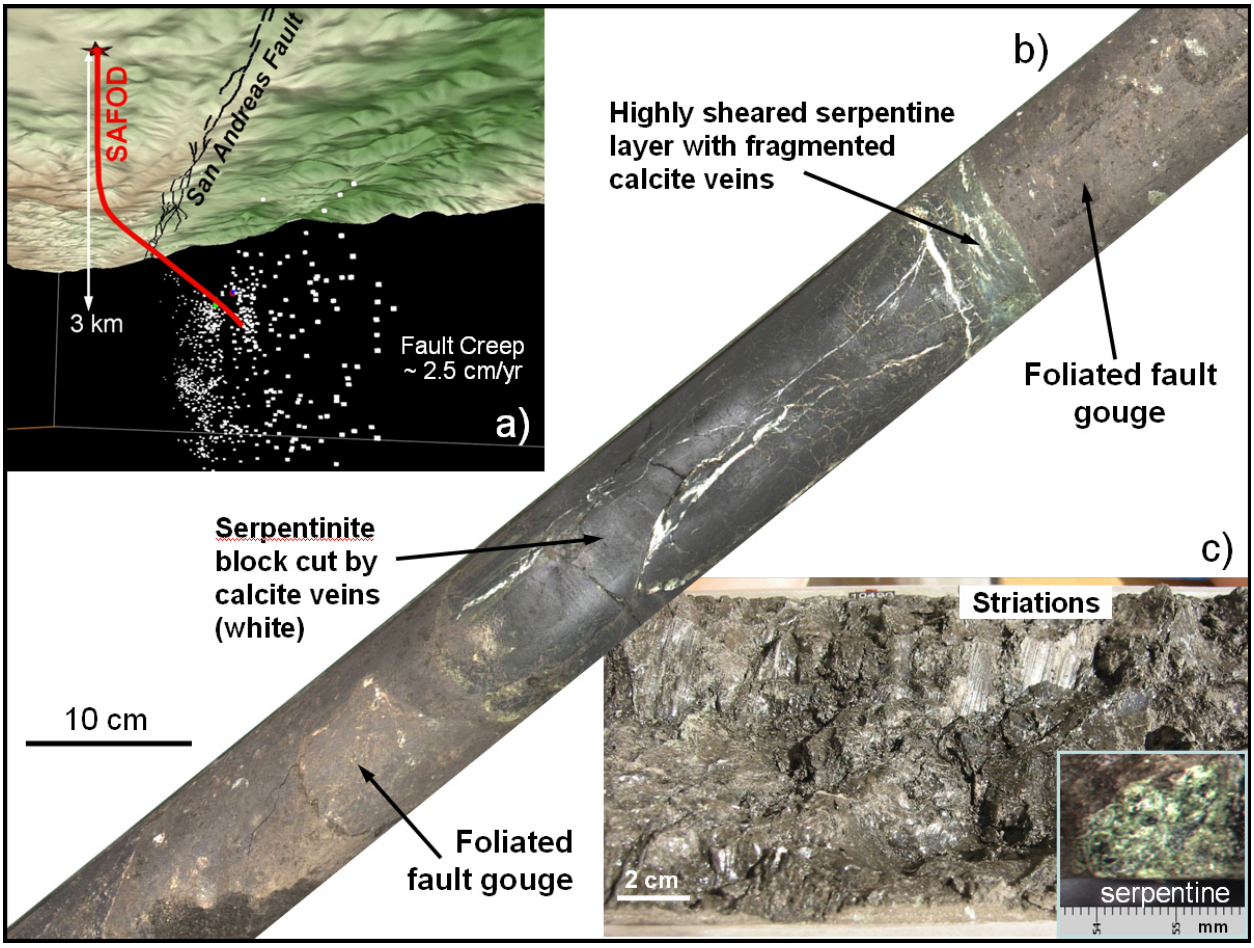

Figure 1. a) Seismicity of the San Andreas Fault as seen from a vantage point in the earth looking to the northwest. Hypocenters of microearthquakes (white dots) were determined by Haijiang Zhang and Cliff Thurber (Univ. Wisconsin) utilizing data from the Parkfield Area Seismic Observatory, supplemented by data from local USGS and U.C. Berkeley network stations. The SAFOD borehole is shown in red, extending downward from the surface facility (star). The surface trace of the fault is shown in black draped over the topography (3-D EarthVision plot by Luke Blair, USGS). b) Photograph of the SAFOD core obtained in 2007 from the casing deformation zone (active fault) at a measured depth of 3194 m, showing serpentinite block surrounded by a foliated fault gouge. c) Close up of foliated fault gouge from split core section immediately below core shown in Figure 1b, illustrating highly sheared internal structure with anastomozing, slickensided surfaces (see striations labeled in photograph) and serpentine porphyroclast (inset).

Detailed Distribution and Activity of
Small Repeating Earthquakes at the Kanto Region, central Japan

Hisanori Kimura[1], Tetsuya Takeda[1], Yohei Yukutake[2], Kazushige Obara[1], Keiji Kasahara[3]
1 National Research Institute for Earth Science and Disaster Prevention, Japan
2 Hot Spring Institute of Kanagawa Prefecture, Japan
3 Earthquake Research Institute, University of Tokyo, Japan
kimura@bosai.go.jp

At the Kanto region, the Philippine Sea plate (PHS) and the Pacific plate (PAC) are subducting, where numerous repeating earthquakes were found, based on waveform similarity analysis of seismograms recorded by Kanto-Tokai network (1979-2003) (Kimura et al., 2003; 2006) and a portion of Hi-net data (2003-) of National Research Institute for Earth Science and Disaster Prevention (NIED) (Kimura et al., 2007). Highly similarity of seismograms shows that repeating earthquakes at Kanto can be regarded as repetition of rupture at the same fault and can be regarded as an indicator of relative plate motion, the same as at other regions (Nadeau et al., 1995; Igarashi et al., 2003; Matsubara et al., 2005). To understand detailed configuration and interaction of plates, we studied detailed distribution and activity of repeating earthquakes.

We determined high-precision relative hypocenter distribution by Double-Difference method (Waldhauser and Ellsworth, 2000) with waveform correlation for seismic clusters of the PHS and PAC and obtained detailed hypocentral distribution near the plate boundary. Most M3-class repeating earthquakes are located within 40 m and 140 m, at largest, for the PHS and the PAC, respectively. Larger distances for the PAC would be caused by location of the target region at the edge of the seismographic network. Considering fault size of used events, they are likely to occur at the same location.

Hereafter, we will explain about results from two distinctive seismic clusters. At the southwestern Ibaraki, north of Kanto, significant linearly distributing seismic clusters are observed and repeating earthquakes also occur (Fig. 1). Repeating earthquakes are distributed along a plane and its dip angle is almost the same with a dip angle of low-angle nodal plane of focal mechanism of repeating earthquakes. Dip angles of seismic plane are 36° and 26° for northern and southern part of the cluster, respectively. Widths of the seismic cluster are 3 km and 6 km for northern and southern part, respectively. The changing locations of dip angle and width are almost the same.

At the other cluster, significant temporal change of activity is observed. Off the Boso Peninsula, southeastern Kanto, activations of repeating earthquakes synchronizing with the Boso slow slip events (SSEs), which repeat with time interval of 5-7 years, were observed. Recurrence time averaged for each sequence of M3-class repeating earthquakes off the Boso Peninsula is 1.5 - 19.4 years with total average of 9.2 years. These events have close relation with SSEs. At offshore region, no repeating earthquakes occurred after the previous SSE on 2002. However, numerous repeating earthquakes occurred synchronizing with the 2007 SSE (Fig. 2). Since repeating earthquakes at Kanto can be regarded as an indicator of plate motion, this result strongly indicates that plate interface is locked between SSEs and interplate slip is accelerated synchronizing with the Boso SSE, causing repeating earthquakes.

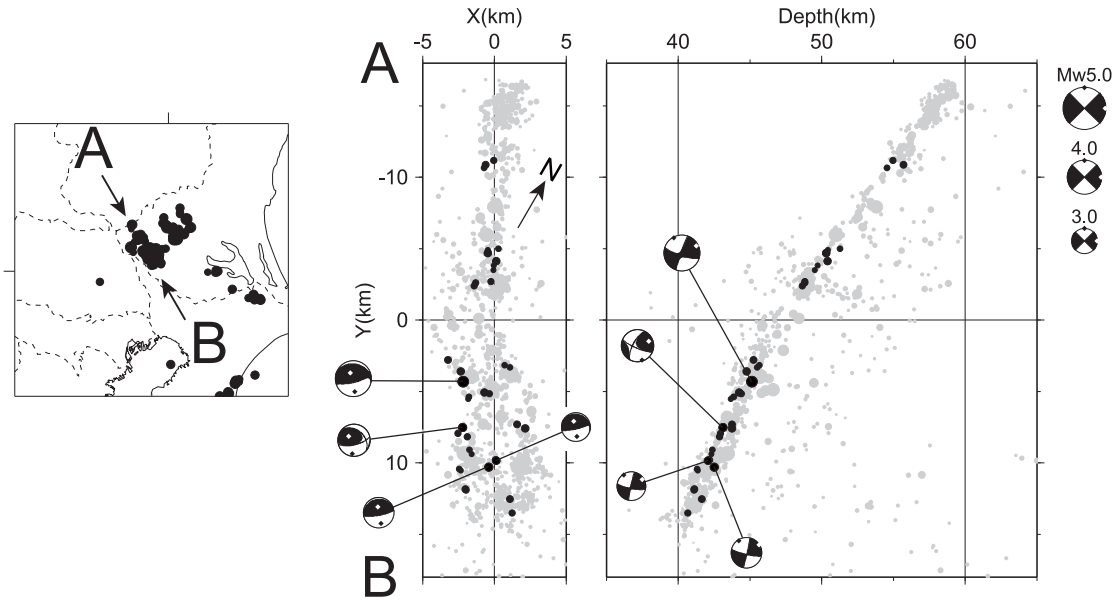

Figure 1 Epicentral distribution of repeating earthquakes on the PHS (left). Vertical cross section and epicentral distribution of repeating (solid circle) and background (gray circle) earthquakes (right). F-net moment tensor solutions of repeating earthquakes are also shown.

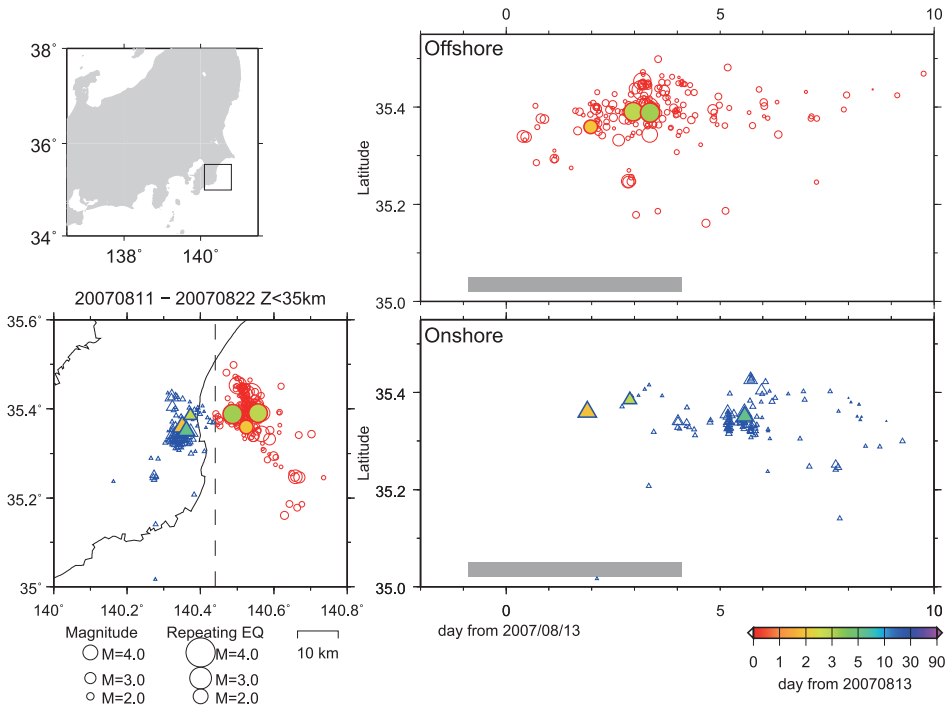

Figure 2 Activity of repeating and background earthquakes synchronized with the 2007 Boso SSE. Map of the target region (upper left), epicentral distribution (lower left), and space-time plot projected to N-S direction (right panels) are shown. Events at onshore and offshore regions are denoted by blue triangles and red circles, respectively. Gray thick line represents period of transient crustal tilt change (Sekine et al., 2007).

What can we Learn About Frictional Properties of Faults from Postseismic Earthquake Studies?

Kaj M. Johnson[1], Junichi Fukuda[1], Shinichi Miyazaki[2], and Paul Segall[3]
[1]Indiana University, [2]University of Tokyo, [3]Stanford University

Current afterslip modeling efforts in the geodetic community are moving away from a purely kinematic approach, in which slip is estimated using standard inversion methods, towards dynamic models that incorporate stress boundary conditions and fault rheology. A common approach is to model geodetic postseismic time-series data with single-degree-of-freedom spring-slider models with a friction law prescribed at the base of the slider and an imposed sudden displacement of the spring to represent an earthquake. An increasingly popular approach to modeling afterslip with a continuum fault is to impose a velocity-strengthening rheology on a fault in an elastic half-space, subject the fault to a sudden change in stress due to imposed distribution of coseismic slip, and use boundary element techniques to solve for the evolution of afterslip.

The friction parameter $\sigma(a-b)$ inferred below seismogenic depths using these types of models and GPS postseismic time series data for a number of earthquakes are surprisingly similar and typically in the range 0.1-0.5 MPa. This is about an order of magnitude lower than would be expected on faults at hydrostatic pore pressures suggesting either that pore pressure is elevated above hydrostatic on faults or that a-b is smaller for real faults than in the laboratory.

However, there are limitations of both of these modeling approaches. The spring-slider models assume slip occurs at a point and neglects the effect of an expanding afterslip zone. The velocity strengthening models neglect the state evolution effect incorporated in rate-and-state friction. Both models assume initial conditions on the fault immediately after the earthquake can be determined from steady-state sliding before the earthquake. Both models assume the earthquake can be imposed instantaneously and that the instantaneous velocity after the earthquake can be determined from the instantaneous stress change.

We show that some of the assumptions are questionable in the context of a model for 1D fault with earthquake cycles controlled by rate-and-state-dependent friction. We compare results from the two afterslip models with the postseismic phase of slip in the 1D rate-state friction models. We find that effect of state evolution on the fault as the afterslip zone expands and propagates into the velocity strengthening region is a significant factor in the rate of postseismic moment release on the fault. Models that neglect state evolution during afterslip may lead to misestimates of friction parameters using real data if the critical slip distance in the rate-state formulation is of order 1 mm or larger. We also find that assuming steady-state sliding before the earthquake and imposing sudden coseismic slip leads to underestimates of the amount of postseismic slip surrounding coseismic rupture because the initial sliding velocity is too low. Models assuming velocity-strengthening friction may lead to underestimates of postseismic slip or overestimates of the amount of coseismic slip needed to drive afterslip.

We utilize the 1D fault model to estimate the rate of propagation of the afterslip front into the velocity-strengthening region of the fault and compare with surface creep measurements following the 2004 Parkfield, CA earthquake. The creep meters show that slip on the fault at the

surface is delayed 1-2 hours after the time of the earthquake (Figure 1). This 1-2 hour delay constrains the critical slip distance on the fault to be about 1 mm.

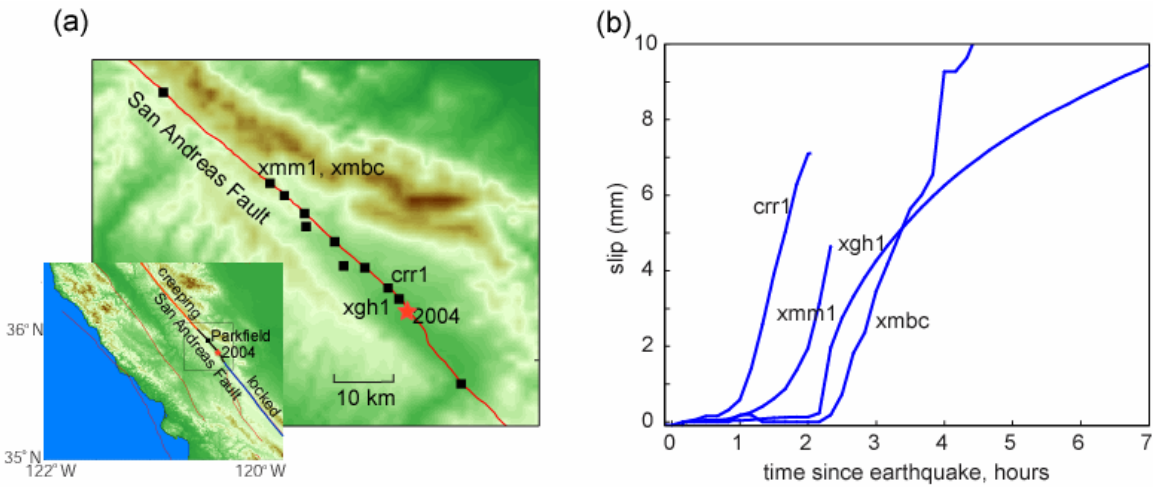

Figure 1. (a) Location of 2004 Parkfield earthquake. (b) Creepmeter records (10 minute samples) at sites spanning the fault and labeled in (a).

Micro-, Nano- and Picoearthquakes: Implications for Fault Friction and Fault Mechanics

By William L. Ellsworth [1.] and Kazutoshi Imanishi [2.]
1. US Geological Survey, Menlo Park, CA USA
2. Geological Survey of Japan, A.I.S.T. Tsukuba, Japan

The deployment of instrumentation within seismically active crustal rocks in deep boreholes and mines has opened a new window for the study of the earthquake source. Advances in both sensors and high-temperature electronics enable recording of seismic waves over a very broad frequency spectrum (D.C. to several KHz) and amplitude spectrum (Earth noise floor to several g acceleration) in these challenging underground environments. By reducing the distance between source and receiver to a few hundred meters or less, it becomes possible to observe dynamic processes on space and time scales that approach those of laboratory experiments. Key questions that can be addressed in the near-source region include scaling of apparent stress and static stress drop, the minimum size of earthquakes, and the time, length and displacement scales of frictional evolution during nucleation.

Earthquake source parameters determined using a variety of methods indicate that there is no breakdown in apparent stress or stress drop scaling for Mw > 0. Within any magnitude band, stress drops range between 0.1 and 100 MPa. The highest values are comparable to the laboratory-derived frictional strength of faults.

Using deep borehole seismometers in the main hole of the San Andreas Fault Observatory at Depth (SAFOD) and in the Long Valley Exploratory Well (LVEW) in the center of Long Valley Caldera, CA, we have observed earthquakes at the lowest limit of magnitude detection (currently Mw -3.5 at SAFOD). The smallest events have source dimensions < 1 m, indicating that if there is a minimum earthquake size, it must lie at lower magnitude and spatial scales. Mean displacements in the smallest events are on the order of 100 microns, suggesting that the displacement weakening distance is smaller still. The rate of fault weakening can be studied using the earliest part of the P-wave arrival. We apply Kostrov's 1964 model for self-similar crack growth to determine the dynamic stress drop. For earthquake sources at distances of less than 1 km, we find no evidence for a slow initiation process. Instead, these earthquakes begin abruptly with the dynamic stress drop typically reaching 5 MPa within the first few milliseconds of rupture. These results suggest that displacement weakening distances are small, comparable to values measured in the laboratory.

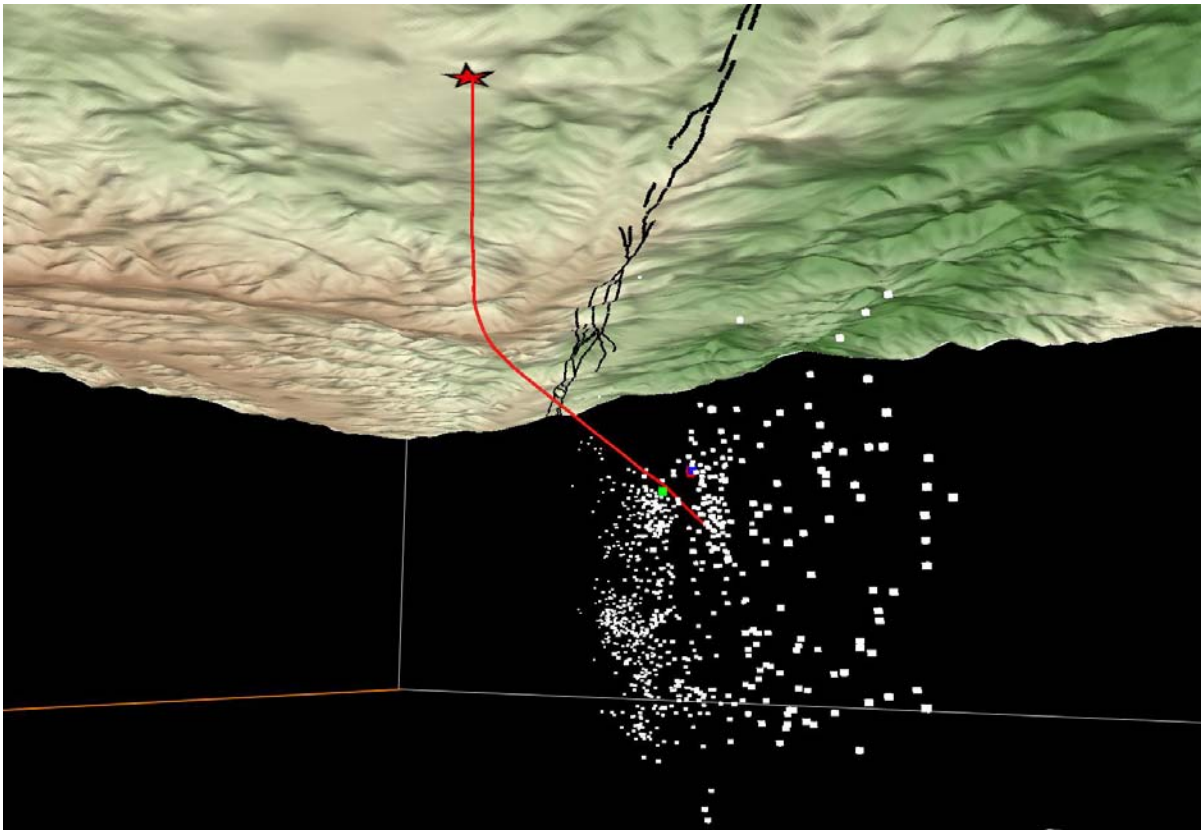

Figure 1. The San Andreas Fault Observatory at Depth Main Hole (red star) follows a diagonal path from the Pacific to North American Plate, intersecting the seismically active fault (squares) at approximately 3 km depth. View is from below, with the surface trace of the fault (black) and surface topography shown. The SAFOD target earthquakes include the "San Francisco" (red), "Los Angeles" (blue) and "Hawaii" (green) repeating earthquakes. Illustration by Luke Blair (USGS).

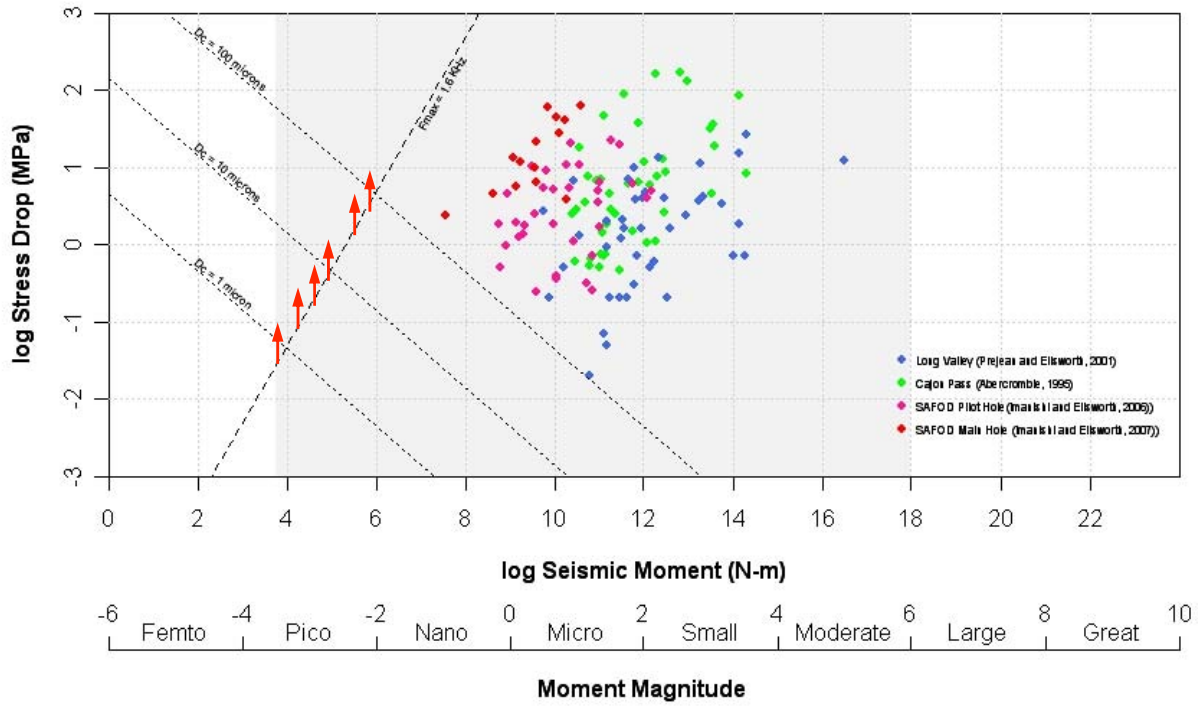

Figure 2. Stress drop scaling diagram showing measurements from deep boreholes in California. Nano- and picoearthquakes recorded in the SAFOD Main Hole have corner frequencies higher than the maximum frequency observable (1.6 KHz) and consequently must have stress drops above the scaling line indicated by red arrows. Scaling lines for mean slip in hypothetical minimum earthquakes are shown for several values of the displacement weakening distance, Dc. Shaded area corresponds to range of earthquakes observed at SAFOD to date.

Monitoring Rupture Process of Giant Earthquakes Using the Japanese Hi-net Array

Miaki Ishii[1], Eric Kiser[1] & Peter M. Shearer[2]
1 Dept. Earth & Planetary Sciences, Harvard University, Cambridge, MA
2 Scripps Institution of Oceanography, University of California, San Diego, La Jolla, CA

The High Sensitivity Seismograph Network (Hi-net) is one of the world's finest seismographic networks, consisting of more than 700 stations distributed throughout Japan. Its borehole instrumentation ensures high-quality data, and provides an opportunity for investigating characteristics of earthquakes in detail. We take advantage of this dense network, and empirically back-project the recorded seismograms to regions around the hypocentre. This is computationally very inexpensive, and provides estimates of the spatiotemporal variations in relative energy radiation which can be used to infer various characteristics of the event. One appealing feature of the back-projection approach for studying earthquake characteristics is that it can be performed in near realtime, as soon as the first-arriving seismic waves are recorded at the Hi-net stations. The back-projection method has been applied successfully to the series of giant earthquakes along the Sumatran-Sunda subduction zone (Figure 1). Estimates of the magnitude, rupture speed, duration, extent, direction, area, and spatiotemporal variations are obtained for each event. The rupture areas lie next to one another along the trench, and agree well with slip areas of historical earthquakes. They also highlight a large gap in slip around Siberut island where a large earthquake in 1797 with estimated magnitude of 8.8 caused much damage at Padang, the capital and largest city of West Sumatra. Since October 2000 when the Hi-net data became available, there have been more than 20 earthquakes with magnitude greater than 7.8 that are good candidates to be studied using the back-projection method. Unlike the Sumatran earthquakes, many of these earthquakes have slip planes that are not subhorizontal.
The resolution in depth is extremely poor using only the P waveform, but it can be improved if depth phases, i.e., pP and sP, are included in the analysis. We investigate the characteristics of giant earthquakes and explore the capabilities and limitations of the back-projection technique with combination of different phases. The resolvability of rupture depends on the source location with respect to Japan and availability of depth phases.

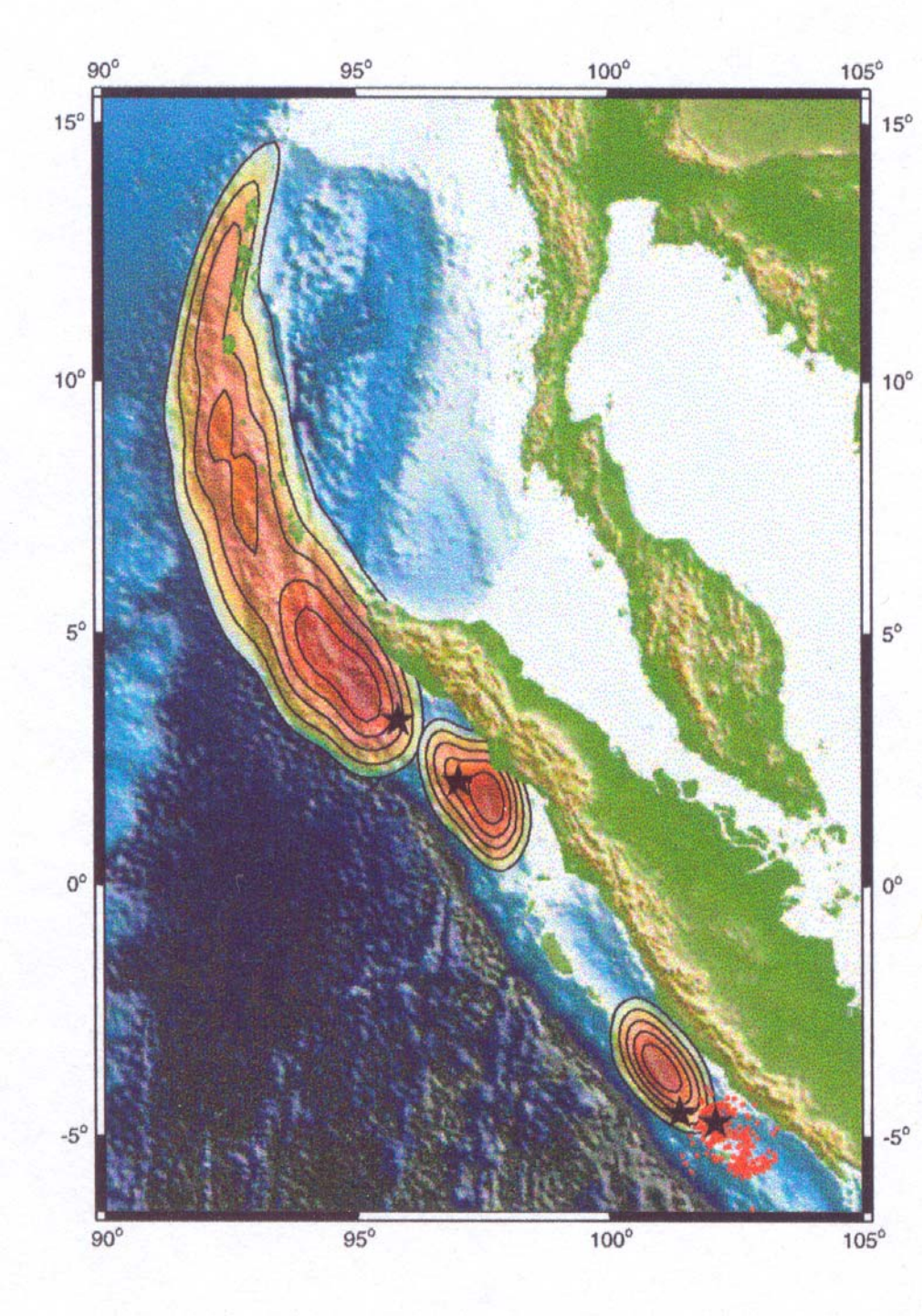

Figure 1: Spatial Variations in Earthquake Energy Radiation of the Three Giant Events in the Sumatra Region. Inferred rupture using the data recorded at the Hi-net stations for the 2004 Mw 9.3 Sumatra-Andaman earthquake (contoured red-orange pattern in the northwest), 2005 Mw 8.7 Nias earthquake (contoured red-orange pattern in the middle), and 2007 Mw 8.4 Pagai earthquake (coloured and contoured region in the south). The black stars indicate the epicentral locations. The black star and red dots southeast of the 2007 event are the epicentre and one month of aftershocks associated with the 2000 Mw 7.9 Enganno earthquake, respectively.

Strong Ground Motion Prediction Using the Ambient Seismic Field

Gregory C. Beroza and German A. Prieto

Department of Geophysics, Stanford University, Stanford, CA, 94305-2215, USA

The waves generated by faulting represent the primary threat posed by most earthquakes. Complex geological structure, such as sedimentary basins, can have a controlling influence on the strength and duration of strong ground motion, but it is difficult to model accurately because we lack detailed knowledge of the elastic and anelastic structure of the crust. We demonstrate that it is possible to extract reliable phase and amplitude response, which includes the effects of complex crustal structure, for the elastodynamic Green's function from the ambient seismic field. We demonstrate the approach by predicting complex ground motion for a moderate ($M_w = 4.63$) earthquake in southern California as recorded in the Los Angeles Basin. We compare real earthquake records with ground motions predicted using ambient-noise Green's functions. Both show strong amplification at stations within the basin relative to those "hard rock" sites outside the basin, especially for the horizontal components of motion. A similar result was obtained through numerical simulation for the same earthquake by Graves [2008]. This suggests a novel approach to seismic hazard analysis in which ground motion from hypothetical future earthquakes is simulated directly, without the need for modeling the detailed heterogeneity of the Earth's crust as an intermediate step, at least in the period range of 4-10 seconds. These periods are outside the range of primary engineering interest (0.1 to 1 seconds); however, they are quite important case of structures, such as bridges and very tall buildings, which have fundamental modes of oscillation in that range. Extending the method to shorter periods is an important research direction. One approach is to use ambient-noise Green's functions to improve models of three-dimensional crustal structure, which can be used as input for more accurate simulations of strong ground motion at all frequencies. The ambient-noise approach has the distinct advantage that it is "active," in that seismologists can design experiments to determine station-to-station Green's functions that target areas of particular concern.

SESSION V

ABSTRACTS

How the Continents Deform: The Evidence from Tectonic Geodesy

Wayne Thatcher
U. S. Geological Survey
Menlo Park, California 94025
thatcher@usgs.gov

Space geodesy now provides quantitative maps of the surface velocity field within tectonically active regions, supplying constraints on the spatial distribution of deformation, the forces that drive it, and the brittle and ductile properties of continental lithosphere. Deformation is usefully described as relative motions among elastic blocks and is block-like because major faults are weaker than adjacent intact crust. Despite similarities continental block kinematics differs from global plate tectonics: blocks are much smaller, typically ~100-1000 km in size; departures from block rigidity are sometimes measurable; and blocks evolve over ~1-10 Ma timescales, particularly near their often geometrically irregular boundaries. Quantitatively relating deformation to the forces that drive it requires simplifying assumptions about the strength distribution in the lithosphere. If brittle/elastic crust is strongest, interactions among blocks control the deformation. If ductile lithosphere is the stronger, its flow properties determine the surface deformation and a continuum approach is preferable.

Block modeling of GPS velocity fields worldwide is providing hundreds of new decadal fault slip rate estimates that can be compared with independent Holocene (<10 ka) to late Quaternary (<125 ka) rates obtained by geological methods. A compilation of over 40 available GPS/geologic comparisons shows general agreement but a subset of apparently significant outliers. Some of these outliers have been discussed previously and attributed either to a temporal change in slip rate or systematic error in one of the estimates. I suggest 4 criteria for assessing the differing rates. (1) Is there even-handed evaluation of random and systematic errors? (2) Are rate estimates obtained by more than one geodetic or geologic method? (3) Is proposed rate change mechanism consistent with examples of changes in style and rate of deformation preserved in the geologic record? (4) Is there a quantitative analysis of mechanism proposed to explain rate change?

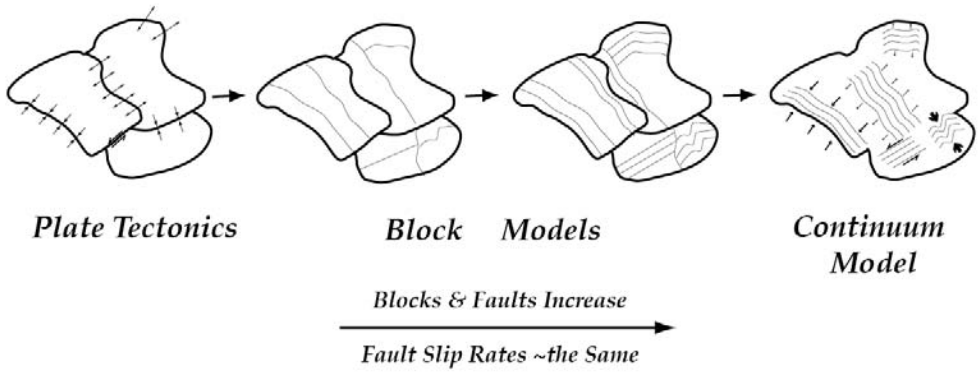

Figure 1: Cartoon showing the transition from global plate kinematics through continental block models to continuum model. Bold lines denote major block boundary faults and thin lines are faults delimiting smaller blocks.

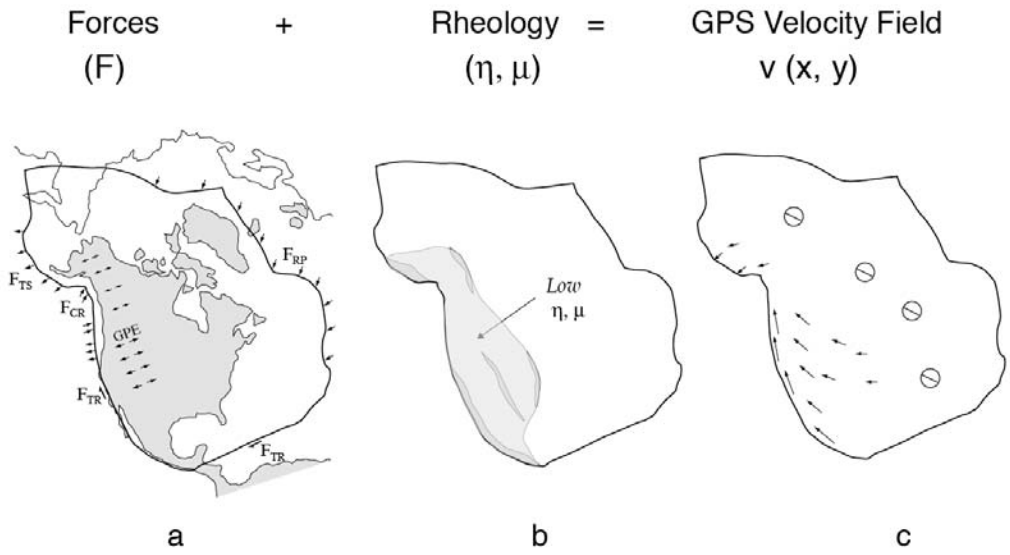

Figure 2: Schematic illustration showing how applied forces and lithospheric rheology determine the GPS velocity field of North American plate. Abbreviations: gravitational potential energy gradients – GPE; collision resistance – F_{CR}; ridge push – F_{RP}; transform resistance - F_{TR}; trench suction – F_{TS}; □ – friction coefficient for crustal faults; □ – viscosity of ductile lithosphere. In Figure 2c arrows are GPS velocities relative to stable North America (screwheads).

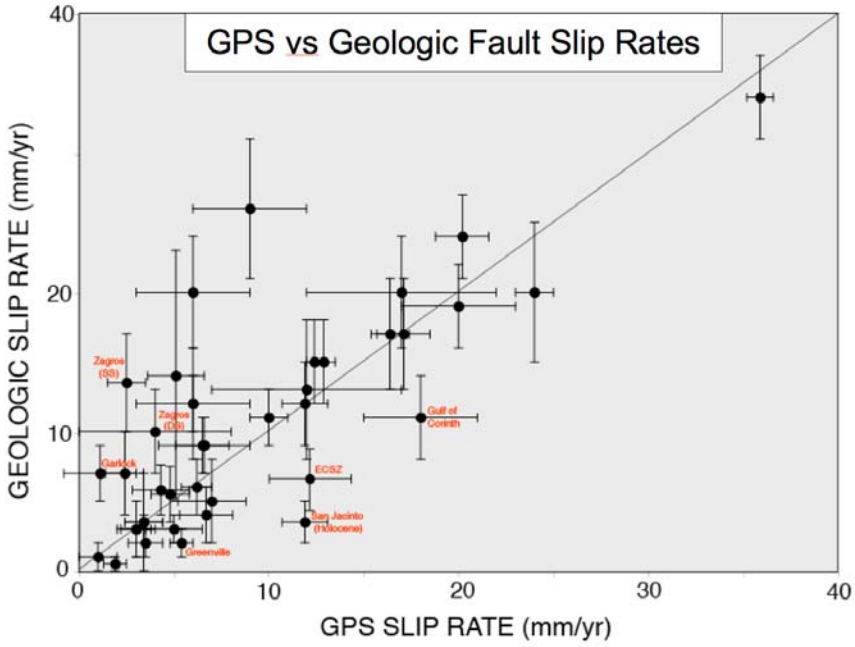

Figure 3: GPS versus geologic slip rates, with 1 SD error bars as assigned by each investigator.

Observation Well Network of Groundwater and Borehole Strain Monitoring for the Prediction Research of the Tonankai and Nankai Earthquakes

Observation well network of groundwater and borehole strain monitoring for the prediction research of the Tonankai and Nankai earthquakes

Norio Matsumoto (n.matsumoto@aist.go.jp), Naoji Koizumi, Makoto Takahashi, Yuichi Kitagawa, Satoshi Itaba, Ryu Ohtani and Tsutomu Sato
Geological Survey of Japan, the National Institute of Advanced Industrial Science and Technology (AIST)

In the past, large earthquakes about magnitude 8 or higher have occurred along the Nankai and Suruga troughs, offshore from central to southwest Japan at intervals of about 90 - 150 years (Ando, 1975). Recent events were the 1944 Tonankai (M 7.9) and the 1946 Nankai (M 8.0) earthquakes along the Nankai trough after 90 - 92 years from the 1854 Ansei Tokai (M 8.4) and the 1854 Ansei Nankai (M 8.4) earthquakes.

Preseismic hydrological anomalies at fifteen wells several days before the 1946 Nankai earthquake were reported by Hydrographic Bureau (1948). The reported phenomena were turbid groundwater, decreases of groundwater level or hot spring discharge. Furthermore, Shigetomi et al. (2005) found several ancient writings that report preseismic decreases of groundwater level before the 1854 Nankai earthquake.

Short-term slow slip events (SSEs) are recursively observed every six months at an adjacent area of the focal zones of the Nankai, Tonankai and Tokai earthquakes (Obara et al., 2004; Hirose and Obara, 2006). The corresponding magnitude and duration of SSEs are about Mw 6.0 and several days, respectively.

We are constructing 12 observation sites in and around focal zones of Nankai, Tonankai and Tokai earthquakes to monitor groundwater and borehole strain (Figure 1). The 30, 200 and 600 m-depth wells are constructed in one observation site. Groundwater level and groundwater temperature will be observed at each well, and the multi-component borehole strainmeter (Ishii's strainmeter or the Gladwin tensor strainmeter) is installed at the bottom of either the 600 m-depth well or the 200-m depth well. We expect to observe groundwater level and/or strain changes associated with the preseismic hydrological anomalies, SSEs, preslips and co- and afterseismic crustal deformation.

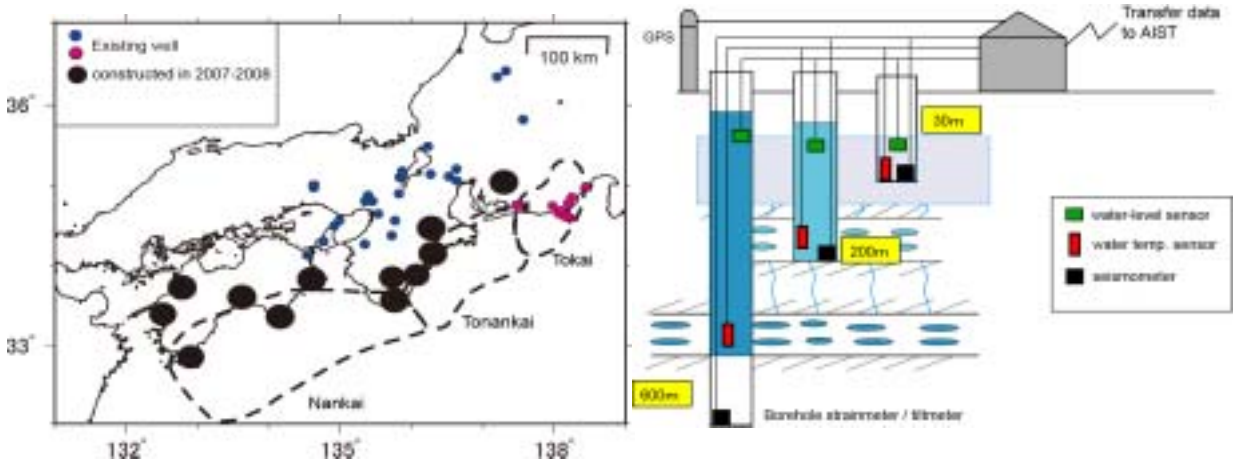

Figure 1 Location and specification of new observation site

Stress Evolution of the San Andreas Fault System: Hindcast Stress Accumulation Models and Stress Rate Uncertainties

Bridget Smith-Konter[1], Teira Solis[1], and David T. Sandwell[2]
[1]University of California at San Diego, La Jolla, CA
[2]The University of Texas at El Paso, El Paso, TX

Major ruptures along transform faults such as the San Andreas Fault System (SAFS) are driven by stress that has accumulated in the upper locked portion of the crust. Interseismic stress rates of the SAFS, derived from the present-day geodetic network spanning the North American-Pacific plate boundary, range from 0.5 - 7 MPa per century (Fig. 1), are inversely proportional to earthquake recurrence intervals (500-20 yrs), and vary as a function of fault locking depth, slip rate, and fault geometry. Hindcast calculations of accumulated stress over several earthquake cycles (Fig. 2), consistent with coseismic stress drops of ~3-8 MPa, also largely depend on the rupture history of a fault over the past few thousand years. These more speculative results indicate that the southern San Andreas, which has not ruptured in a major earthquake in over 300 years, is currently approaching a historically critical stress level.

Substantial uncertainties, however, in paleoseismic slip history, combined with ongoing discrepancies in geologic/geodetic slip rates and variable locking depths throughout the earthquake cycle, can introduce uncertainties in stress rate and in present-day stress accumulation calculations. For example, a number of recent geodetic studies have challenged geologic slip rates along the SAFS, varying by as much as 25% of the total slip budget; geodetically determined locking depths, while within the bounds of seismicity, typically have uncertainties that range from 0.5 - 5 km; uncertainties in paleoseismic chronologies can span several decades, with slip uncertainties on the order of a few meters.

Here we assess the importance of paleoseismic accuracy, variations in slip rates, and basic stress model components using a 3-D semi-analytic time-dependent deformation model of the SAFS. We perform a sensitivity analysis of Coulomb stress rate and present-day accumulated stress with respect to the six primary parameters of our model: slip rate, locking depth, mantle viscosity, elastic plate thickness, coefficient of friction, and slip history. In each case, we calculate a stress derivative with respect to a parameter over the estimated range of uncertainty, as well as any tradeoffs in parameters. Our results suggest that a 25% variation, or exchange, of slip rates between the primary SAFS and faults of the Eastern California Shear Zone (ECSZ) yields a respective decrease (SAFS) and increase (ECSZ) of stress rate by only 0.5 MPa per century. Alternatively, variations in locking depth spanning respective fault depth uncertainties can increase/decrease stress rates by as much as 2-3 MPa per century. We also examine stress accumulation changes based on a suite of plausible historical faulting scenarios; for example, when only 70% of paleoseismic slip events are accounted for in the model, we calculate a ~0.5-3.0 MPa increase in earthquake cycle stress accumulation spanning several segments of the SAFS. Stress variations of these magnitudes have critical implications for seismic hazard analyses given that modeled stress accumulation levels of the southern San Andreas appear to be approaching those of historically great events (~7^{+} MPa).

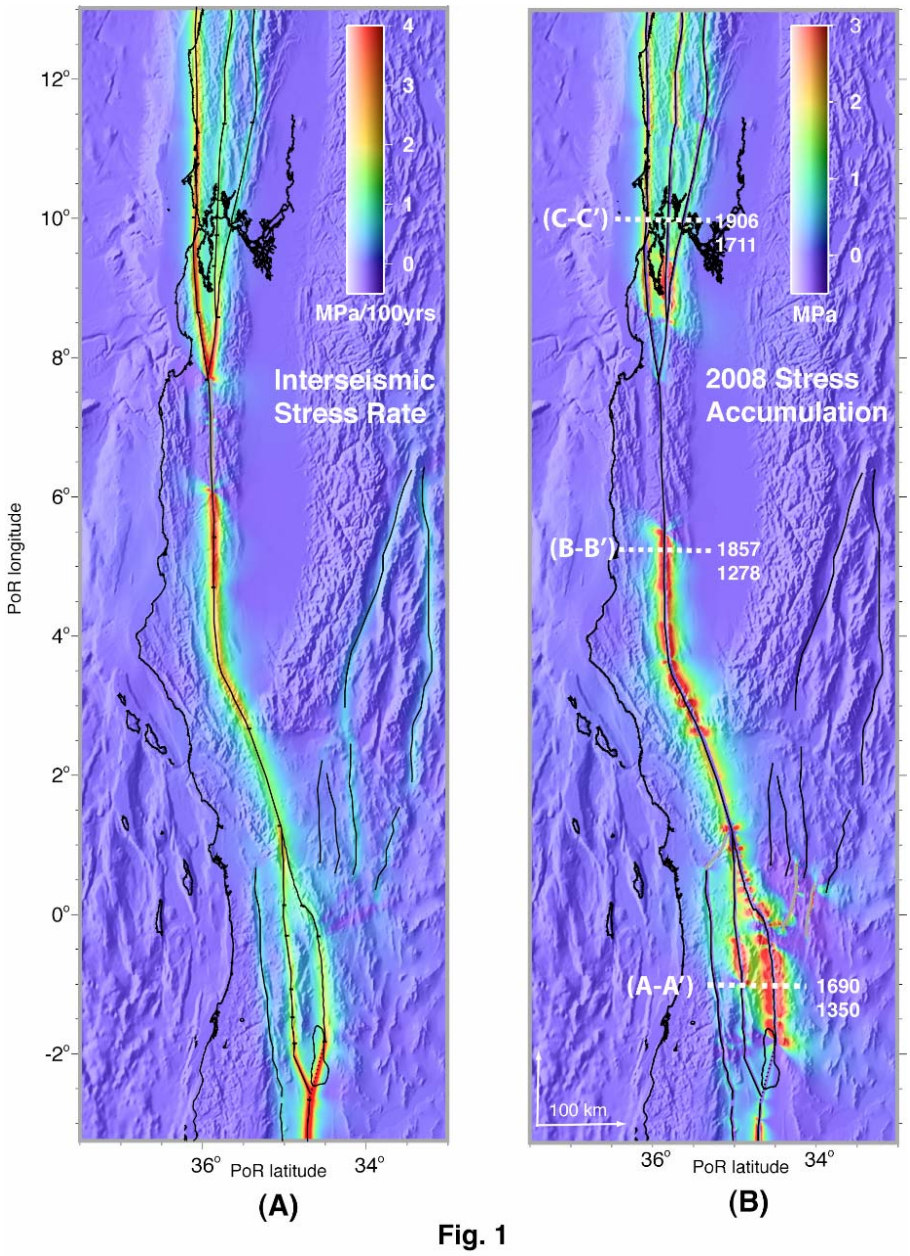

Fig. 1

Fig 1. **(A**) Coulomb stress accumulation rate of the SAFS, evaluated at ½ of the locking depth, in MPa/100 yrs, projected into Pole of Rotation (PoR) coordinate system [*Wdowinski et al*., 2007]. Color scale is saturated at 4 MPa/100yrs. **(B)** Present-day (calendar year 2008) Coulomb stress accumulation of the SAFS based on 75 historical and prehistorical earthquake ruptures. Color scale is saturated at 3 MPa to emphasize significant regions of accumulated stress. White dashed lines represent locations of acquired across-fault model profiles plotted in Fig. 2: (A-A') length-averaged rupture trace of an estimated ~1690 event [*Shifflett et al*., 2002] and regional location of an estimated penultimate event of ~1350 along the Coachella segment [*Sieh and Williams*, 1990]; (B-B') approximate epicenter of the 1857 Fort Tejon earthquake and regional location of an estimated penultimate event of ~1278 [*Young et al*., 2002]; (C-C') approximate epicenter of the 1906 San Francisco earthquake and regional location of an estimated penultimate event of 1711 [*Kelson et al.*, 2006].

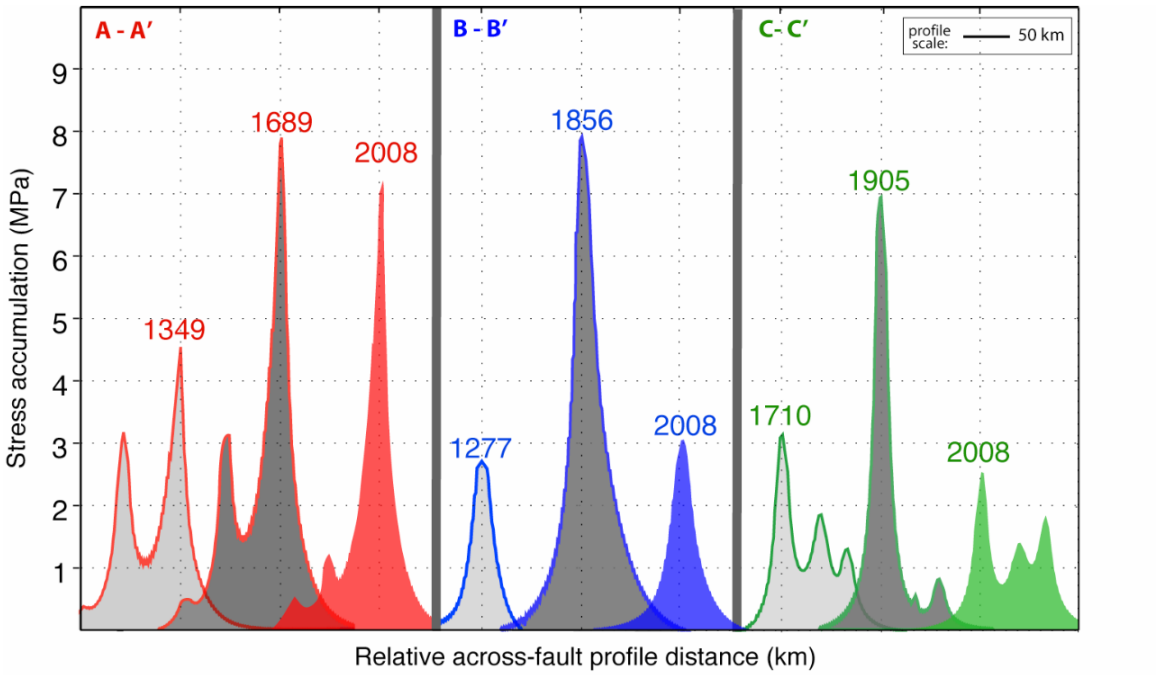

Fig. 2

Fig. 2. Across-fault yearly stress profiles, evaluated at ½ the locking depth, based on historical and prehistorical earthquake activity of the SAFS. Profile A-A' (red) crosses the southern SAFS region; profile B-B' (blue) crosses the central SAFS; profile C-C' (green) crosses the northern SAFS. Stresses are computed for calendar year 2008 (solid color profiles), as well for the years just prior to the most recent event (dark gray fill) and the penultimate event (light gray fill) for each plotted region. Multiple peaks per profile represent stress levels on paralleling fault segments at the indicated observational year.

SAR-derived Deformation Fields and a Fault Model of the 2008 Wenchuan Earthquake

Mikio TOBITA, Hiroshi YARAI, Takuya NISHIMURA, SAR team in GSI
Geographical Survey Institute, Japan
Email: tobita@gsi.go.jp

A huge Mw7.9 earthquake struck the western Sichuan province, China, on May 12, 2008. The co-seismic deformation is investigated using Synthetic Aperture Radar (SAR) data. The ALOS "Daichi" satellite data are used to generate interferograms and pixel offset maps of the co-seismic surface displacement field.

Figure 1 shows the interferograms from ascending orbits. Interferometric SAR data show edges of the rupture area clearly. The estimated length of the rupture area is about 285 km. Pixel offset maps also show location of surface ruptures. In northeastern part of hypocentral area, surface rupture runs along the Beichuan fault. In southwestern area, interferograms show large deformation around the Pengguan fault, which runs south of the Beichuan fault. Pixel offset data indicate both the Beichuan fault and the Pengguan fault rupture on this area.

We invert the InSAR data for slip distribution of the Wenchuan earthquake rupture. We set geometry of faults from fringe pattern of InSAR images and results of seismic wave inversion. Dip of northeastern faults (55°) is steeper than southwestern fault (40°). We estimate amplitude and direction of slip on each 5x5km sub-fault. Figure 2 shows estimated results. Near main shock area, estimated slip shows mostly reverse fault motion and slightly right-lateral slip. Large slip is estimated at deep (15-30km) part. On the other hand, estimated slip of other area shows large right-lateral motion and slip area locates at shallow (0-10km) part. The maximum slip is 11 m at near Beichuan, about 150 km northeast from the hypocenter. The seismic moment derived from estimated fault parameters is 9.2×10^{20} Nm (Mw 7.9). These features are consistent with other results, such as waveform inversion and field survey of surface ruptures.

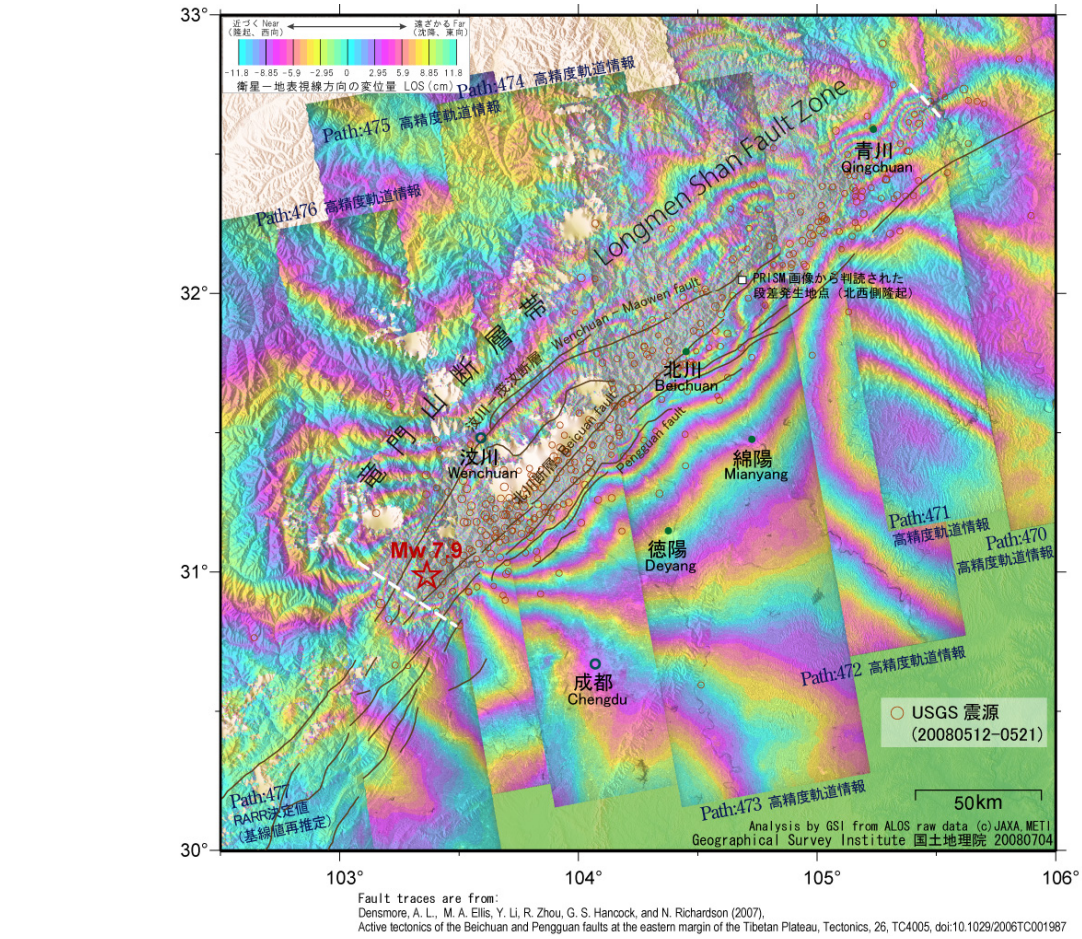

Figure 1. ALOS interferograms of the 2008 Wenchuan earthquake.

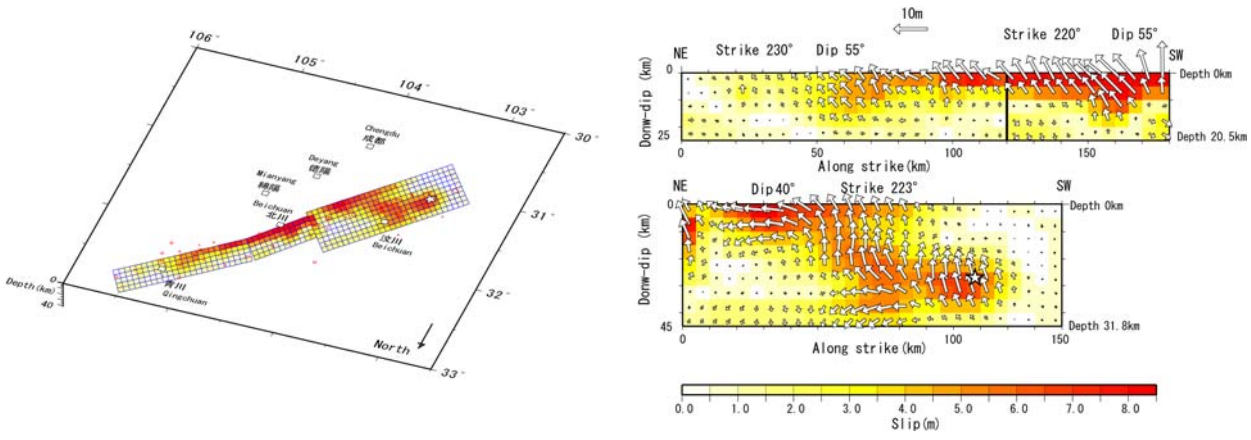

Figure 2. Slip distribution from the inversion of the InSAR displacements. Red-yellow-white color denotes the amplitude of the slip displacements, and arrows show slip directions of hanging wall, i.e., northern side of the fault. Star indicates epicenter.

Atmospheric, Topographic, Crustal and Parameterization Errors: At What Point do they Significantly Affect our Models of Moderate to Large Earthquakes?

Rowena Lohman
Cornell University
Ithaca, NY

In the immediate aftermath of a large earthquake, rapid and accurate characterization of the location, source geometry and magnitude of the event allows emergency relief organizations to assess the severity of the earthquake and to direct their efforts towards areas that may have sustained damage. In the weeks to months following an earthquake, the focus turns to that of analysis and improving our understanding of the seismogenic process. At this stage, more detailed characteristics of the earthquake are required, including the precise location, geometry and slip distribution, for later comparison with postseismic deformation, mapped fault locations, the historical earthquake record, etc. Although there is more time available to perform these types of analyses than there is for immediate disaster response, earthquake research, especially that involving the study of multiple earthquakes and their statistical behavior, is still limited by both the time it takes to learn and implement new computational tools and by the time that it takes to run them. Although the datasets and tools that we have at our disposal are constantly improving, it may not always make sense to apply them to a particular problem if the cost is too high. On the other hand, there are many problems that we cannot yet address because our knowledge of the exact fault geometry, crustal elastic structure, and other parameters is not good enough. Determining the level of sophistication required by a given problem can often be as time consuming as solving the problem itself.

One possible tool is the use of synthetic tests that can assess the bias introduced by neglect both of 3-D variations in crustal elastic structure and of complicated fault geometries during interpretations of geodetic observations of strain along fault zones. These biases can easily be compared to the uncertainties associated with noise in the data, such as that result from variations in atmospheric water vapor in InSAR or GPS observations. We explore these constraints on several M6 earthquakes in Iran as well as larger events elsewhere. The use of synthetic tests can allow both the determination of when existing information needs to be included, as well as the identification of regions that require better constraints in the future.

Physical Source Modeling for the 2008 Iwate-Miyagi Nairiku, Japan, Earthquake: The Effects of Frictional Heterogeneity due to Geothermal Anomaly near Volcanoes

Ryosuke Ando (Active Fault Research Center, AIST)

The Mw 6.9 Iwate-Miyagi Nairiku earthquake on June 14 occurred near a volcanic front in northern Honshu (also refer Toda et al. in this abstract volume), provides us a unique opportunity to physically concern the effect of geothermal structures on the stressing conditions of inland earthquakes. The observed lower limit of the aftershock distribution, reflecting the base of the brittle seismogenic zone, appears to be the deepest near the hypocenter, close to the middle of the estimated main-shock rupture area, and to become gradually shallower to south and steeply to north along strike. There are quaternary active volcanoes near the ends of the rupture area, in which low S-wave velocity anomalies are also situated deep down More over, these aftershocks and coseismic slip estimated by seismic and geodetic inversions appear to be distributed keeping away from such low velocity zones. Thus, it should be fare to consider that these high temperature zones make the thermal anomaly that course the along-strike variation in the base depth of the seismogenic zone that are determined by the geothermal gradient.

In this study we try to explain several characteristic phenomena in the aftershock distributions and the coseismic dynamic rupture process in terms of a basic physical model called the “deep slip” model (e.g. Scholz, 2002; Tse and Rice, 1986), consisting of an unstable frictional fault in the upper crust and an underneath localized ductile shear zone in the lower crust. In order to consider the geothermal anomaly along the fault, we assume a dipping fault embed in the 3-D half space with horizontal variation in the frictional property related to the brittle-ductile transition determined by the geothermal structure.

As for the computation, we develop the current model including the quasi-static stressing process and dynamic rupture process based on the boundary integral equation method (BIEM). Regarding the treatment of the free surface in BIEM, while the quasi-static process is modeled by an existing analytical expression (Okada, 1992), in the dynamic process, the surface is numerically treated as a virtual crack with the zero traction condition.

Referring the aftershock distribution, we assume a non-uniform depth distribution in the brittle-ductile transition along strike. With the simulation, we find the rupture is nucleated at the deepest portion in the brittle zone and propagated mainly toward south. The slip also tends to be concentrated in the shallow depth as the rupture propagates to south. These calculation results seem to reproduce the overall observed characteristics of this event.

SESSION VI

ABSTRACTS

Prehistoric Earthquakes in the Puget Lowland, Washington

Brian L. Sherrod, bsherrod@usgs.gov, U.S. Geological Survey, Department of Earth and Space Sciences, Box 351310, University of Washington, Seattle, Washington 98195

As recently as 1998, field evidence could confirm only two faults with evidence of past earthquake activity. Coastal marsh deposits and LIDAR topographic data now show evidence for past earthquakes on at least nine fault zones in the Puget lowland. Three fault zones, the Seattle fault zone, Tacoma fault, and the Southern Whidbey Island fault zone (SWIFZ), cut through the heavily populated portions of central Puget Sound. Faults in five other areas, namely the Boulder Creek fault in Whatcom County, Darrington– Devils Mountain fault zone, Olympia fault, the northern margin of the Olympic Mountains, and the southeastern Olympic Mountains, show that the area of active Holocene faulting extends over the entire Puget Sound lowland.

LIDAR scarps have been identified in several areas not associated with the nine zones noted here but have yet to be investigated. LIDAR data covers about 70% of the Puget Sound basin, but key areas with suspected crustal faults in northwestern Washington have yet to be flown. Still, the combination of paleoseismological field investigations and LIDAR imaging allowed remarkable progress in understanding the Holocene earthquake history of greater Puget Sound in the last 10 years. The new observations are an important addition to observations used to calculate the National Hazard Maps.

Fault Model of the 2007 M6.8 Chuetsu-oki Earthquake, central Japan and Triggered Episodic Deformation in the Adjacent Active Folding area

Takuya NISHIMURA[1]*, Mikio TOBITA[1], Makoto MURAKAMI[1], Hiroshi YARAI[1], Tomomi AMAGAI[1], Midori FUJIWARA[1], Akira SUZUKI[1], Fumi HAYASHI[1], Hiroshi UNE[1], Mamoru KOARAI[1], Toshihiko KANAZAWA[2] and Masanao SHINOHARA[2]
[1]Geographical Survey Institute, Japan
[2]Earthquake Research Institute, University of Tokyo, Japan
Email: t_nisimura@gsi.go.jp

The Niigata-ken Chuetsu-oki earthquake in 2007 (M=6.8, hereafter Chuetsu-oki earthquake) occurred west off Kashiwazaki city in the Sea of Japan, on July 16, 2007. It is a shallow reverse-type earthquake in the Niigata-Kobe Tectonic Zone where recent GPS observations show a large amount of compression in east-west direction. Here we present the coseismic deformation, a fault model to explain the deformation (Nishimura *et al.*, 2008b), and the deformation that cannot be explained by the coseismic fault model.

Using the fault geometry inferred from an accurate aftershock distribution (Shinohara et al., 2008), we estimated the slip distribution on the faults by inverting the observed geodetic data including GPS, InSAR (Fig. 1), and leveling. Considering the misfit and the estimated slip distribution, we suggest that the major fault of the Chuetsu-oki earthquake dips to southeast and that the minor fault dipping to northwest ruptured in the northeastern part of the source area simultaneously. The interesting feature of the deformation clarified by InSAR data is the narrow uplift belt in the active folding belt, which is ~6 km east of the aftershock area (Nishimura *et al.*, 2008a). This uplift zone parallel to the anticline axis can be interpreted as the episodic growth of active fold (Fig. 2). The uplift has been probably caused by a shallow aseismic slip triggered by an increase in static stress due to the earthquake.

References

Nishimura, T., M. Tobita, H. Yarai, T. Amagai, M. Fujiwara, H. Une, and M. Koarai (2008a) Episodic growth of fault-related fold in northern Japan observed by SAR interferometry, *Geophys. Res. Lett.*, 35, L13301, doi:10.1029/2008GL034337, 2008.

Nishimura, T., et al. (2008b) Crustal deformation and a preliminary fault model of the 2007 Chuetsu-oki earthquake observed by GPS, InSAR, and leveling, *Earth, Planets, and Space, in press.*

Shinohara, M., et al. (2008), Precise aftershock distribution of the 2007 Chuetsu-oki earthquake obtained by using an ocean bottom seismometer network, *Earth Planets Space, in press.*

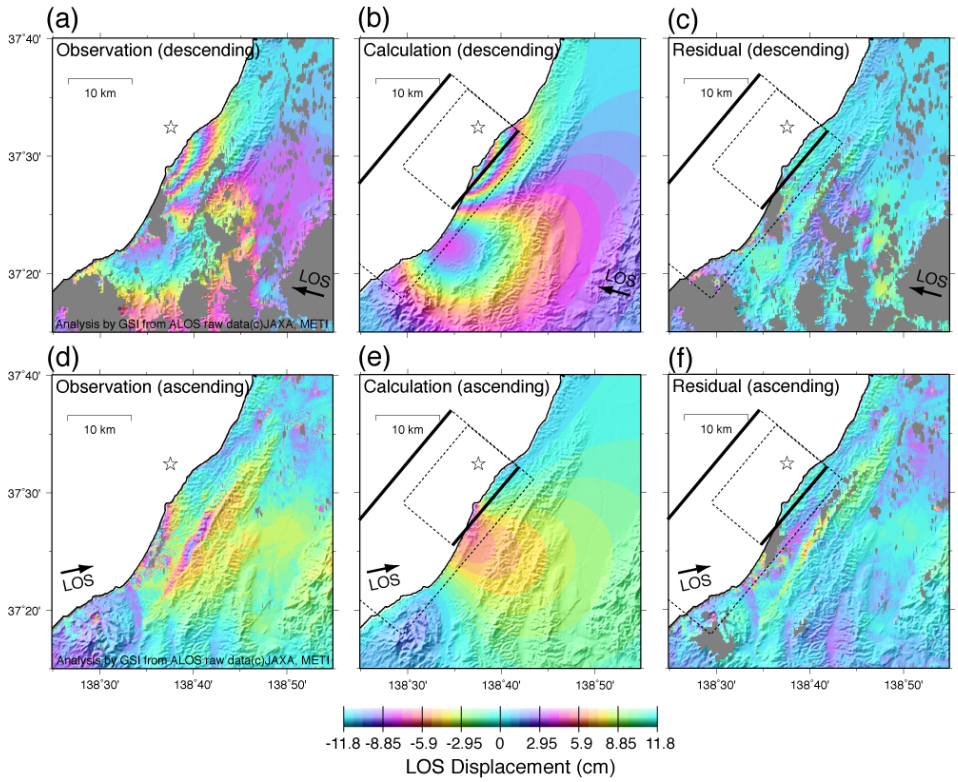

Figure 1. The interferograms showing the deformation for the 2007 Chuetsu-oki earthquake. (Nishimura *et al.*, *submitted to ADGOS*) (a) Observed interferograms formed from the descending orbit data acquired on January 16 and July 19, 2007. (b) Descending orbit interferograms calculated using the fault model. (c) Residual interferograms for the descending orbit data. (d) Observed interferograms formed from the ascending orbit data acquired on June 14 and September 14, 2007. (e) Ascending orbit interferograms calculated using the fault model. (f) Residual interferograms for the ascending orbit data.

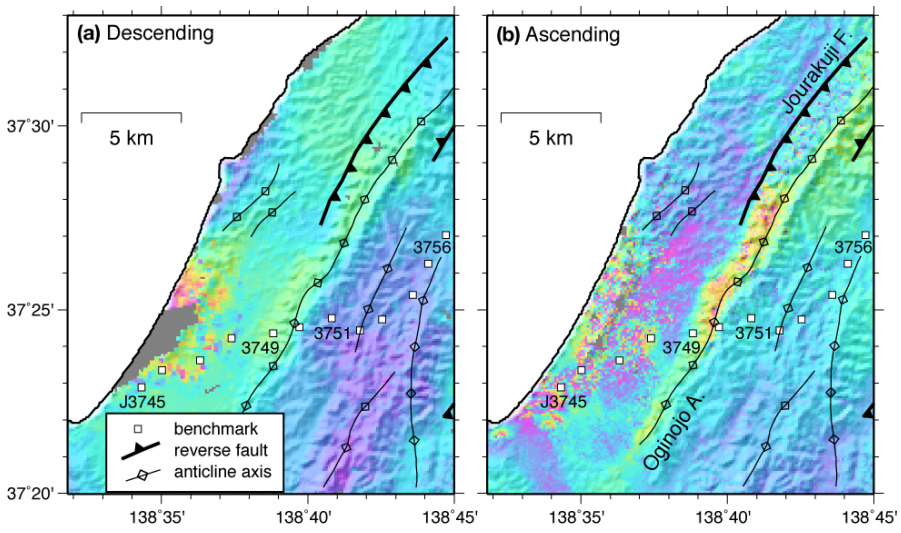

Figure 2. Residual LOS displacement of the main-shock fault model and tectonic structure (*Nishimura et al.*, 2008a). The uplift band parallel to the Oginojo anticline is clarified particularly in the ascending data.

Comparison of Satellite Image Interpretations between ALOS/PRISM and IKONOS, in the case of Landslides Triggered by Wenchuan (Sichuan) EQ

[*]Hiroshi P. SATO and [**]Edwin Harp
[*]Geographical Survey Institute (GSI), [**]United States Geological Survey (USGS)

The M7.9 earthquake occurred on 12 May 2008 in eastern Sichuan Province of the People's Republic of China (http://earthquake.usgs.gov/eqcenter/eqinthenews/2008/us2008ryan/, accessed on 15 September). This earthquake caused thousands of landslides covering a wide area of 285 km x 20 km. The affected area is so wide that satellite imagery is convenient to map landslides, but there are few studies to compare characteristics of landslide interpretation between the 2.5 m-resolution Advanced Land Observing Satellite (ALOS)/Panchromatic Remote-sensing Instrument for Stereo Mapping (PRISM) image and the 4 m-resolution IKONOS color mono image. To discuss their advantages and disadvantages, we compared them at Maowen, 112.8 km north of Chengdu. PRISM and IKONOS images were taken on 4 June and on 23 May, respectively, and their coverage areas are 42.6 km NS x 43.7 km EW and 11 km x 11 km, respectively. The study area is 70.7 km^2, where both images are overlapped and cloud-free.

First, we interpreted landslides using the PRISM 3-D view at ca.1:10,000 scale. The number of interpreted landslides is 170 as shown in Fig. 1, the range and average of their areas are 170-30,000 m^2 and 2,400 m^2, respectively.

We prepared a pan-sharpened IKONOS image, where a 4 m-color image was overlain on 1 m-panchromatic image, and we compared the PRISM image with the IKONOS image. As a result, the IKONOS image shows a bright white scar where the greenish vegetation is denuded, whereas the PRISM image shows a pale gray landslide that is not so clearly defined (Fig. 2B). It is best to use both PRISM and IKONOS images for comparative interpretation, however the images are not often co-located. With this comparison of PRISM and IKONOS images, we have established that the PRISM images are suitable for identifying and mapping earthquake-triggered landslides larger than 170 m^2 in area.

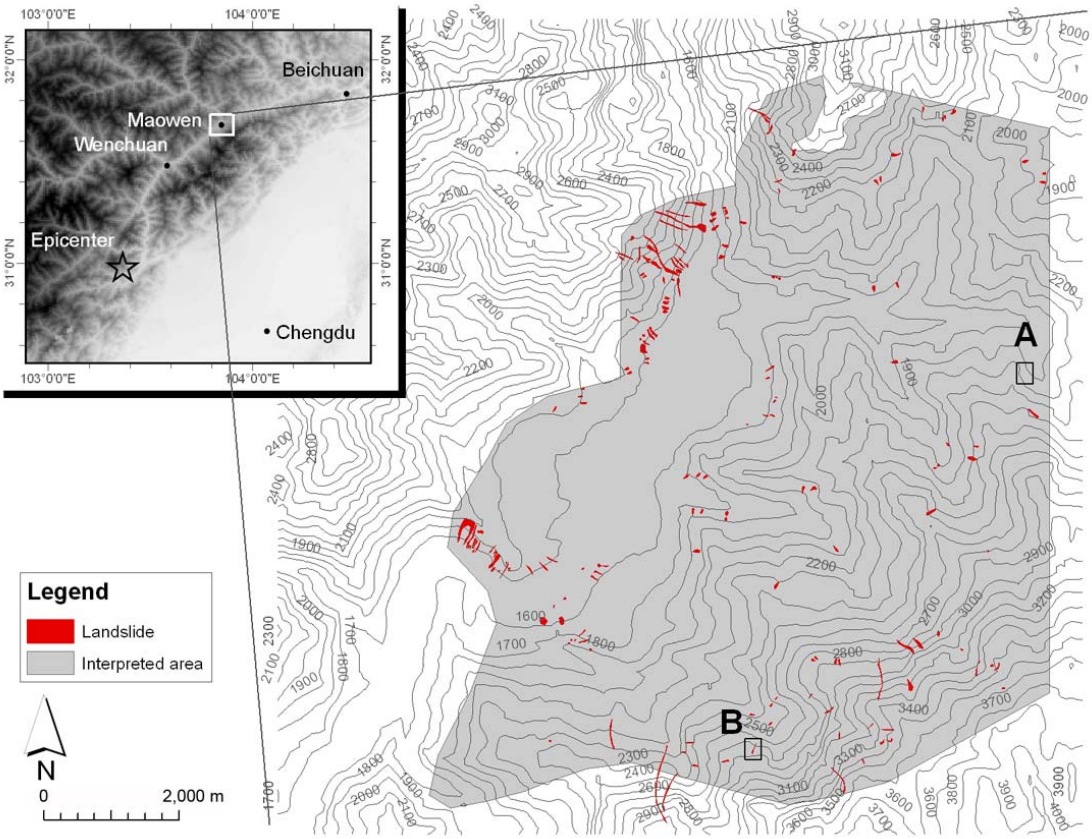

Fig. 1 Landslide interpreted by ALOS/PRISM image in study area. Contour units are meters.

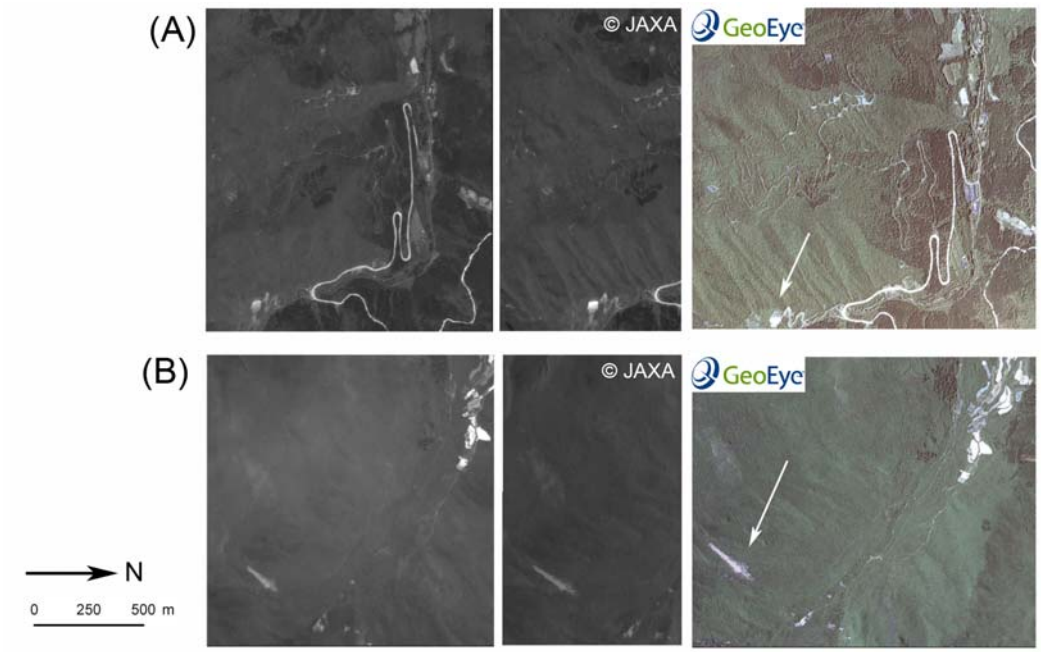

Fig. 2 Comparison of ALOS/PRISM (left, 3-D view) and IKONOS (right, color) images in Fig.1's sites A and B. PRISM image was given by courtesy of Japan Aerospace Exploration Agency (JAXA).

SESSION VII

ABSTRACTS

Inferring Megathrust Slip from Forearc Structure: Promise and Perils

Rich Briggs, US Geological Survey

Megathrust coseismic slip is a primary control on ground shaking and tsunami generation, and consequently there is great interest in developing methods to predict the extent of rupture patches before they break. It has been proposed that readily identified structural or geophysical features - such as forearc basins or gravity anomalies - correlate with slip in historical earthquakes. This has led to the suggestion that the locations of these features might predict the slip patches of future ruptures. There is some promise to this approach, but I will discuss recent great megathrust earthquakes in Sumatra and the Solomon Islands for which detailed coral and GPS geodesy show that megathrust coseismic slip distributions do not obey simple notions of structural or geophysical control. Instead, these rupture areas do not appear to correlate in a simple way with structural or geophysical features.

For example, abundant coral and GPS geodetic data show that slip during the 2005 Mw 8.7 Nias-Simeulue rupture in Sumatra did not occur beneath the forearc basin, but was instead focused beneath the outer arc high. Thanks to the presence of outer arc islands that allowed abundant measurements of surface deformation in the region surrounding the slip patch, the slip distribution for this megathrust rupture is among the best yet obtained - and the data show that slip occurred well updip of the forearc basin and squarely on a positive gravity anomaly. The 2007 Mw 8.1 Solomon Islands earthquake ignored what might have seemed a major structural control before the rupture: it ruptured through a subducting triple junction. The final lateral extent of the rupture appears to correspond to a subducting ridge on the downgoing plate at one end, and a probable fault in the overriding plate on the other - correlations that are possible only *a posteriori*.

Apparent correlations between megathrust slip and forearc structure or gravity usually rely on finite fault models derived from teleseismic or limited geodetic or tsunami data, but the uncertainty in slip models is not usually addressed in this context. Inversions based on teleseismic body waves, surface waves, sparse geodetic measurements, or tsunami waves often give highly variable solutions, and the results are subject to further uncertainty depending on model fault geometry and structure. Based on the recent ruptures in Sumatra and the Solomon Islands, it appears to be premature to forecast global megathrust rupture areas based on existing structural and geophysical proxies.

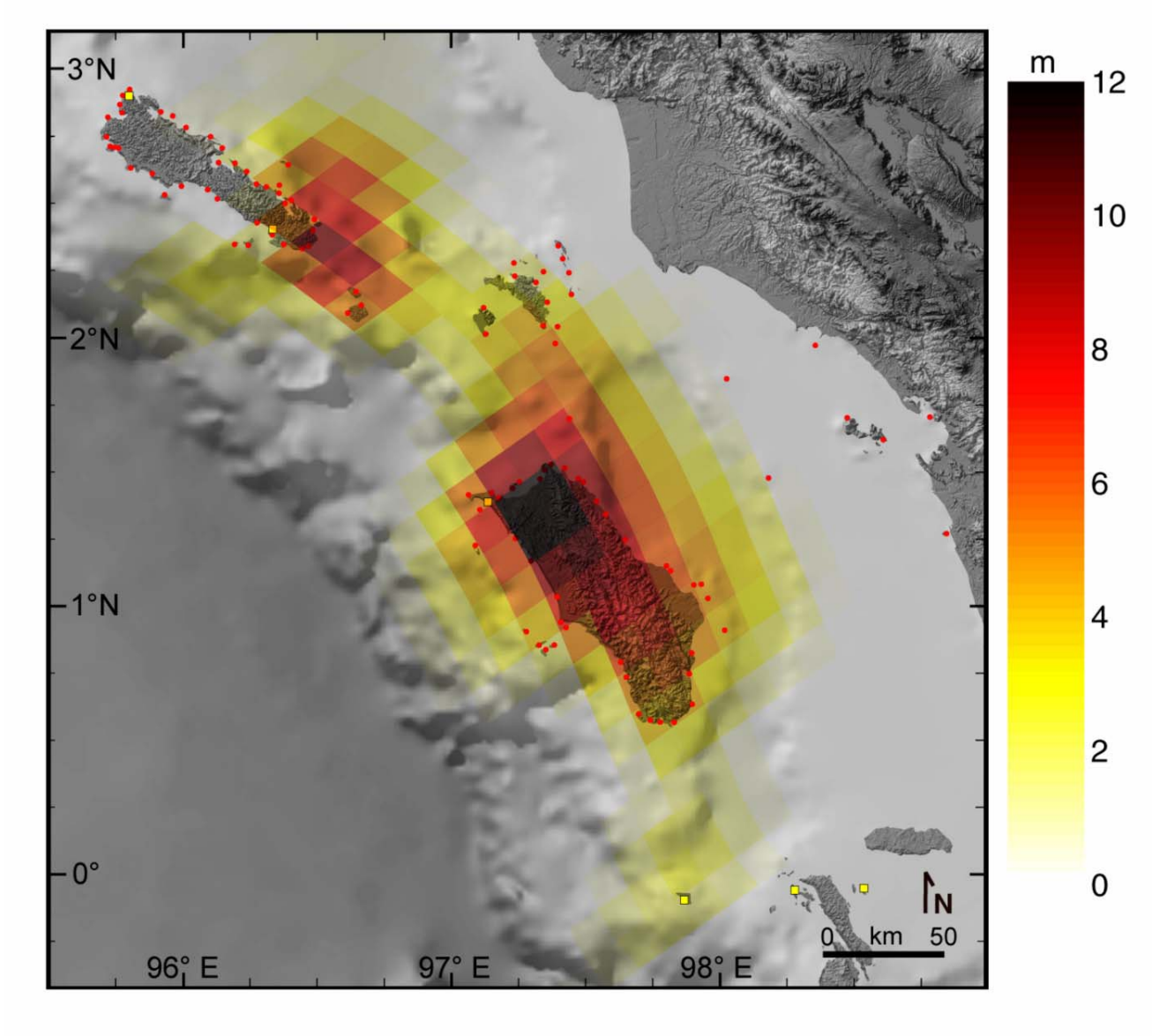

Figure 1: Megathrust slip during the 2005 Mw 8.7 Nias-Simeulue rupture off western Sumatra. Slip was concentrated beneath the outer arc rather than the forearc basin.

Resolving the Geometry of Global Subduction Zone Interfaces a priori - Working Towards Improved Earthquake Source Modeling

By Gavin Hayes, US Geological Survey

A key step in many earthquake source inversions requires knowledge of the geometry of the fault on which the earthquake occurred. Our knowledge of this surface is often uncertain, however, and as a result fault geometry misinterpretation can map into significant error in the final temporal and spatial slip patterns of these inversions. Relying solely on an initial hypocenter and CMT mechanism can be risky when establishing rupture characteristics needed for rapid tsunami and ground shaking estimates.

Here we attempt to improve the quality of fast finite-fault inversion results by combining, a priori, several independent and complementary datasets to more accurately constrain the geometry of the seismic rupture plane of subducting slabs. Unlike previous analyses aimed at defining the general form of the plate interface, we require mechanisms and locations of the seismicity considered in our inversions to be consistent with their occurrence on the plate interface, by limiting events to those with well-constrained depths and with CMT solutions indicative of shallow-dip thrust faulting. We construct probability density functions about each location based on formal assumptions of their depth uncertainty and use these constraints to solve for the `most likely' fault plane, exploring fits with both planar and polynomial geometries. Where available, data from shallow active seismic experiments across trenches are also used as additional constraint.

We show that by using the aggregated data sets this method produces a fault plane that is more consistent with all of the data available than is the plane implied by the initial hypocenter and CMT mechanism, allowing us to rapidly determine more accurate initial fault plane geometries for source inversions of future earthquakes. We use these geometries to explore the effect on finite fault model slip distributions, and show that the model changes can have a significant affect on assumed seismic hazard.

Maps describing the subduction interface geometry constraint for the Sumatra Trench at the location of the 01/22/2008 Mw6.2 Nias Islands earthquake. (a) Basemap of Sumatra subduction zone. Earthquake locations from the gCMT catalog and NEIC catalog (gray circles) are shown. Red rectangle indicates the area shown in cross-section (c); all earthquakes within this area may be used to constrain trench geometry. Red star indicates reference (new earthquake) location; yellow star represents equivalent gCMT centroid location. (b) Probability functions describing interface dip likelihood. The right panel describes results from a maximum likelihood approach; the left for weighted least-squares (red and gray solid lines) and SVD (dashed black vertical line) (c) Cross-section of subduction zone taken perpendicular to the average strike of gCMTs that match selection criteria and whose equivalent EHB or NEIC locations lie within the red box from (a). Gold CMTs are mechanisms from the gCMT catalog plotted at their equivalent EHB location; orange CMTs are mechanisms at their event location in the NEIC catalog. These mechinisms represent events used to constrain geometry. Light and dark gray circles are events from the EHB catalog south and north of the plane of the cross-section, respectively. These are not used to constrain geometry because either (i) they did not have a mechanism in the gCMT catalog, or (ii) their mechanism did not match selection criteria. The trench location is marked with a red square, labeled 'Trench'. Probability density functions for EHB and NEIC locations are shown as green lines. The black solid line describes the best fitting planar geometry; the red line is the equivalent polynomial geometry. The initial locations of the 'new event' used to help constrain geometry are shown by black circles and marked with arrows. PDFs for these locations are shown in red; the most likely depth for each location is marked with a white star. The best-fitting fault plane from the gCMT catalog for the new event is shown with a black dashed line. (d) Variation in dip of best-fitting fault planes from the gCMT catalog for all events used to constrain trench geometry across the plane of the cross-section. Individual event dips are shown with small dark gray circles, sized with magnitude. Large mechanisms indicate the average dip in 20km bins across the plane of the cross-section. Light gray mechanisms represent a bulk average; dark gray represents a moment-weighted average.

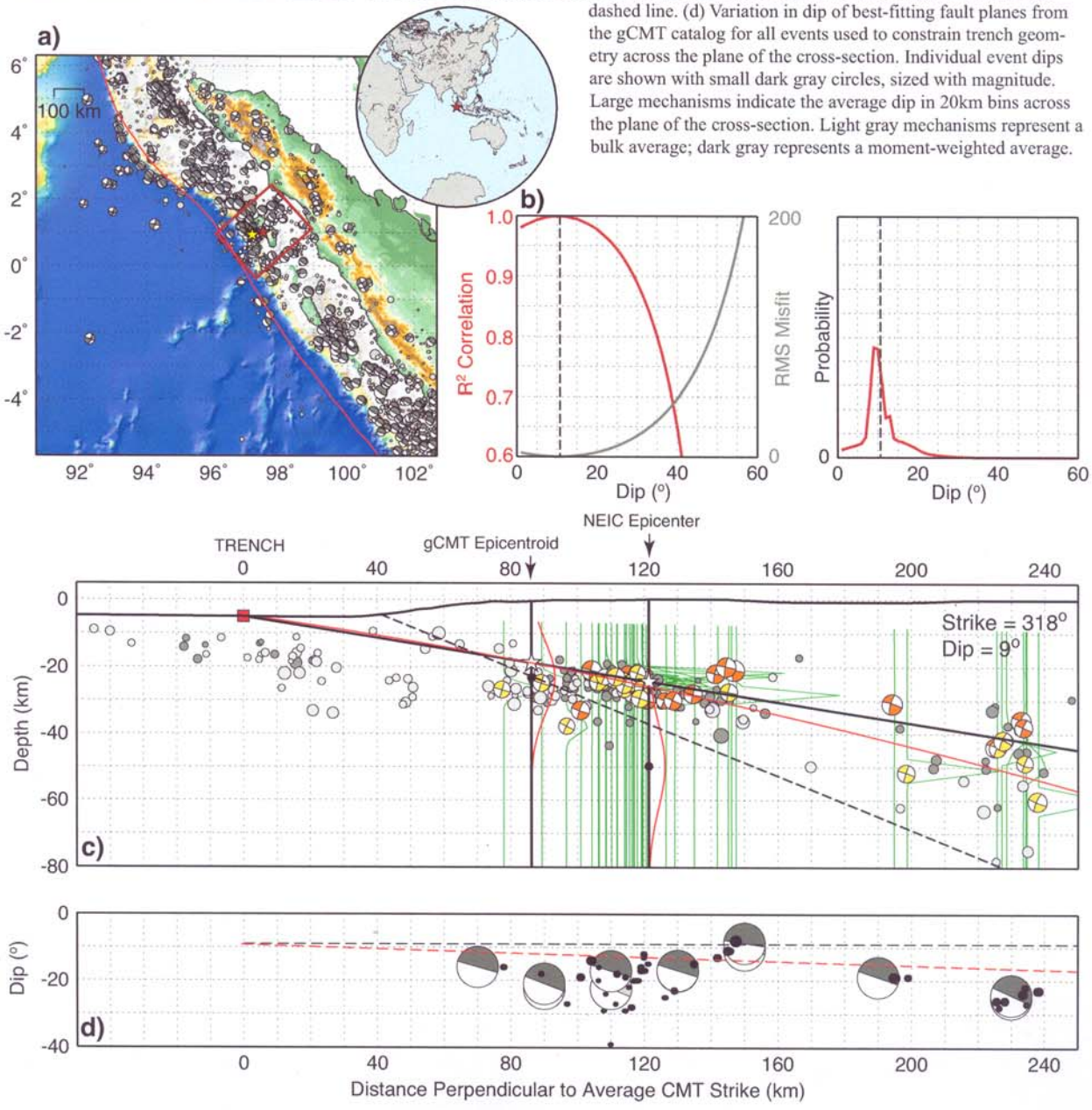

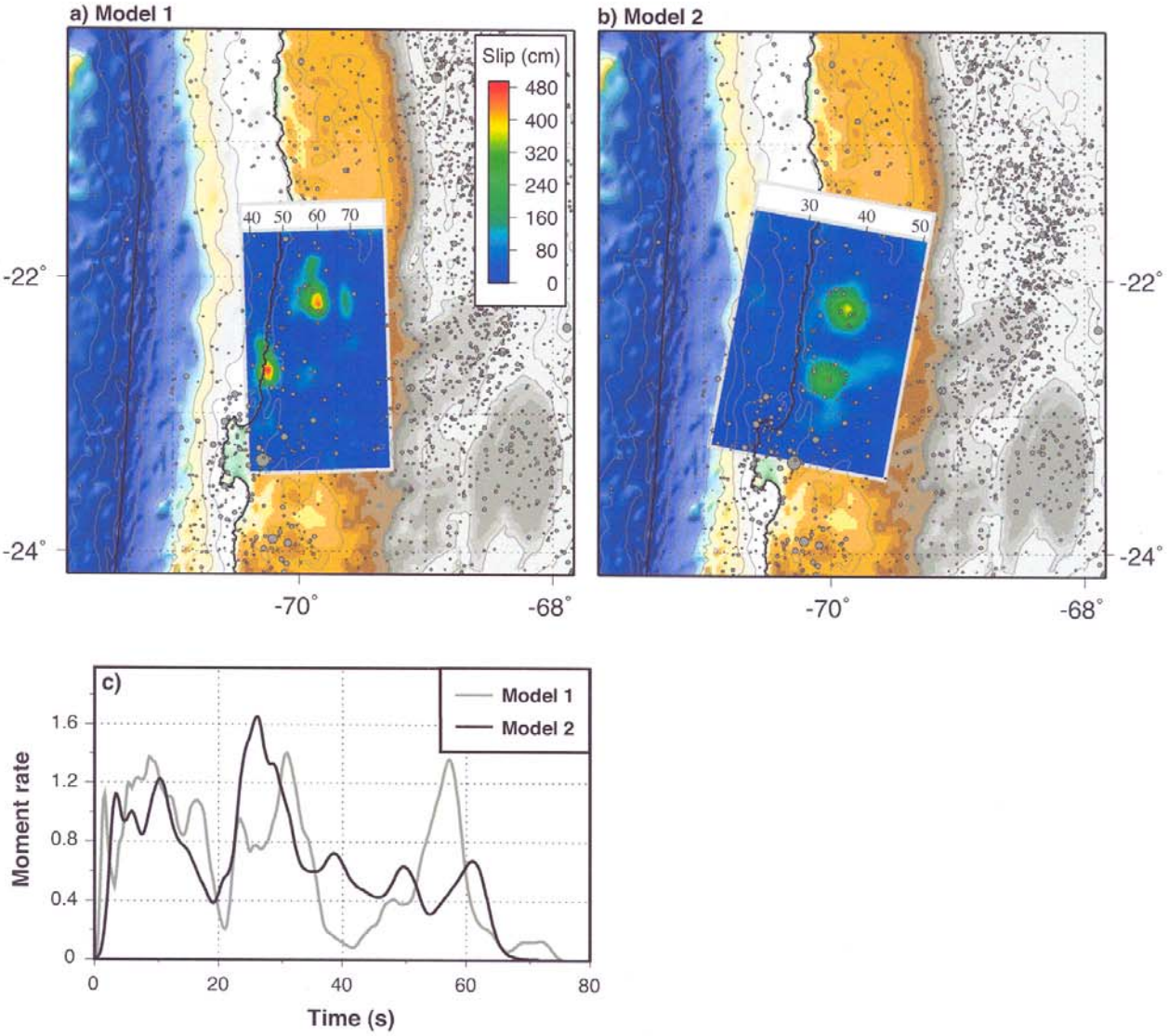

Finite fault inversions demonstrating the change in modeled slip distributions using fault planes based on **(a)** the gCMT best-fitting fault plane at the initial NEIC catalog hypocenter, and **(b)** the most-likely fault plane from our probabilistic subduction interface inversion. These models constrain the slip history of the earthquake based on the finite fault inverse algorithm of Ji et al. (2002), analyzing 13 teleseismic broadband P waveforms, 6 broadband SH waveforms, and 23 long period surface waves selected based upon data quality and azimuthal distribution. In each figure, the surface projection of the fault plane used in the inversion is colored based on slip amplitude. The scale at the top of each model relates to the depth distribution of the fault plane. Dark gray circles represent background seismicity up to the day prior to this event, scaled by magnitude. The thick black lines represent the plate boundary and the coastline; light gray lines represent contours of bathymetry data (from the Marine Geoscience Data System, http://www.marine-geo.org) at 1000m intervals. **(c)** Moment-rate time functions for each finite fault model, in units of 10^{19} N.m/s.

The 2004 Great Sumatra Earthquake as a Critical Phenomenon and an Accelerating Seismicity along the Indian-Eurasian Plate Boundary Zone

Shin-ichi NOGUCHI, National Research Institute for Earth Science and Disaster Prevention, shin@bosai.go.jp

The spatio-temporal distribution of global seismicity since 1900 demonstrates a long-term cyclic activity along the Eurasian/Indian-Australian plate boundary zone from around 1990. We apply two models of time-to-failure analysis to the seismic activity in the broad area before the 2004 Sumatra earthquake M_w9.3 and to the currently accelerating activity in the Indo-Himalaya collision zone, based on the Harvard/Global CMT and USGS/NEIC catalogs. Calculating the curvature parameter of the acceleration of the cumulative Benioff strain (Bowman *et al*., 1998) in circular areas around the 2004 Sumatra earthquake, we estimate an optimum critical region radius 3200 km centered at point near Nicobar Islands. We use both the power law function and the log-periodic function added to the power law relation to determine parameters by the nonlinear least-square method. The better fitting of the log-periodic function with final failure time t_f=2005.3 may indicate an intrinsic oscillatory behavior of the seismic strain release before the 2004 event in the hierarchical fault network approaching to the critical point. This is consistent with the increase of clustering and larger events and the Gutenberg-Richter relation extending systematically to larger magnitude range in the later period before the 2004 final rupture.

As for the accelerating cumulative Benioff strain in the Indian-Himalayan collision zone, we obtain an optimum area radius 2600 km centered at 28°N and 90°E. The area includes the latest and largest Sichuan earthquake of May 12, 2008 M_w 7.9 since 1976. The two time-to-failure functions predict further large event(s) with the final fracture time 4-5 years from now. To clarify the ongoing crustal activity, a comprehensive and interdisciplinary investigation is necessary.

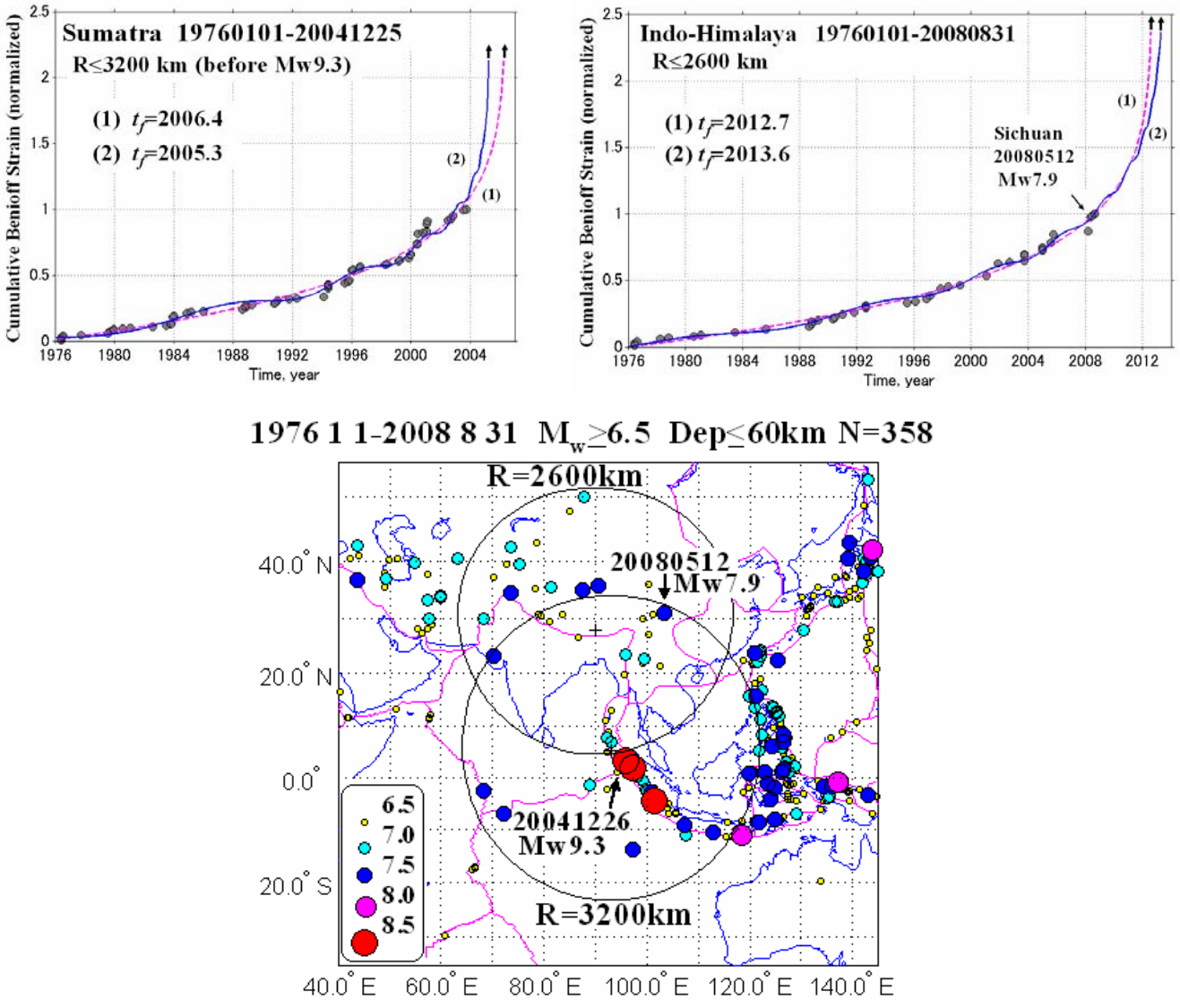

Figure 1. Two time-to-failure models, (1) the power law model by Bufe and Varnes (1993) and (2) the log-periodic model added to the power law function by Sornette & Sammis (1995), are applied to the cumulative Benioff strains of earthquakes with $M_w \geq 6.5$ in the Sumatra-Andaman region radius 3200 km before the 2004 Sumatra earthquake, and in the Indian-Himalayan region radius 2600 km for the period 1976-2008. Though the latest Sichuan earthquake of May 12, 2008 M_w7.9 is the largest event in the Indian-Himalayan circular region since 1976, the time of final failure t_f (years) calculated from the models predict further large event in 4-5 years later.

Previous Tsunamis in Thailand

Kruawun Jankaew[1], Brian F. Atwater[2], Yuki Sawai[3], Montri Choowong[1], Thasinee Charoentitirat[1], Maria E. Martin[4], Amy Prendergast[5]

[1]Department of Geology, Faculty of Science, Chulalongkorn University, Phayathai Road, Phatumwan, Bangkok 10330, Thailand. [2]U.S. Geological Survey at Department of Earth and Space Sciences, University of Washington, Box 351310, Seattle, Washington 98195-1310, USA. [3]Geological Survey of Japan, National Institute of Advanced Industrial Science and Technology, Site C7 1-1-1 Higashi, Tsukuba 305-8567, Japan. [4]Department of Earth and Space Sciences, University of Washington, Box 351310, Seattle, Washington 98195-1310, USA. [5]Geoscience Australia, GPO Box 378, Canberra, Australian Capital Territory 2601, Australia.

Sheets of sand show probable precedents for the 2004 Indian Ocean tsunami at a grassy beach-ridge plain 125 km north of Phuket. The 2004 tsunami, running 2 km across this plain, coated the ridges and intervening swales with a sheet of sand commonly 5-20 cm thick. The peaty soils of two marshy swales preserve the remains of several earlier sand sheets less than 2,800 years old. If responsible for the youngest of these pre-2004 sand sheets, the most recent full-size predecessor to the 2004 tsunami occurred about 550-700 years ago.

Studies of Seismicity and Paleoseismicity in the Kuril Biocomplexity Project [KBP]

Joanne [Jody] Bourgeois (University of Washington) and many others

KBP is a five-year project involving an interdisciplinary team of American, Japanese and Russian scholars and students examining a 5000-year history of human-environmental interactions along the Kuril Island chain in the northwest Pacific. Amongst geological and geophysical objectives, we are studying the volcanic, tectonic and coastal history of these islands. In addition, we have been able to facilitate the placing of permanent and campaign GPS stations in the central and northern Kurils, from Urup to Paramushir. We have just completed our third [and last] major field season, concentrating on the central Kuril Islands, which we have visited by chartered ship [funded primarily by the U.S. National Science Foundation.

Our coastal geology group's original plan was to survey the record of tsunami deposits along the Kuril Islands, examining spatial and temporal variations in tsunami prehistory as a proxy for paleoseismicity of the islands. Our first field season was 2006 summer, and in the following winter, two great earthquakes struck the central Kuril Islands in an identified seismic gap. Both these earthquakes were tsunamigenic. Thus in the summers of 2007 and 2008 we added a component of post-earthquake and tsunami study to our field plan. Currently we are processing our field data and planning joint workshops to exchange data and analyses amongst U.S., Russian and Japanese scientists and students.

KBP website address: http://depts.washington.edu/ikip/index.shtml

SESSION VIII

ABSTRACTS

Phenomenology of Deep Episodic Tremor and Slip in southwest Japan
—Spatiotemporal Characteristics and Segmentation—

Kazushige Obara
NIED (National Research Institute for Earth Science and Disaster Prevention),
3-1 Tennodai, Tsukuba, Ibaraki, 305-0006, Japan, obara@bosai.go.jp

The phenomenology of episodic slow earthquake in the transition zone at the deeper side of the mega-thrust zone on the subducting plate interface in southwest Japan is investigated on the basis of the data obtained from the dense seismic and geodetic network. Slow earthquakes include deep low-frequency tremors [Obara, 2002], deep very-low-frequency earthquakes [Ito et al., 2007], and short-term slow slip events [Obara et al., 2004]. Low-frequency tremors and very-low-frequency earthquakes are characterized by long-period seismic waves having a dominant frequency of 2 Hz and 0.05 Hz, respectively. A short-term slow slip event is recognized by ground tilting lasting for several days. Based on the space-time activity of tremors, the belt-like distribution of tremors is divided into some segments bounded by aseismic gaps. The repetition property of slow earthquakes depends on the segment size. In large segments longer than 100 km, the coupling phenomena of slow earthquakes occur with a recurrence interval of approximately 6 months. In smaller segments, tremor episodes that occur with a recurrence interval of a few months occasionally accompany the slight ground tilting caused by a small-sized slow slip event. Assuming all tremor episodes to be caused by a slow slip event, the apparent seismic moment of a slow slip event is estimated from the number of detected tremors and the area of each tremor episode. The apparent slip history estimated from all tremor episodes is almost constant in each segment. This indicates that the tremor activity is a good proxy for slow slips. Some segments indicate an along-strike variation of tremor seismicity and VLF earthquakes. Along-strike inhomogeneity on the plate interface might affect the tremor migration. The initiation and direction of tremor migration have some variations within a segment. In many cases, the tremor migration that corresponds to the rupture front of a slow slip event starts or stops at the edge of a segment bounded by the gap. The tremor occasionally propagates beyond the gap to a neighboring segment. Considering the continuous activity in both segments of the gap, an aseismic slip might propagate through the gap area. Various migration patterns of tremors might be applied to resolving the rupture process of mega-thrust earthquakes at the plate interface.

ETS in Canada: 25 Years of Observations

Garry Rogers, Honn Kao, Herb Dragert, Shao-Ju Shan, Kelin Wang
Geological Survey of Canada, Pacific Geoscience Centre, Sidney BC

The northernmost part of the Cascadia subduction zone in Canada is the region subducting the youngest lithosphere. It contains two separate oceanic plates, Juan de Fuca and Explorer, subducting at different rates and thus hosting different forearc temperature regimes. Analysis of continuous seismic and GPS data collected in the last decade (1997-2007) establish the most comprehensive contemporary observational basis for northern Cascadia episodic tremor and slip (ETS) events. Analysis of paper seismograms prior to continuous digital recording has extended the documentation of tremor episodes beneath southern Vancouver Island back for another 15 years (Figure 1).

Since continuous GPS data became available on southern Vancouver Island in 1994, tremor events exceeding one-week duration have had a one-to-one correlation with GPS observed slip events. These ETS episodes last anywhere from a week to a month. The average repeat time for ETS events beneath southern Vancouver Island over 25 years is about 14.5 months. Halting and jumping are very common in ETS migration patterns and migration along strike of the subduction zone can a happen in both directions, although south to north is the most common. Migration speed varies from ~5 to ~13 km/day. About one quarter of the tremor occurs in short lived tremor events of a few hours to a few days which usually have no resolvable GPS signature. However, a combination of GPS and PBO strainmeter observations allowed characterization of slow slip during one of these short tremor episodes.

The tremor depth distribution shows a peak in the 25-35 km range where strong seismic reflectors in a low shear wave velocity zone (i.e. the E-layer) are located. Existence of tremors in the vicinity of the E-layer is also confirmed by independent waveform analysis. In addition, a preliminary search indicates that some very-low frequency earthquakes (VLFE) may have occurred at the depth of the E-layer with low angle thrust faulting mechanisms. Our observations suggest that a significant portion of the tremor and perhaps some of the slip is associated with the E-layer which is above the interpreted plate interface in the most commonly used plate geometry model. One of the most interesting observations is that the two largest crustal earthquakes on Vancouver Island in the last century, 1918 (M=6.9) and 1946 (M=7.3) are located in a persistent tremor gap, suggestive of some as-yet unknown connection that leads to this anti-correlation (Figure 2).

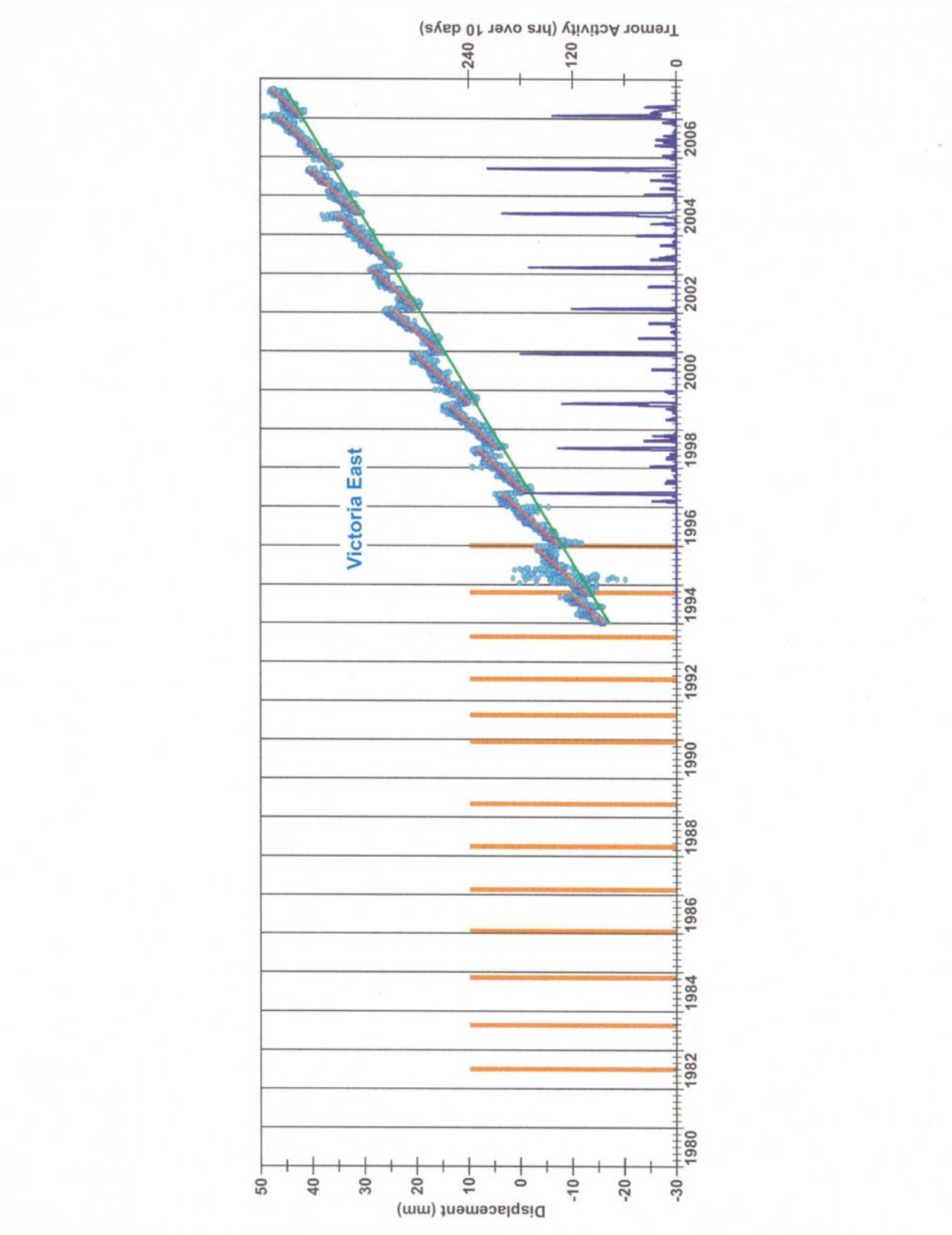

Figure 1: Blue dots show the GPS east component in Victoria. Graph below shows total number of hours with tremor activity in a ten day period. Vertical orange bars are tremor events identified from paper seismograms.

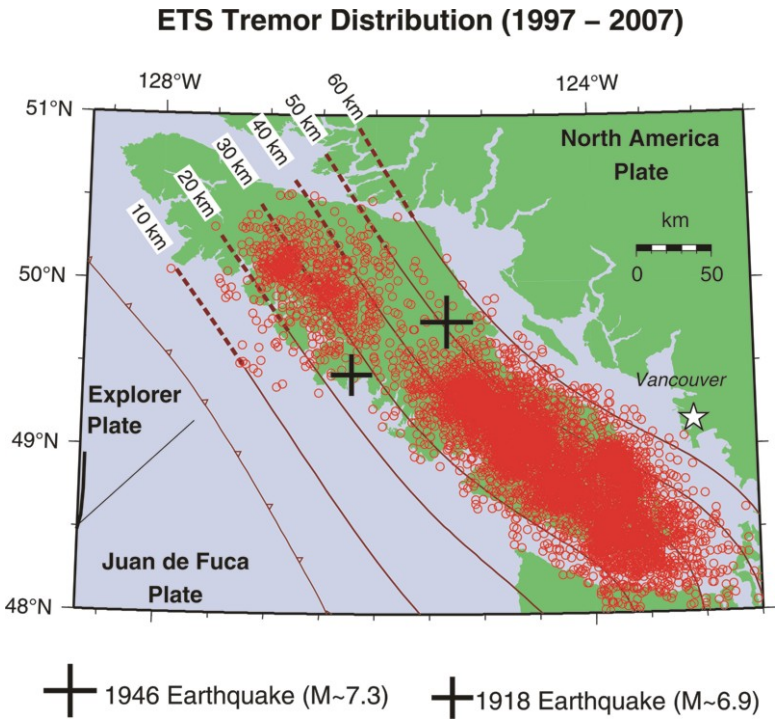

Figure 2: Red circles are tremors and black crosses are large crustal earthquakes.

Modeling Short-term Slow Slip Events in the Deeper Parts of the Nankai Trough Subduction Zone

Bunichiro Shibazaki
International Institute of Seismology and Earthquake Engineering,
Building Research Institute, Tsukuba, Japan
bshiba@kenken.go.jp

We have developed a 3D model of the short-term slow slip events (SSEs) on the subduction interface beneath Shikoku, southwest Japan, considering a rate- and state-dependent friction law with a small cut-off velocity to an evolution effect (Shibazaki and Shimamoto, 2007). We assume low effective normal stress and small critical displacement at the SSE zones. On the basis of the hypocentral distribution of low-frequency tremors (LFTs) determined by Obara (2008), we set three SSE-generation zones: a large segment beneath western Shikoku and two smaller segments beneath central and eastern Shikoku. The numerical results show that the events reproduced by the model beneath western Shikoku have longer lengths (around 100 km) in the horizontal direction and longer recurrence times (0.25–0.5 years) than the events beneath central and eastern Shikoku (20–40 km and 0.2–0.3 years). The numerical results are consistent with the observations of Obara (2008) in that the events at longer segments have longer recurrence intervals. The activity of SSEs is determined by a segmentation structure in the frictional properties at the transition zone. We also report the results of numerical modeling on the SSE activity beneath the Kii Peninsula and the Tokai region.

Next, we attempted to model the very-low-frequency (VLF) earthquakes accompanied by short-term SSEs, on a 2D thrust fault. We consider a local patch in which the friction parameters are varied. There exist two plausible models for generating VLF earthquakes. In the case that the critical displacement is very small at the patch, fast multiple slips occur at the patch. In the case that the effective normal stress is high at the patch, the patch acts as a barrier to SSEs; when it ruptures, however, rapid slip occurs. Because the source time functions of these cases are somewhat different, it will be possible to assess which model is more appropriate for VLF earthquakes.

Cycles Within Cycles - Repetitive Tremor of and Between Cascadia 14-month ETS Episodes

Ken Creager[1], Aaron Wech[1], John Vidale[1] and Tim Melbourne[2]
1. University of Washington 2. Central Washington University

We present a comprehensive view of tremor activity during the past 4 episodic tremor and slip (ETS) episodes in northern Cascadia as well as during one inter-ETS period. Automatically detected and located tremor epicenters provide a high-resolution map of Washington's slow slip region. Thousands of epicenters from each of the past four ETS events from 2004—2008 provide detailed map-view constraints that correlate with geodetic estimates of the simultaneous slow slip activity. Epicenters from both ETS and inter-ETS tremor are bounded between the 30—45 km plate interface depth contours and locate approximately 75 km east of previous estimates of the locked portion of the subducting Juan de Fuca plate. Based on the high spatio-temporal correlation between tremor and slip, the tremor duration and slip magnitude relationship and the similarity in map view and duration of ETS and inter-ETS tremor, we suggest that the well-resolved, sharp updip edge of the tremor epicenters reflects a change in plate interface coupling properties. This region updip of the tremor epicenter boundary likely accumulates stress with the potential for coseismic shear failure during a megathrust earthquake. Alternatively, slip in this region could be accommodated by slow slip events with sufficiently long recurrence intervals that none have been detected during the past 10 years of GPS observations

We detect 35 tremor swarms during one 15-month long inter-ETS period. The number of hours of tremor per swarm ranged from about one to 50 hours, adding up to 193 hours. The inter-ETS tremor swarms generally locate along the downdip side of the major ETS events, and account for approximately 45% of the time tremor has been detected during the last entire ETS cycle, which includes the May, 2008 ETS episode. Many of the inter-ETS events are near carbon copies of each other in duration, spatial extent and propagation direction, as is seen for the larger 14-month-interval events.

These 35 inter-ETS swarms plus one major ETS episode follow a power law relationship such that the number of swarms, N, exceeding duration τ is proportional to $\tau^{-0.6}$. If we assume that seismic moment is proportional to τ as proposed by Ide et al. [Nature, 2007], we find that the tremor swarms follow a standard Gutenberg-Richter logarithmic frequency-magnitude relation, $\log_{10}N = a\ 10^{-bMw}$, with b = -0.9, which lies in the range for normal earthquake catalogs. Furthermore, the major ETS events fall on the curve defined by the inter-ETS swarms, suggesting that the inter-ETS swarms are smaller versions of the major 14-month ETS events.

Assessment of Slow Slip Events on the Cascadia Subduction Zone, 1998-2008

David Schmidt and Haiying Gao
Department of Geological Sciences, University of Oregon

We invert for the time dependent slip history of slow slip events on the Cascadia subduction zone using GPS data from 1998 to 2008. We process continuous GPS data from the PBO, PANGA and WCDA networks from the past decade using GAMIT/GLOBK processing package. GPS time series are inverted for fault slip using the Extended Network Inversion Filter. This inversion methodology filters out the uncorrelated benchmark motion and random white noise in the GPS time series, and estimates the reverse fault slip that best models the temporally and spatially correlated surface deformation. 16 slip transients have sufficient station coverage to solve for the slip distribution on the plate interface. Limited station coverage south of Portland restricts our analysis primarily to events on the northern half of the subduction zone.

Of the 16 events resolved, 11 slip patches are centered in northwestern Washington, and 5 slip patches are located in southwestern Washington and northwestern Oregon. Some slip events are complex, such as the February 2003 event where sub-events extend from Portland to southern Vancouver Island. One additional event is resolved near Cape Blanco in southern Oregon where the recent installation of stations has improved resolution beginning in 2007. Our time dependent inversion allows for the discrimination of sub-events and the propagation direction from the hypocenter. The identification of sub-events and the along-strike extent of slip suggest a segment boundary just to the south of Seattle where events tend to rupture on a northern segment and southern segment in western Washington. This segment boundary correlates roughly with geologic and tectonic boundaries. A proposed tear in the subducting plate near the southern end of Puget Sound, as supported by intra-slab seismicity, would disrupt the geometry of the plate interface and introduce structural boundaries between the segments. Additionally, the northern terminus of the Siletzia terrain is found in southwestern Washington, and marks a change in tectonic environment as the rigid Oregon forearc migrates northward causing north-south transpression. Therefore, these structural and tectonic controls may influence slow slip and act to segment along-strike behavior.

Over a ten-year period, total strain release from slow slip events is non-uniform along-strike with the greatest cumulative slip (27 cm) centered beneath Port Angeles in northwestern Washington. This slip patch also exhibits the most regular recurrence interval relative to other locations along-strike and the largest slip per event. The spatial extent of the slip patch beneath Port Angeles correlates with the along-strike bend of the Cascadia subduction zone in northwestern Washington. Enhanced crustal seismicity and high strain rates indicate that compressional stressing rates are at a maximum around the structural bend in the plate boundary. This suggests that plate geometry plays an important role in controlling the along-strike characteristics of slow slip. We hypothesize that a higher stressing rate on the plate interface in northwestern Washington results in lower recurrence intervals and higher slip amplitudes for slow slip events.

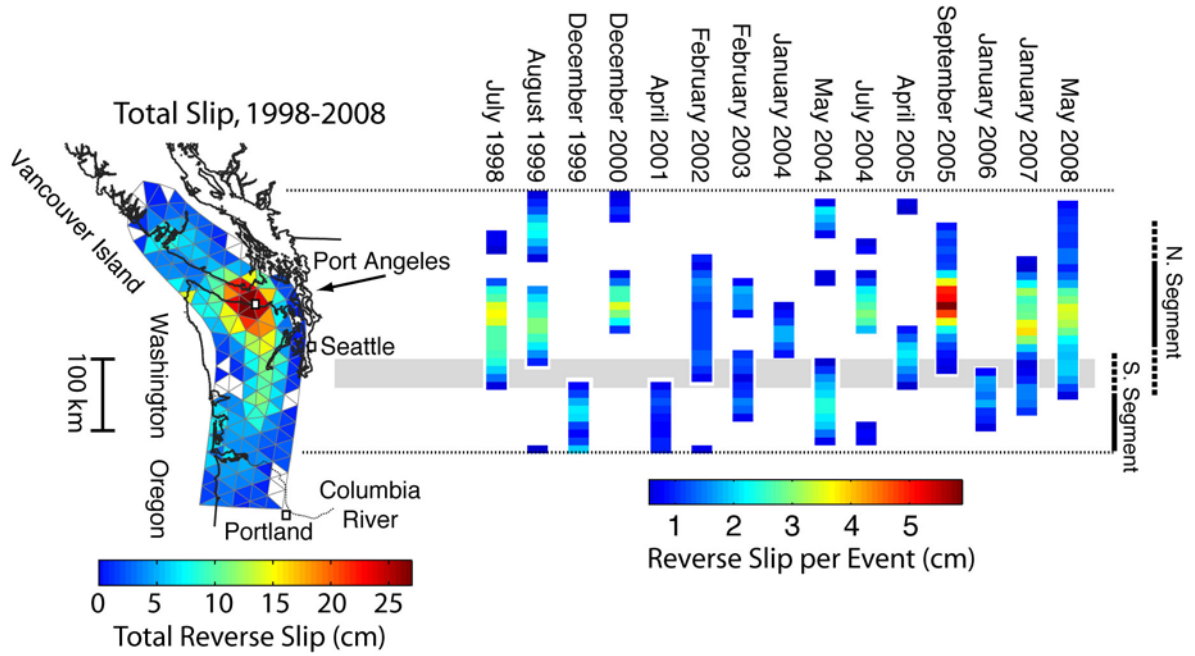

Figure: Total slip (left plot) is calculated by summing the slip distribution from slow slip events on the northern half of the Cascadia subduction zone. The along-strike slip profile is plotted for each event (right plot). Profiles are taken along the 35 km depth contour on the plate interface for fault slip greater than 5 mm.

Detection of Short Term Slow Slip Event by GEONET Routine Analysis

Tetsuro IMAKIIRE
Geographical Survey Institute (GSI)

GEONET, the continuous GPS observation network of GSI, revealed Tokai slow slip event started from the fall of 2000. GEONET was very effective to detect and monitor the long term slow slip event, as the time constant of the phenomenon is long enough to apply the filtering to remove the trend, annual variation and noise derived from atmospheric perturbation. On the other hand, GEONET has not been able to detect the crustal deformation caused by short term SSE in Tokai region. As the accuracy of GEONET final solution (F2) evaluated is as large as 2.8mm in the horizontal components (Hatanaka et al., 2003), after removing the annual variation, it is considered to be difficult to detect the signal of short-term SSE, which is as small as one millimeter.

However, Hama et al. (2008) reported that data stacking of more than one hundred GPS sites in Tokai region is effective to reduce the noise from observed coordinates. They pointed out the horizontal movement caused by short term SSE in December 2004 can be detectable on several GEONET sites. Even though their analysis was based on the coordinates of GPS observation sites by the solution of different strategy, same noise reduction method is applicable to GEONET final solution. The F2 solution data of 84 GEONET sites from January 2004 to December 2005 in same target area and were used to verify the effectiveness of the method. As a preliminary result, it is difficult to determine a threshold value to "detect" SSE occurrence, but can estimate the displacement by SSE, if its occurrence is proved by other observations.

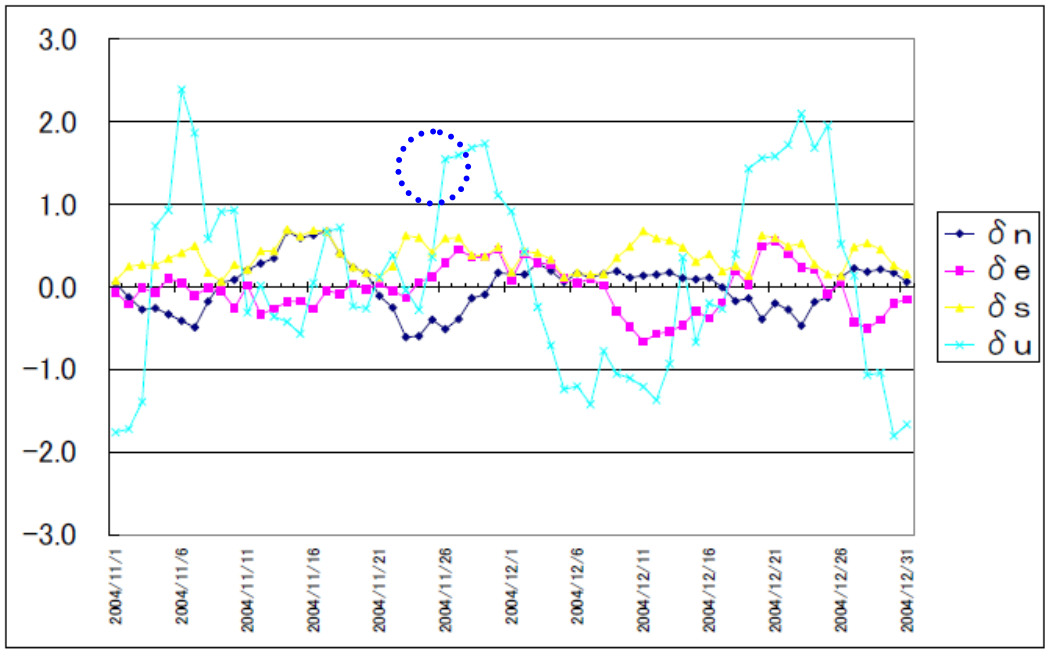

Fig.1 Possible crustal deformation caused by Tokai short term SSE from Dec. 17 to 20, 2004, observed by GEONET (Toyohashi-2 site)

References

Yuki HATANAKA, T. Iizuka, M. Sawada, A. Yamagiwa, Y. Kikuta, J. M. Johnson, C. Rocken (2003) : Improvement of the Analysis Strategy of GEONET, Bull. Geogr. Surv. Inst., 49, 11-37

Hiroe HAMA, M. Satomura, S. Shimada, T. Kato, K. Sayanagi (2008): The crustal movements caused by the short-term slow slip events in the Tokai region by using dense GPS observation net data, Abstracts Japan Geoscience Union Meeting 2008, D107-005

What Does Tremor Really Look Like? Results from a 1km, 80-Element Array on Hard Rock

John E. Vidale[1], Ken Creager[1], Zhigang Peng[2], Abhijit Ghosh[1], and Justin Sweet[3]
[1] University of Washington, Seattle, Wash. U.S.A., [2] Georgia Institute of Technology, Atlanta, Ga. U.S.A., [3] Northwestern University, Evanston, Ill., U.S.A.

Part I - Initial results from an 84-element array

Aspiring to see more intimate details, we placed an 84-element short-period vertical-component array with an aperture of 1km on a hard rock mountain over the path of Cascadia tremor. This site is coincident with a stellar 6-station three-component CAFE array (see talk by K. Creager). Texans, which are convenient to deploy but require recycling for fresh batteries every four days, recorded the seismograms. We recorded 8 days in March and 17 days in May 2008. We find most of the arrivals at high frequencies, especially in the stacks, are P-waves, due to the network constitution. The March week contains only six intermittent hours of tremor detectable by the usual envelope analysis of data from the regional network, but array beamforming shows much more continuous activity, and extending about a half day longer. We also pick up a later episode of weak tremor that contains probably the first glance of low-frequency earthquake in Cascadia. The May field season recorded full-blown tremor passing directly underneath in startling detail. The tremor source region in preliminary images is more compact than the cloud of locations determined from envelope correlation, but also with an apparently persistent patchwork of regions that do and do not generate tremor. Further analysis and future deployments with multiple dense arrays show great promise for getting to the bottom of the issue of tremor generation.

Part II - Tremor triggered near Parkfield by teleseismic waves

We perform a systematic survey of triggered tremor around the Parkfield section of the San Andreas fault for the 31 teleseismic earthquakes since 2001 with Mw > 7.5 and depth < 100 km. We identify triggered tremor as bursts of high-frequency (2-8 Hz), non-impulsive seismic energy that are generated during the passage of teleseismic waves and coherent among many stations. 10 teleseismic events triggered clear tremor around Parkfield. About 35% of the tremor is concentrated south of Parkfield near Cholame, where ambient tremor has been identified previously, and 23% near Bitterwater in the creeping section of the San Andreas fault. Tremor is most commonly initiated by and in phase with the Love wave particle velocity. However, the pattern becomes complicated with the arrival of the Rayleigh waves, and sometimes tremor continues after the cessation of the surface waves. We identify two cases where tremor is triggered during the teleseismic PKP phase. These observations indicate a mixture of driven, instantaneous, perhaps Coulomb-friction response with an added component of self-sustaining activity more suggestive of ongoing slow slip or triggered fluid flow. We also examine the ambient tremor occurrence rate before and after the teleseismic events, and find the aforementioned transient increase of tremor rate during the passage of the teleseismic surface waves, followed by a period of relative tremor quiescence. This suggests that the occurrence time of tremor is temporally advanced by the dynamic stress of the teleseismic waves. Larger amplitude in the teleseismic waves correlates well with the occurrence of triggered tremor, and the inferred tremor-triggering threshold at Parkfield is ~2-3 KPa. The relatively low triggering threshold suggests that the effective stress at the tremor source region is very low, most likely due to near-lithostatic fluid pressure.

SESSION IX

ABSTRACTS

Recurrence Behavior of Short-term Slow Slip and Correlated Non-Volcanic Tremor Episodes in western Shikoku, southwest Japan

Hitoshi Hirose (hirose@bosai.go.jp) and Kazushige Obara
National Research Institute for Earth Science and Disaster Prevention (NIED)

Slow slip events (SSE) that accompany non-volcanic low-frequency tremor (episodic tremor and slip; ETS; Rogers and Dragert, 2003) have repeatedly occurred along the Nankai trough subduction zone in southwest Japan (Obara et al., 2004; Hirose and Obara, 2005, 2006). In the western Shikoku region, one of the most active ETS region in southwest Japan, ETS has been observed every six months with the NIED Hi-net tiltmeter network and has been documented over 10 episodes since 2001. The previous studies have analyzed static offsets in tilt records to obtain a simple rectangular fault model for each episode. However, the tiltmeters have recorded signals of crustal deformation due to SSEs with sub-day time resolution that are beneficial for investigating detailed slip processes of SSEs. Moreover, slip distributions over a number of SSE cycles provide useful information about the repeating nature of slip events on the plate interface. In this study, we apply a newly-developed time-dependent slip inversion method to the tilt records for seven SSEs (2002–2007) to retrieve source slip processes of these episodes.

For each SSE, slip migrates along the strike direction of the subducting Philippine Sea slab at a rate of approximately 10 km/day (Fig. 1). Comparing the slow slip area with epicenters of accompanying non-volcanic tremors in sub-day time resolution, we find that the two phenomena are located on a smaller area than previously reported and migrate as a group (Fig. 1). A moment rate function for each SSE exhibits good correlation with the temporal change in tremor activity. A comparison of the slip distributions of all SSEs shows that there is a patch of slow slip (approximately 30 km in diameter) that is shared by all the episodes. In addition, the location of the slip patch is in good agreement with the epicenters of tremors and very low-frequency earthquakes. These lines of evidence suggest that a recurrence of SSEs in the western Shikoku region may be caused as recurrent slip on the patch area and that these "slow earthquakes" might be different manifestations of a single slip process on the deep plate interface.

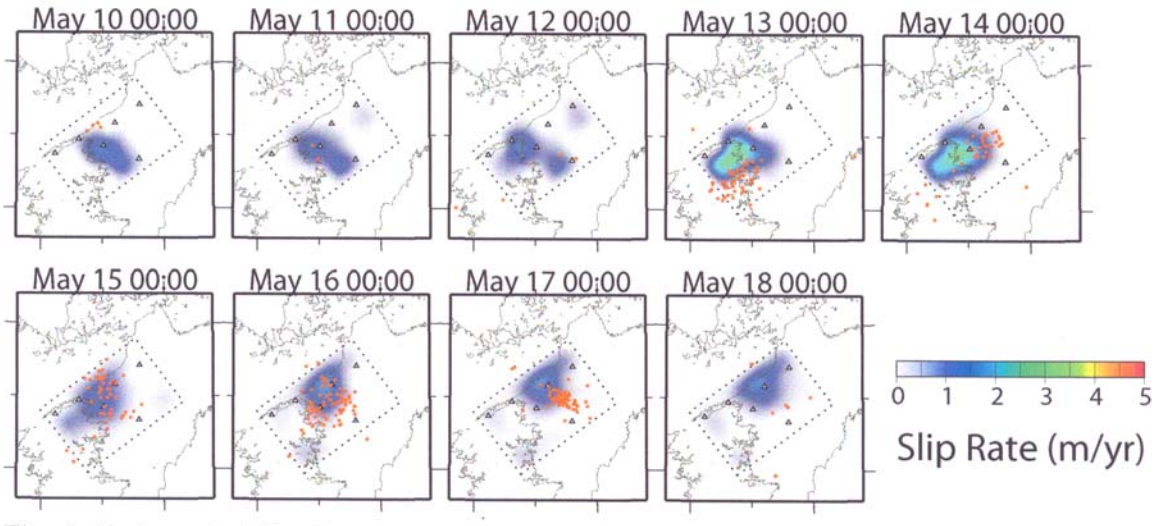

Fig. 1: Estimated daily slip rate distributions of the May 2005 SSE. Times for each frame are 00:00 JST. Orange dots show the tremor epicenters that occurred within a one-day-long time window from 12:00 on the previous day to 12:00 on the day of each frame. A rectangle with broken lines in each frame denotes the modeled region.

Bursts and Waves: The Response of Non-Volcanic Tremor to External Stressing

Justin Rubinstein, US Geological Survey, Menlo Park, CA

Nobody seems to think that tremor and slow-slip can do it on their own. Many authors have sought to understand tremor as the response of the transition zone to outside forcing. Numerous studies have shown that very small stresses can influence significantly the generation of tremor. Efforts to explain tremor and slow-slip through outside forces began quite early in the study of the topic with speculation that the Chandler wobble triggered the repeated slow-earthquakes in Cascadia. More recently, authors have shown that during ETS events, tremor is strongly influenced by the tides, its amplitude rising and falling at the tidal periods of 12.4 and 24 hours. The strong shaking of earthquakes has also been shown to influence the generation of tremor, with the Sumatra earthquake triggering tremor across much of Japan and the Denali earthquake triggering tremor in several locations across California.

Here, I review the predominant ways in which tremor and slow-slip are believed to be affected by outside stresses and the approximate amplitudes of these stresses. Given this information and the assumption that tremor is the product of frictional slip on the plate interface I assess the implications of the small stress perturbations strongly influencing the generation of tremor. While many have speculated that very low effective pressures are needed to produce this triggering behavior, I will argue that low effective pressure is unnecessary.

Observations and Implications of Triggered Tremor

Joan Gomberg, US Geological Survey, Seattle, WA

The growing number of observations of tremor triggered by the passage of seismic waves is providing key constraints on mechanisms of tremor generation. Triggered tremor has the same characteristics as ambient tremor but appears temporally modulated by the triggering seismic waves. I review some of the constraints already established and others that future studies may provide. I also summarize ongoing research focused on testing the hypothesis that triggered tremor serves as an indicator of slow slip. While tremor itself may or may not itself relax ongoing tectonic deformation, slow slip does need to be considered in the accounting of the deformation budget. If this hypothesis were correct, triggered tremor would be a useful tool for detecting slow slip in the many regions with triggered seismic stations but lacking geodetic and continuous seismic monitoring. This hypothesis is premised on the now established correlation between rates of ambient tremor activity and slow slip. Thus, if the probability of triggering tremor depends on the ambient tremor rate, we can infer that it also depends on the amplitude or rate of slow slip. We test the assumption that the probability of triggering tremor depends on the ambient tremor rate by employing ideas used to study earthquake triggering. We measure tremor rates for Cascadia using new tremor catalogs containing quiet times punctuated by episodes of slow slip and increased tremor activity. We also document the characteristics of large teleseismic waves that passed through the region during this period, and which of this triggered tremor. Preliminary results suggest triggered tremor is more probable during periods of increased ambient tremor activity, but that the size of the triggering waves also is an important factor.

Surface Wave Triggering Potential

By
David P. Hill
U.S. Geological Survey, MS 910
Menlo Park, CA 94025
hill@usgs.gov

The capability of dynamic stresses associated with surface waves from large, distant earthquakes to trigger local earthquakes in the brittle crust as well as bursts of non-volcanic tremor associated with the episodic tremor and slip (ETS) beneath subduction zones and the San Andreas Fault System at depths of 20 to 30 km is well established. Likely triggering processes, however, remain a matter of discussion. Here, I explore the potential of fundamental mode, 15- to 30-s Love and Rayleigh waves for triggering non-volcanic tremor through frictional failure on critically-stressed thrust and vertical strike-slip faults at depths of 20 to 30 km using a Mohr's circle representation for dynamic stress perturbations and the Coulomb failure criteria (see Hill, 2008). Well documented instances of triggered non-volcanic tremor along the Nankai (Japan) and Cascadia (North America) subduction zones involve strike-parallel wave propagation along slabs with dips of 10 to 15 degrees at depth of 20 to 30 km (e.g. Rubinstein et al, 2007; Miyzawa and Brodsky, 2008). For this configuration, dip-parallel dynamic stresses associated with Love waves hold a greater potential for triggering frictional failure along the slab interface than those associated with Rayleigh waves. In the case of near-lithostatic pore pressure within the subduction interface, however, the peak amplitude of the Rayleigh wave dilatational stress, which is just ~20% of the peak Rayleigh wave traction stress at these depths, may induce shear failure through pore-pressure re-distribution via extensional (Griffith) failure along sub-vertical fractures. Documented instances of triggered non-volcanic tremor beneath the San Andreas Fault system in California are also associated with strike-parallel wave propagation (Gomberg et al, 2008). In this case Love waves also hold a greater potential for triggering strike-slip shear failure on vertical faults than Rayleigh waves, although again, the relatively weak Rayleigh wave dilatational stress may play an indirect role through the dynamic redistribution of pore-pressure under conditions of near-lithostatic pore pressure. The observation that Rayleigh waves appear to trigger non-volcanic tremor along the Nankai subduction zone and the San Andreas Fault system is consistent with pore-pressure re-distribution playing a significant role in both environments in contrast to simple shear failure beneath Cascadia.

References:

Gomberg, et al., 2008, Science, v. 319, p. 173.
Hill, D.P., 2008, BSSA, v. 98, pp. 66-92.
Miyazawa, M. and E.E. Brodsky, 2008, JGR, v. 113, doi:10.1029/2006JB004890.
Rubinstein, J. et al., 2007, Nature, v. 448, pp. 579-582.

Toward a Source Spectral Model of the ETS Process

by Heidi Houston, Dept. Earth and Space Sciences, University of Washington

The physical processes involved in Episodic Tremor and Slip (ETS) are not understood. Examination of possible source spectral models for ETS and comparison with those appropriate for earthquakes could help elucidate the physics of ETS. Although individual earthquakes may deviate, the standard source spectral model for earthquakes is the omega-squared model, in which displacement spectral amplitudes at frequencies above a corner frequency fall off as the inverse of frequency squared. In contrast, tremor has been observed to fall off roughly as the inverse of frequency over 1 to 10 Hz, i.e., as ω^{-1}. The direct observation of a truly broadband spectrum of ETS is difficult, if not impossible, due to the very long durations involved and the weak signal. However, observations of the amplitudes of tremor and a handful of very-low-frequency events (VLFs) can be compared to the long-period moment of an entire ETS inferred from GPS measurements. Source spectral amplitudes (i.e., a moment-rate spectrum) can be estimated from tremor recordings by assuming that they consist primarily of direct far-field S waves and then applying an empirical calibration to account for reverberations at the stations. The calibration is developed from recordings of small earthquakes whose magnitudes are known. The moment rates obtained for short representative intervals of tremor (e.g., 20 minutes to 1 day) are adjusted to that expected for the ~14 day duration of the 2005 Cascadian ETS.

A simple ω^{-1} model for ETS has a flat portion of the spectrum and a higher-frequency portion falling off as the inverse of frequency:

$$M(\omega) = M_0 \frac{\omega_c}{\omega + \omega_c},$$

$$\omega_c = \frac{2}{T}.$$

In the simplest version, the corner frequency between the portions would be set by the duration T of the entire ETS process and is thus very small indeed. This model under-predicts observed spectral amplitudes of Cascadia tremor at 1-10 Hz during ETS by about two orders of magnitude (Figure 1). Inferences of spectral amplitude at ~100 s from VLFs observed in Japan (Ide et al., 2008) are also under-predicted, although not as badly. One possible solution involves a higher corner frequency, for example, that associated with the daily or twice-daily tidal cycles, which have been shown to affect tremor generation (e.g., Rubenstein et al., 2008). Another possibility involves a spectral bump at high frequencies due to small-scale patchiness or to a difference in the physical process generating high frequencies and that responsible for slow slip. It should also be noted that above some frequency, the source spectrum must fall off faster than $\omega^{-1.5}$ to avoid an energy catastrophe. As more observations of the amplitudes of ETS processes at various frequencies become available, from a variety of instrument types, we will be able to discriminate between the possibilities and obtain spectral models of the ETS source.

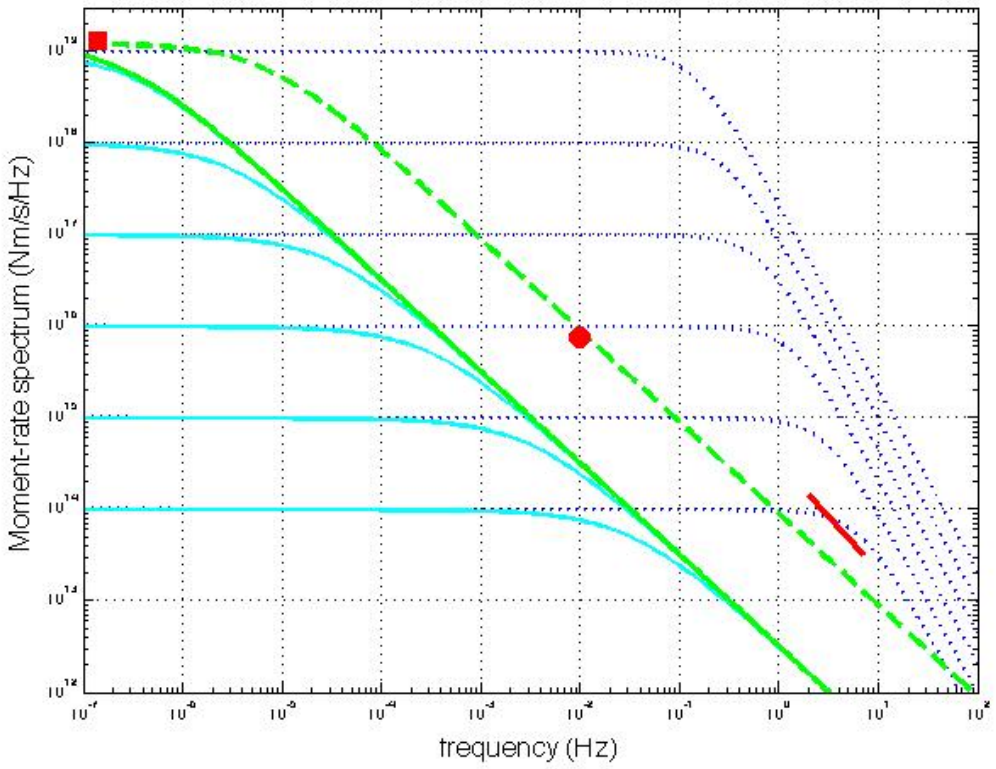

Figure 1. Comparison of spectral source model for ETS process and observations of spectral amplitude. ω^{-1} models (cyan lines) with corner frequencies set by a moment release rate of M_W 6.7 per 14 days. ω^{-2} models (dotted blue lines) with corner frequencies set by stress drop 3 MPa are shown for comparison. Total moment of 2005 Cascadia ETS inferred from GPS by Melbourne and coworkers (red square). Estimated moment-rate spectrum of 2005 Cascadia ETS tremor for 14 days (red line). Estimated moment-rate spectral amplitude of VLF's in Japan (Ide et al., 2008, GRL) scaled to 14 days (red circle). The simplest ω^{-1} model for a M_W6.7 14-day ETS under-predicts moment rates inferred from tremor and VLF observations (solid green line). Dashed green line shows ω^{-1} model with corner frequency corresponding to 0.5 day rather than 14 days.

Seismic Exploration of Deep Low-frequency Tremor Area in western Shikoku, Japan

Tetsuya Takeda[1], Kazushige Obara[1], Yoshikatsu Haryu[1], Youichi Asano[1], Takuto Maeda[1], Katsuhiko Shiomi[1], Tomotake Ueno[1], Takanori Matsuzawa[1], Yohei Yukutake[2], Makoto Matsubara[1], Hitoshi Hirose[1], and Shutaro Sekine[1]
1 National Research Institute for Earth Science and Disaster Prevention (NIED), Japan
2 Hot Spring Institute of Kanagawa Prefecture, Japan
ttakeda@bosai.go.jp

Low-frequency tremor, first found in southwestern Japan, is a seismic phenomenon that would be attributed to subduction system of the Philippine Sea plate. We carried out a seismic reflection survey in March 2008 to reveal the structure around the source region of tremor in western Shikoku, Japan. The survey had two reflection profiles, Line-SN and Line-WE, whose lengths are 75 km and 85 km, respectively (Figure 1). Six blasts of 500 kg were used as controlled sources. Such large sources enable us to detect reflected waves from the Philippine sea plate at depths of ~40 km. 341 seismometers with the natural frequency of 2 Hz (L-22D) were deployed with the average separation of 333 m for Line-SN and 500 m for Line-WE, respectively. We retrieved high S/N data for all blasts. The data was analyzed with typical seismic processing; the CDP editing, the filtering, the muting, the NMO correction, and the depth conversion. We assumed a homogeneous medium with velocity of 6.4 km/s.

From the obtained seismic profiles, we identified abundant reflectors. In the Line-SN, we can trace a strong and continuous reflector, which has a north dip of 8 degrees at depths of 22~35 km. We interpreted the reflector as the upper boundary of the Philippine Sea plate. Another reflector, whose amplitude is smaller than that of the plate boundary, is identified at depths of 30~42 km. The reflector is interpreted as the Moho discontinuity in the Philippine Sea plate, because it is below and parallel to the plate boundary and is consistent with the oceanic Moho discontinuity estimated by the receiver function analysis. These interpretations show that the thickness of the oceanic crust is about 8 km and the hypocenters of tremor concentrate near the plate boundary. Along the dip of the Philippine Sea plate, the reflection from the plate boundary around the tremor is not clear, whereas we observed a strong reflector from down-dip extent of the slab. It suggests that such difference is a key to understand the physics of the tremor.

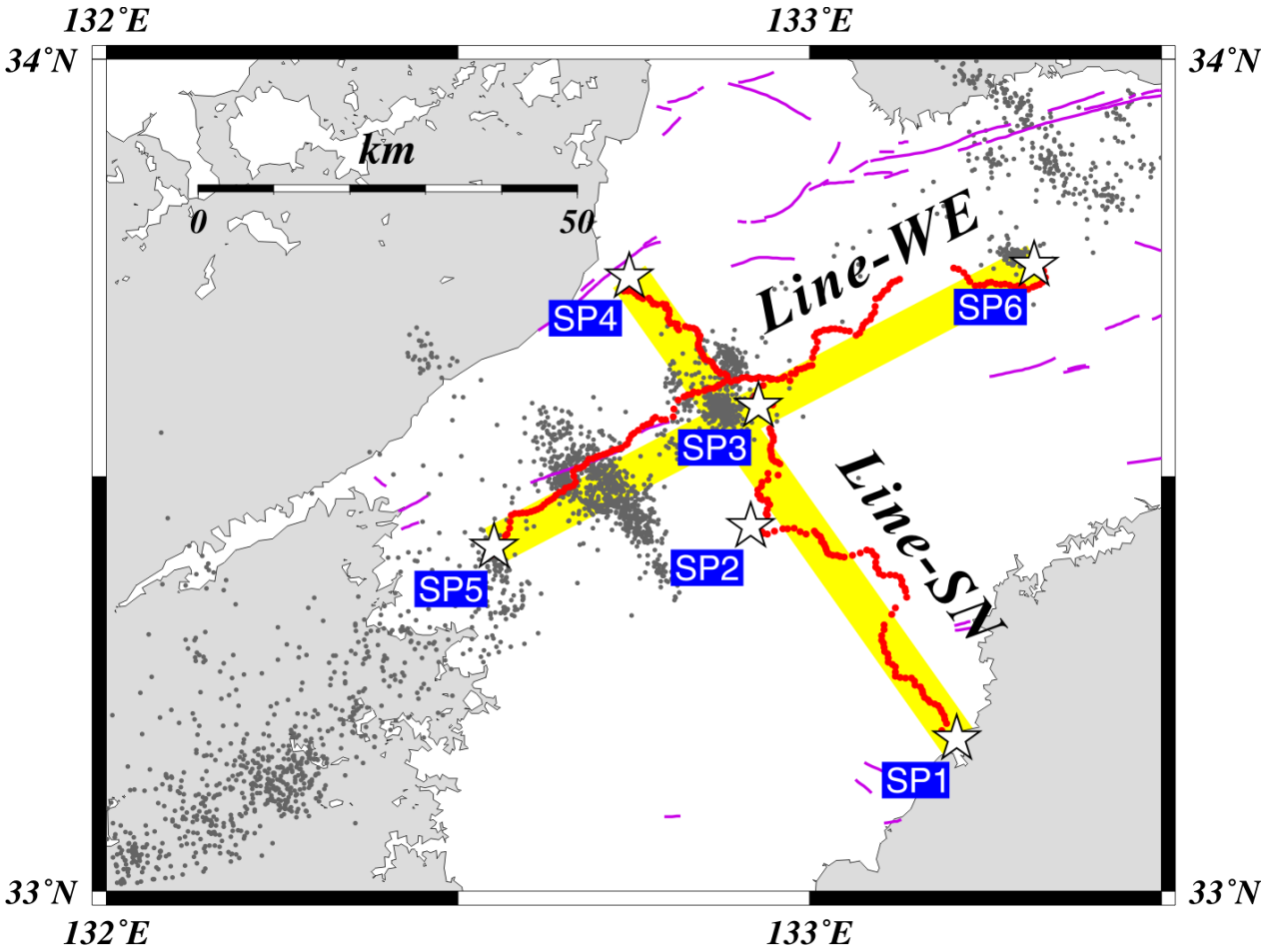

Figure 1 Location map of two seismic reflection profiles (Line-SN and Line-WE). Stars denote blasts. Red dots indicate seismic stations. Gray dots indicate epicenters of low-frequency tremor by Japan Meteorological Agency.

Precise Relative Location of San Andreas Fault Tremors near Cholame, CA Using Seismometer Clusters: Slip on the Deep Extension of the Fault?

David R. Shelly[1], William L. Ellsworth[1], Trond Ryberg[2], Christian Haberland[2], Gary S. Fuis[1], Janice Murphy[1], Robert M. Nadeau[3], Roland Bürgmann[3]
[1]*U.S. Geological Survey, Menlo Park, CA 94025*
[2]*GeoForschungsZentrum, Potsdam, Germany*
[3]*Berkeley Seismological Laboratory, University of California, Berkeley, CA 94720*

Non-volcanic tremor, similar in character to that generated at some subduction zones, was recently identified beneath the strike-slip San Andreas Fault (SAF) in central California (Nadeau and Dolenc, 2005). Using a matched filter method, we closely examine a 24-hour period of active SAF tremor and show that, like tremor in the Nankai Trough subduction zone, this tremor is composed of repeated similar events. We take advantage of this similarity to locate detected similar events relative to several chosen events. While low signal-to-noise makes location challenging, we compensate for this by estimating event-pair differential times at "clusters" of nearby temporary and permanent stations rather than at single stations. We find that the relative locations consistently form a near-linear structure in map view, striking parallel to the surface trace of the SAF. Therefore, we suggest that at least a portion of the tremor occurs on the deep extension of the fault, similar to the situation for subduction zone tremor. Also notable is the small depth range (a few hundred meters or less) of many of the located tremors, a feature possibly analogous to earthquake streaks observed on the shallower portion of the fault. The close alignment of the tremor with the SAF slip orientation suggests a shear slip mechanism, as has been argued for subduction tremor. At times, we observe a clear migration of the tremor source along the fault, at rates of 15-40 km/hr.

POSTER SESSION ABSTRACTS

Modeling the Slip Distribution and Fault Geometry of the February 21, 2008 Mw 6.0 Wells Nevada Earthquake Using InSAR

Charles Wicks, USGS Menlo Park, CA

On February 21, 2008 a Mw 6 earthquake shook northeastern Nevada near the city of Wells, causing damage to many buildings especially in the old town, but no deaths. The earthquake occurred on a NNE striking normal fault north of Wells. The fault does not appear to be related to any mapped active fault from the USGS Quaternary faults and folds database (black lines in Figure 1). The earthquake occurred in what can be considered a typical Basin and Range setting.

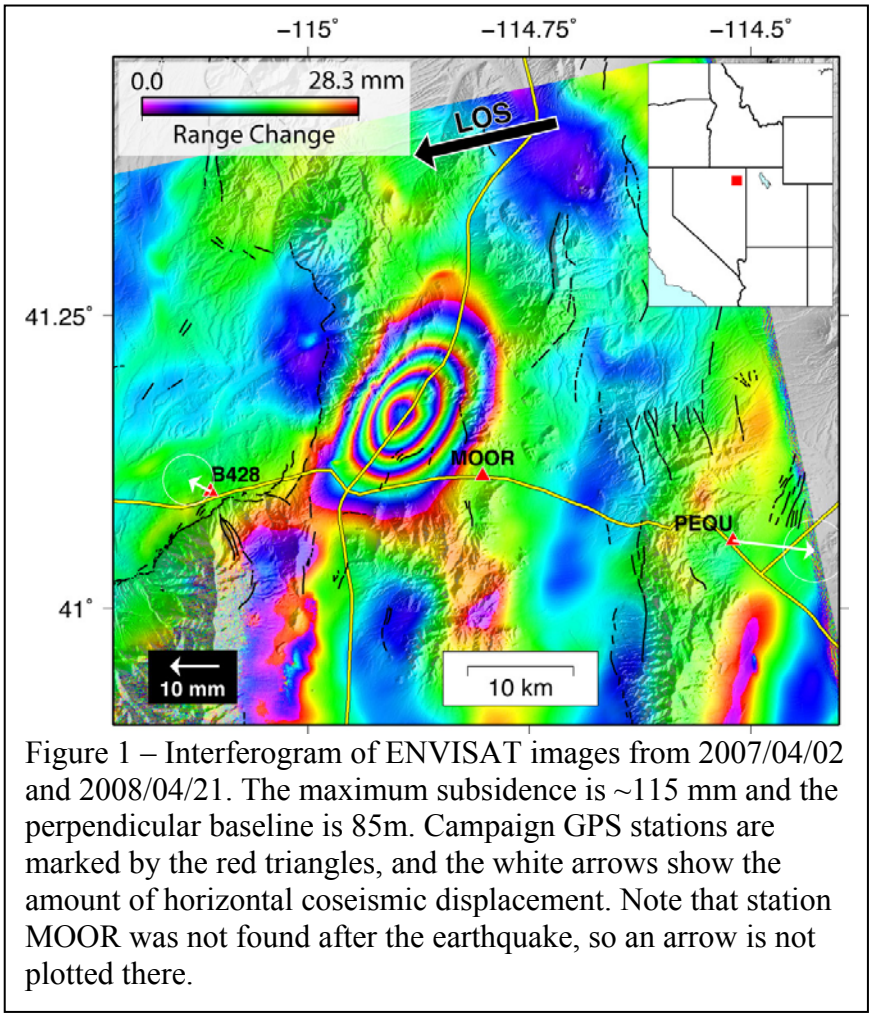

Figure 1 – Interferogram of ENVISAT images from 2007/04/02 and 2008/04/21. The maximum subsidence is ~115 mm and the perpendicular baseline is 85m. Campaign GPS stations are marked by the red triangles, and the white arrows show the amount of horizontal coseismic displacement. Note that station MOOR was not found after the earthquake, so an arrow is not plotted there.

Preliminary modeling of ENVISAT interferograms yields a fault that dips 30-45 degrees to the east, with the top of the fault at about 6 km and slip of over one meter. The surface trace of the fault would then fall in the next basin to the west. If I introduce curvature to the fault and force the surface trace to fall on the east side of the mountain range on the west side of the deformation field (Figure 1) the depth, dip and amount of slip remain nearly the same, but the dip at the surface is about 65 degrees…a listric fault.

The incidence angle of the ENVISAT data is steep, about 23 degrees and I hope to have RADARSAT and ALOS data that have incidence angles that are shallower and more sensitive to horizontal displacements. This data should give better constraints on the fault parameters and its possible listric nature.

Anomalous Depth Distribution of Deep Low-Frequency Earthquakes at the northeast Tokai District

Fuyuki Hirose (MRI), Junichi Nakajima (Tohoku Univ.), and Akira Hasegawa (Tohoku Univ.)

Deep low-frequency earthquakes are distributed in a belt-like form along the isodepth contour of 30 km depth of the upper plate boundary of the Philippine Sea slab as pointed out by Obara [2002]. Hirose et al. [2007] confirmed this features on the basis of precisely determined geometry of the Philippine Sea slab, but further revealed that at the northeastern Tokai district deep low-frequency earthquakes are distributed away from the isodepth contour of 30 km depth of the plate boundary and lie on the isodepth contour of 40 km depth. Shelly et al. [2006] and Ide et al. [2007] analyzed mechanism of deep low-frequency earthquakes and insisted that deep low-frequency earthquakes are generated by shear slip on the plate interface. If they occur on the plate boundary even in the Tokai district, it is expected that their depths become deeper toward the northeastern Tokai. It is known that many deep low-frequency earthquakes occur during continuous deep low-frequency tremors [Shelly et al., 2007] and tend to occur in succession in the Tokai district [Kobayashi et al., 2006], which makes it difficult to pick P and/or S phases accurately. As a result, the depth distribution of deep low-frequency earthquakes is scattered in the depth range of 20-50 km.

To constrain and precisely estimate the depth of deep low-frequency earthquakes, we selected 69 deep low-frequency earthquakes from 1582 events in the JMA catalogue that occurred from November 1, 2002 to December 31, 2006 in the Tokai district. The selection is based on the following criteria; (1) P-wave arrival times are picked at more than 3 stations, (2) total number of P- and S-wave arrival times picked are 10 or more, and (3) the magnitude is greater than 0.0. We checked waveforms of the 69 events and re-picked P- and S-wave arrival times. In the picking procedure, we noticed several wrong phase pickings resulting from the continuous occurrence of low-frequency earthquakes. Some of events with wrong phase pickings were located at a depth of ~45 km in the JMA catalogue with travel-time residuals of more than 1 sec. We excluded those wrong pickings and unclear phases and picked only clear phases in each seismogram, which yields 53 deep low-frequency earthquakes recorded by 10 or more stations. Then, the 53 events were relocated with one-dimensional JMA2001 seismic velocity model [Ueno et al., 2002]. After that, they were relocated with the three-dimensional velocity structure estimated by Hirose et al. [2007], by applying DD location algorithm [Waldhauser and Ellsworth, 2000], together with ordinary earthquakes that occurred within the slab and in the overriding plate.

As a result, deep low-frequency earthquakes were clustered and located at depths of ~30 km in the southwestern part and at depths of 35-40 km in the northeastern part, indicating a gradual deepening of deep low-frequency earthquakes from southwest to northeast. Distribution of deep low-frequency earthquakes agrees with almost the plate boundary estimated by Hirose et al. [2007]. This result supports the idea that deep low-frequency earthquakes occur on the plate boundary [Shelly et al., 2006; Ide et al., 2007]. It is very important for considering the extent of the source area of the anticipated Tokai earthquake that the depth of deep low-frequency earthquakes becomes locally deep to about 40 km at the northeastern Tokai district.

The IRIS DMC: Global Real-Time Collection and Distribution of Seismological Data and Products

By Rick Benson[1] and Tim Ahern[1]
[1] Incorporated Research Institutions for Seismology (IRIS), Seattle, Wash. U.S.A.

IRIS was founded in 1984 with support from the National Science Foundation, and is a consortium of over 100 US universities dedicated to the operation of science facilities for the acquisition, management, and distribution of seismological data. IRIS programs contribute to scholarly research, education, earthquake hazard mitigation, and the verification of a Comprehensive Test Ban Treaty.

This poster will focus on updated activities within IRIS Data Management Center, located in Seattle, WA, which operates a core facility that coordinates data collection and delivery within a global, and highly collaborative, "network of networks" that not only includes the IRIS GSN, IRIS PASSCAL and much of the EarthScope (USArray, SAFOD and PBO) data collections, but more than a hundred non-IRIS-managed local, regional, and national networks that now openly exchange data predominantly in real-time. At the core is an 80 terabyte, online seismological waveform archive, with an accompanying large relational database, that enables researchers the ability to access either all data that is either currently collected in real-time, or from a collection that spans over 40 years of collected time-series data.

There are 4 topics to present:

1) We will show what is behind the current effort to archive 20 Tb of data while distributing nearly 35Tb annually, in addition to servicing close to a million requests for data (the sum of both real-time and customized).

2) It's no longer enough to simply collect and distribute data on demand, so the current, continuously streaming low-latency data that now comes into the BUD (Buffer of Uniform Data) system undergoes significant QC through the QUACK (Quality Analysis Control Kit) framework. Measurements taken include data completeness, signal RMS, and advanced signal analysis aimed at measuring background noise levels, helping indicate station quality problems with minimal delay. In addition, latencies for both import and export delivery are tracked and exported to web interfaces for simple searching and viewing.

3) We are now building a broad range of services that leverage data discovery and access, utilizing both SOAP and REST-style web services. These will provide streamlined access to station metadata, waveform inventory, and data products from within the SPADE product archive.

4) Finally, the IRIS DMC now plays an important "additional" role of contributing data to networks that perform monitoring and require low-latency data, and this is accommodated by serving data through an augmented SeedLink server that currently clusters data from over 1700 stations, with more than 16,000 discreet channels. In addition to seismic, real time feeds included in this highly available mix of data are strong-motion (engineering), pressure, strain, gravimeter and infrasound data.

We intend to present snapshots of the data holdings, life cycle and services that are openly available to anyone, anywhere, at any time.

National Seismic Hazard Maps for Japan (2008)

The Headquarters for Earthquake Research Promotion*
Earthquake and Disaster-Reduction Research Division, Research and Development Bureau,
Ministry of Education, Culture, Sports, Science and Technology, jishin@mext.go.jp

Seismic hazard-assessment enables the public and private sectors to assess earthquake hazards and prepare for the future earthquakes. In Japan, the Headquarters for Earthquake Research Promotion (HERP) released National seismic hazard maps in 2005, and revised them by adding new knowledge about the nature of earthquakes every year. The seismic hazard maps prepared by the Earthquake Research Committee in HERP consist of two types of maps, 'Probabilistic Seismic Hazard Map' and 'Seismic Hazard Maps for Specified Seismic Source Faults (Scenario Earthquakes)'.

The 'Probabilistic Seismic Hazard Map' shows the possibilities of strong motions all over Japan. The regional differences of the possibilities of ground motion levels are presented in it. In contrast, the 'Seismic Hazard Maps for Specified Seismic Source Faults' show the special distribution of earthquake motions which will be generated around a single fault.

The 'Probabilistic Seismic Hazard Map', indicates the possibility of strong motions within the next 30 years at every location (1 km mesh) on the map. This map takes into consideration of the following:

- Characteristic earthquakes that occur along major active fault zones,
- Large earthquakes that occur at the oceanic plate boundary (called 'subduction zone earthquakes'), and
- Background earthquakes whose fault locations are not identified in advance.

'Seismic Hazard Maps for Specified Seismic Source Faults' pay attention to specific seismic source faults, and indicate the detailed special distribution of seismic intensity around the scenario earthquakes. Broadband time histories of earthquake ground motions are evaluated at the base rock level of each mesh for estimating seismic intensity. Maps providing such information are prepared and will be useful for the mitigation of earthquake disaster.

In order to improve these maps, we need more detailed information about the active faults such as paleo-seismic events and underground structures. HERP is discussing how to effectively improve the National seismic hazard maps.

*The Headquarters for Earthquake Research Promotion (HERP) was launched in 1995, after the 1995 Hyogo-ken Nanbu Earthquake. It's based on a Special Measure Law on Earthquake Disaster Prevention. Under this framework, the Earthquake Research Committee of HERP collects, arranges, analyzes and evaluates survey results on earthquakes. Also, in order to reduce damages from earthquake, HERP has been making efforts to promote investigation and spread basic knowledge of earthquake.

Crustal Movements Detected by Seafloor Geodetic Observation

M. Sato, H. Saito, Y. Matsumoto, M. Fujita, T. Yabuki
(Hydrographic and Oceanographic Department of Japan)
M. Mochizuki, A. Asada (Institute of Industrial Science, University of Tokyo)

1. Introduction

The Hydrographic and Oceanographic Department of Japan (JHOD) and the Institute of Industrial Science have been developing precise seafloor positioning systems using the GPS/Acoustic combination technique and carrying out observations along the major trenches in the Pacific Ocean, such as the Japan Trench and the Nankai Trough. The primary purpose of seafloor geodetic observation is to detect and monitor the crustal deformation caused by the subduction of the oceanic plate near the plate boundary where huge earthquakes repeatedly occur. The original idea dates back to the early work carried out by scientists at the Scripps Institution of Oceanography (Spiess, 1985).

2. Observation system

A schematic picture of the seafloor geodetic observation system is shown in Fig. 1.

This system consists of a seafloor unit with four or three acoustic mirror-type transponders, and an on-board unit with a GPS antenna and an undersea transducer installed on the rigid observation pole of about 8m in length, to which a dynamic motion sensor is also attached.

The system measures ranges from the on-board transducer to the seafloor acoustic transponders through round-trip acoustic travel times in-between. Acoustic wave velocity profiles in the seawater, necessary for transforming travel time into range, are obtained from CTD/XCTD and XBT measurements.

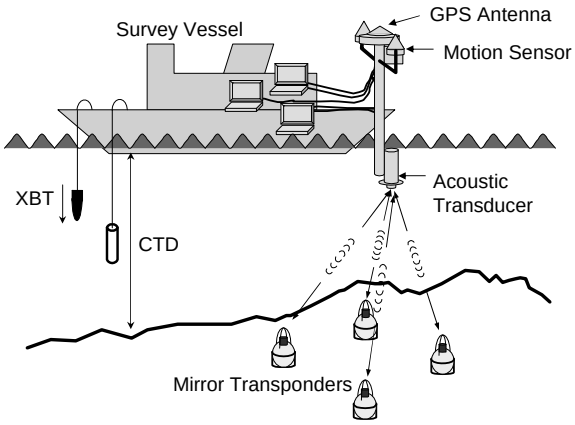

Fig. 1 Schematic picture of the GPS/Acoustic seafloor geodetic observation system.

3. Major results

Off-shore Miyagi Prefecture is one of the most active seismogenic zones in Japan. The Pacific plate is subducting beneath the continental plate at a rate of 9-10 cm/year at the Japan Trench.

From the repeated observations at the seafloor reference points off-Miyagi (MYGI) and off Fukushima (FUKU), we obtained the velocity vector of MYGI of 7.3 cm/year in the direction N60□W and the velocity vector of FUKU of 3.1cm/year in the direction S85□W relative to the stable part of the Eurasian plate (Fig. 2). The velocity of MYGI is fast and close to the subduction velocity of the Pacific plate. In contrast, the crustal velocity of FUKU is significantly slow. The contrast of two results about 100km apart infers the difference of strength of interplate coupling between two regions.

On August 16, 2005, a large earthquake (M7.2) occurred on the plate boundary off Miyagi Prefecture at a depth of approximately 40 km. Its focal region is closely neighbored to a seafloor reference point MYGW, which is located about 10 km east of the epicenter and about 50 km

west of MYGI. Comparing the estimated positions of epochs before and after the earthquake, an eastward co-seismic movement of about 10 cm was detected (Fig. 3). Our result is highly consistent with the synthetic vector both in magnitude and in direction.

We have succeeded in detecting intraplate/interplate crustal movements and a co-seismic displacement with centimeter resolution from multiple campaign observations. Observed seafloor crustal movements close to the focal region expect to provide valuable information for detailed discussion on interplate coupling and slip distribution of the source fault.

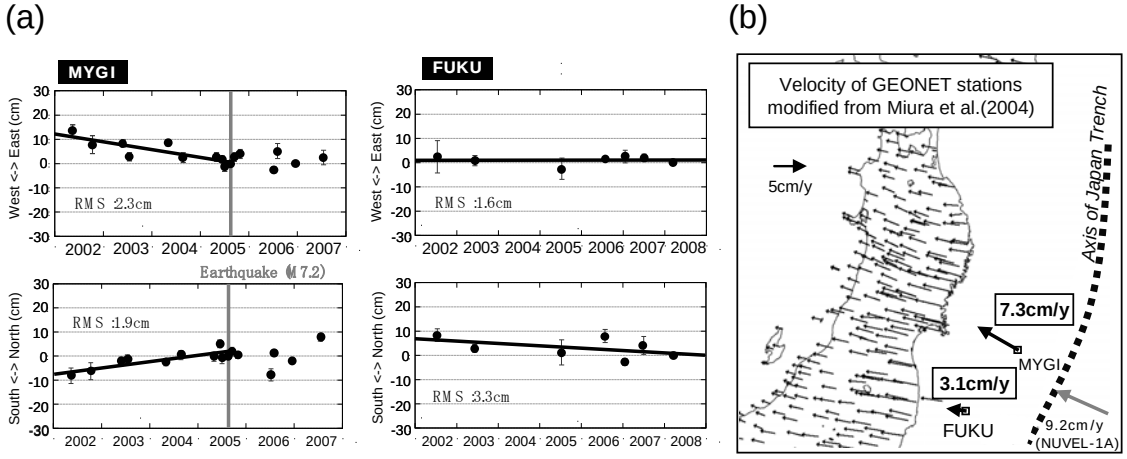

Fig. 2 (a) Time series in the horizontal components of MYGI and FUKU. The reference point is Simosato SLR station in central Japan, with the velocity of 3.2cm/year in the direction N69°W(Sengoku,1998). (b) Velocity vectors of MYGI, FUKU, on-land GPS stations and NUVEL-1A model relative to the stable part of the EU plate.

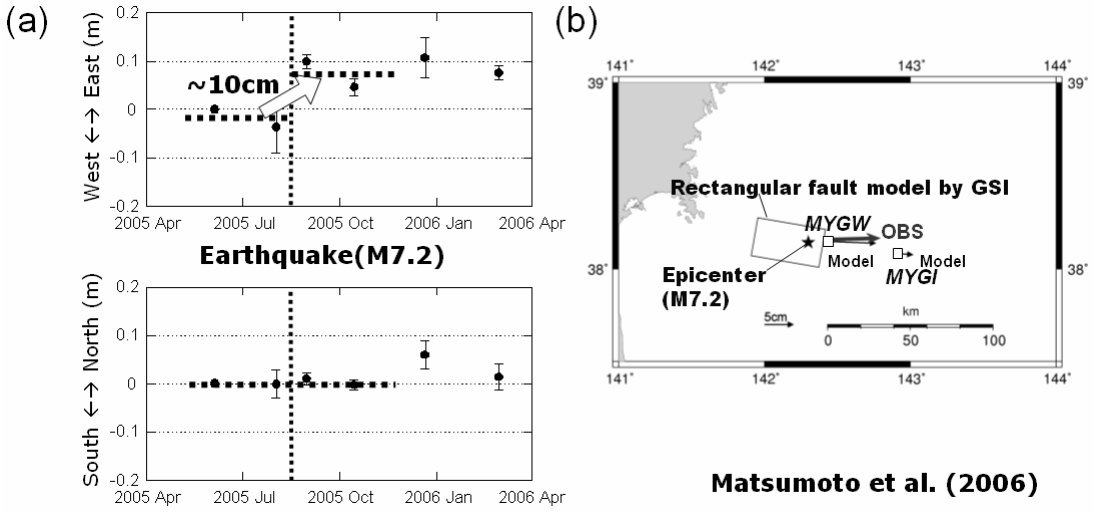

Fig. 3 (a) Time series in the horizontal components of MYGW. (b) Undersea co-seismic horizontal crustal movements associated with the 2005 Off Miyagi Prefecture Earthquake. “OBS” means the observed vector at MYGW and “Model” means synthetic vectors by GSI’s rectangular fault model.

Resolution of the Seventh Joint Meeting of the U.S.-Japan Panel on Earthquake Research (UJNR)
October, 2008

The UJNR Panel on Earthquake Research promotes advanced research toward a more fundamental understanding of the earthquake process and hazard estimation. The Seventh Joint meeting was extremely beneficial in furthering cooperation and deepening understanding of the common problems in both U.S. and Japan.

The meeting included very productive exchanges of information on approaches to systematic observation and modeling of earthquake processes. The Panel recognizes the benefits of working together to achieve our common goal of reducing earthquake risk. We look forward to continued cooperation on issues involving densification of observation networks and the open exchange of data among scientific communities. We recognize the importance of making information publicly available in a timely manner. We also recognize the importance of information exchange on research policy and strategies including framework of research organizations.

Areas of Cooperation

Specific areas of earthquake research where cooperative research between the U.S. and Japan may lead to significant advancement include, but are not limited to:

- Real-time information of seismic, geodetic and strain measurements including borehole strainmeters and ocean bottom seismometers using marine cable
- Technologies for measuring crustal deformation including GNSS, GPS/acoustic, InSAR, LiDAR, VLBI and SLR
- Earthquake recurrence studies using paleoseismic, geodetic and seismic methods
- Laboratory, theoretical and in situ studies of fault-zone physics
- Studies of episodic tremor and slow slip using seismic, geodetic, and borehole strain measurements.
- Systematic studies of earthquake predictability through rigorously evaluated scientific prediction experiments
- Studies of near-source ground motions, geological effects and structural response
- Probabilistic seismic and tsunami hazard estimation incorporating knowledge of current and past behavior, and physics based computational models.

The Panel strongly urges that the appropriate agencies in the U.S. and Japan that are represented on this Panel work together with the academic sector to support and coordinate the scientific work in these areas of cooperation.

The Panel recognizes the importance of promoting exchange of scientific personnel, exchange of data, and fundamental studies to advance progress in earthquake research. Japan and the U.S. should promote these exchanges throughout Asia and the world. The Panel endorses continuation of these activities.

Next Meeting

The next meeting will be held in Japan in the autumn of 2010.